



universität
wien

MASTERARBEIT

Titel der Masterarbeit

„Transmembrane transporters of the liver fluke
Fasciola hepatica“

verfasst von

Sandra Pichler BSc

angestrebter akademischer Grad

Master of Science (MSc)

Wien, 2014

Studienkennzahl lt. Studienblatt:

A 066 834

Studienrichtung lt. Studienblatt:

Masterstudium Molekulare Biologie

Betreut von:

Univ.-Prof. Dr. Harald Sitte

Acknowledgements

First I would like to express my deepest gratitude to Prof. Dr. Harald Sitte for giving me the opportunity to work in his research group and his support and scientific advice.

I feel great appreciation to Prof. Dr. Michael Freissmuth for his support, suggestions and great scientific discussions.

I would also like to thank Prof. Dr. Peter Chiba for giving me the chance to perform experiments within his research group.

My deepest thanks go to my second supervisor Dr. Oliver Kudlacek for his guidance, support and patience. None of this would have been possible without you!

Furthermore, I would like to thank Marion Holy for introducing me to new techniques and her endless moral support.

Special thanks also to Martina and Helmut for answering questions and their help.

I offer a great thank you to my colleagues Mirja, Andreea, Fatma, Thomas, Felix, Tina for making the time enjoyable.

One person I would like to point out is Yaprak Dönmez Cakil. Words cannot express how grateful I am to get to know her. Thank you for everything!

I would also like to take the opportunity to thank my closest friends who never let me down.

Last but not least, my deepest gratitude goes to my parents who made everything possible. Thank you for your endless love, trust and support. I owe everything to you!

Contents

Contents	I
Table of Figures	IV
List of Tables	VI
Abbreviations	VII
Abstract	IX
1 Introduction	1
1.1 <i>Fasciola hepatica</i>	1
1.1.1 Morphology and Taxonomy	1
1.1.2 Life Cycle.....	2
1.1.3 Fascioliasis	4
1.1.4 Triclabendazole and increasing resistance	6
1.2 ATP-binding cassette (ABC) transporters.....	8
1.2.1 Introduction.....	8
1.2.2 Basic structure & mode of action	9
1.2.3 P-glycoprotein / MDR1 / ABCB1	11
1.3 Solute carrier 6A6 (Taurine transporter).....	12
1.3.1 The taurine transporter (SLC6A6).....	12
1.3.2 Taurine	14
1.4 Aim of the study	16
2 Material and Methods	19
2.1 Materials	19
2.1.1 Standard solutions/buffers	19
2.2 Methods.....	22
2.2.1 Cloning	22
2.2.1.1 RNA Isolation from tissue and cells using TRI Reagent®	22

2.2.1.2	Rapid amplification of cDNA ends (RACE)	23
2.2.1.3	Polymerase Chain Reaction (PCR)	24
2.2.1.4	Amplification of full-length cDNA	25
2.2.1.5	PCR product clean-up and agarose gel extraction.....	25
2.2.1.6	Ligation	26
2.2.1.7	Generating competent <i>E. coli</i> bacteria.....	27
2.2.1.8	QuikChange Site-Directed Mutagenesis®	28
2.2.1.9	Transformation	29
2.2.1.10	DNA/Plasmid Isolation.....	29
2.2.2	Cell culture.....	30
2.2.2.1	Cultivation	30
2.2.2.2	Cell counting/seeding	30
2.2.2.3	Transfection	31
2.2.2.4	Stable cell line	33
2.2.3	Western Blot	34
2.2.3.1	Protein preparation.....	34
2.2.3.2	Protein concentration measurement (Bradford reagent)	34
2.2.3.3	SDS-page and blotting	35
2.2.4	Rhodamine123 uptake via FACS.....	37
2.2.5	Uptake	40
2.2.6	Inhibition	41
3	Results & Discussion	43
3.1	<i>Fasciola hepatica</i> MDR	43
3.1.1	Cloning and localization	43
3.1.2	Functional analysis via rhodamine123 accumulation.....	46
3.2	FhepSLC6/Taurine transporter and the human orthologue hTauT	51
3.2.1	Cloning-strategy and verification of localization via fluorescence microscopy	51
3.2.1.1	FhepSLC6.....	51
3.2.1.2	Human taurine transporter hTauT	55

3.2.2	Functional activity	57
3.2.2.1	Uptake: Substrate specificity	57
3.2.2.2	Uptake: temperature dependency of FhepSLC6.....	62
3.2.2.3	Uptake: time dependency of FhepSLC6	63
3.2.2.4	Inhibition.....	65
4	Conclusion & Outlook	71
	References	73
	Sequences.....	77
	Zusammenfassung (Abstract german).....	81
	Curriculum Vitae	83

Table of Figures

Figure 1 Adult <i>Fasciola hepatica</i> & egg.....	2
Figure 2 Life cycle of <i>Fasciola hepatica</i> :	3
Figure 3 <i>Fasciola hepatica</i> infected liver of sheep or cattle	5
Figure 4 Triclabendazole and its metabolites.	6
Figure 5 Schematic overview of ABC transporter function.....	8
Figure 6 Structure based classification of the human ABC transporters.	9
Figure 7 Sav1866 crystal structure.....	10
Figure 8 SLC6 transporter families and their sequence similarities	12
Figure 9 Schematic membrane topology of hTauT.....	13
Figure 10 Schematic model of taurine transport and indicated Na ⁺ /Cl ⁻ exchange.....	14
Figure 11 Structure and biosynthesis of taurine.	15
Figure 12 peCFP-C1 / peYFP-C1/peCFP-N1 schematic vector maps.....	27
Figure 13 Transfection by cationic lipid transfection reagent.....	31
Figure 14 jetPrime [®] DNA Transfection	32
Figure 15 RNAiMAX transfection procedure.....	33
Figure 16 Bradford reagent advanced standard curve	35
Figure 17 Chemical structure of rhodamine123.....	37
Figure 18 Schematic few of FSC and SSC.....	39
Figure 19 5'/3' cDNA fragments FhMDR	43
Figure 20 CFP FhMDR full-length XhoI control digest.....	44
Figure 21 Vector map CFP FhMDR	44
Figure 22 N- or C-terminal CFP tagged FhMDR expressed in RNAi cells.	45
Figure 23 Western Blot with primary antibody against FhMDR.....	46
Figure 24 Viable cells gated in P1.....	48
Figure 25 Rhd123 accumulation	49
Figure 26 Rhd123 accumulation +Tar/GPV31/TCBZ.....	50
Figure 27 Rhd123 accumulation of CFP FhMDR +/- blocker.....	51
Figure 28 Amplification and cloning of FhepSLC6.....	52

Figure 29 Taurine dsMegaprimer for QuikChange (Mutagenesis).....	53
Figure 30 Bsu15I/Clal and EcoRI control digest after mutagenesis.....	53
Figure 31 N-terminally YFP tagged FhepSLC6	54
Figure 32 YFP FhepSLC6.....	55
Figure 33 Amplification and cloning of hTauT	56
Figure 34 Vector scheme of CFP hTauT.....	56
Figure 35 hTauT expressed in HEK293 cells	57
Figure 36 [³ H]-Taurine/[³ H]-GABA/[³ H]-Glycine/[³ H]-Glutamic acid uptake;.....	59
Figure 37 Saturation of [³ H]-Taurine uptake in siRNA knockdown cells.....	61
Figure 38 [³ H]-Taurine uptake related to temperature	63
Figure 39 Time dependent [³ H]-Taurine uptake.....	64
Figure 40 [³ H]-Taurine uptake referring to optimal conditions.....	65
Figure 41 Inhibition curves of different blockers	68

List of Tables

Table 1 Taxonomy of <i>Fasciola hepatica</i>	1
Table 2 3' and 5' primers for RACE for full-length sequence of FhMDR.....	23
Table 3 3' and 5' primers for RACE for full-length sequence of Fh_contig15063.....	24
Table 4 Ligation reaction.....	26
Table 5 QuikChange reaction pipetting.	28
Table 6 QuikChange PCR protocol.....	29
Table 7 Resolving gel/Stacking gel recipe.....	35
Table 8 Antibodies used for Western Blot.....	37
Table 9 List of [³ H] substances.....	40
Table 10 Blocking substances including serial dilution used for inhibition.	42
Table 11 Sample preparation for rhodamine123 accumulation assay.	47
Table 12 [³ H]-Dopamine, [³ H]- 5HT, [³ H]- MPP ⁺ one point uptake.....	60

Abbreviations

aa	Amino acid
ABC	ATP-binding cassette
ATP	Adenosine triphosphate
B _{max}	Maximal binding
bp	Base pair
CFP	Cyan fluorescent protein
CO ₂	Carbon dioxide
cpm	Counts per minute
ddH ₂ O	Double distilled water
DMEM	Dulbecco's modified Eagle Serum
DNA	Deoxyribonucleic acid
<i>E. coli</i>	<i>Escherichia coli</i>
EDTA	Ethylenediaminetetraacetic acid
EtOH	Ethanol
Fhsp/Fh	<i>Fasciola hepatica</i>
FACS	Fluorescence-activated cell sorting
FCS	Fetal calve serum
FMO pathway	Flavin monooxygenase pathway
FSC	Forward scatter
GABA	γ-amino butyric acid
GES	Guanidinoethyl sulphonate
GFP	Green fluorescent protein
HEK	Human embryonic kidney cells
hTauT	Human taurine transporter
K _d	Dissociation constant
kDa	Kilo Dalton
KHP	Krebs-HEPES buffer
K _m	Michaelis-Menten constant
LB medium	Lysogeny broth medium
MDR	Multi drug resistance
ml	Milliliter

mV	Mili Volt
NBD	Nucleotide binding domain
PBS	Phosphate buffered Saline
PCR	Polymerase chain reaction
PDL	Poly-D-lysine
P-gP	P-glycoprotein
RACE	Rapid amplification of cDNA ends
rhd123	Rhodamine 123
RNA	Ribonucleic acid
RT	Room temperature
SERT	Serotonin transporter
siRNA	Small interfering ribonucleic acid
SSC	Side scatter
TauT	Taurine transporter
TBS	Tris buffered saline
TBS-T	Tris buffered saline + Tween20
TCBZ	Triclabendazole
TCBZ.SO	Triclabendazole sulfoxide
TCBZ.SO ₂	Triclabendazole sulfone
TMD	Transmembrane domain
V _{max}	Maximal velocity
YFP	Yellow fluorescent protein

Abstract

Fasciola hepatica is an endoparasitic flatworm of the class Trematoda in the phylum Platyhelminthes. It is also known as the common liver fluke or sheep liver fluke for its eponymous action: the worm actively invades the liver and colonizes the bile duct of its end host. This infestation is referred to as fascioliasis. Beside its threat to human health, the infestation of livestock leads to large financial losses. As vaccinations against this parasite are not yet available, chemotherapy with anthelmintic drugs is the only way to currently control the disease.

The drug of choice against *Fasciola hepatica* infection is triclabendazole (TCBZ) marketed as Fasinex®. This benzimidazole derivative acts on all developmental stages within the end host- from the immature juvenile, to the juvenile and finally adult fluke. TCBZ is the only anthelmintic drug which is specifically available against this fluke.

During the last 20 years, resistance has emerged against triclabendazole in specimen isolated from cattle and sheep of various countries. Many hypotheses were put forth to address the mechanisms underlying resistance. An attractive explanation was provided by the discovery of an ATP binding cassette (ABC) transporter, which showed high homology to P-glycoprotein (P-gP) or MDR1 (multidrugresistance) of the ABC B transporter family. In this scenario, triclabendazole is a substrate for one or several fluke ABC transporters; their overexpression or mutation increases the efflux of triclabendazole.

In spite of its homology to mammalian orthologues of the B subfamily of ABC transporters, the reported *F. hepatica* ABC transporter was only a half-transporter, i.e., conceptual translation of the available sequence predicted 6 transmembrane helices and one nucleotide binding domain. Accordingly, it was of interest to explore the possibility that the published sequence was incomplete. In addition, it is likely that several transporters determine the ability of *F. hepatica* to survive in the hostile environment of the bile. Accordingly, it was reasonable to search for additional transporters. In fact, two full-length cDNAs were identified that encoded two different transmembrane transporter of *F. hepatica* – FhMDR and FhepSLC6. FhMDR is a member of the ATP-binding cassette transporter of the subfamily B. This assignment is based on its homology to the human P-glycoprotein (MDR1/ABCB1). I also attempted to examine the functional properties of heterologously expressed FhMDR using rhodamine123 as a fluorescent substrate. FhepSLC6 encodes a transmembrane transport protein with high homology to the human taurine transporter (SLC6). Thus, the substrate specificity of this transporter was also explored upon heterologous expression and compared to that of the human taurine transporter.

1 Introduction

1.1 *Fasciola hepatica*

1.1.1 Morphology and Taxonomy

Fasciola hepatica is also known as the common liver fluke. It is an endoparasitic flatworm of the class trematoda, which together with its close relative *Fasciola gigantica* cause an infestation, the disease fascioliasis which occurs all over the world preferentially in sheep and cattle. However, humans can also be end hosts and accordingly, these liver flukes are of medical relevance.

This liver fluke is classified as a member of the class Trematoda of the family Fasciolidae specified as *hepatica* based on its final destination within the definite host. The complete taxonomical classification is shown in Table 1.

Table 1 Taxonomy of *Fasciola hepatica*

(<https://www.msu.edu/course/zol/316/fheptax.htm>)

Taxonomy of <i>Fasciola hepatica</i>	
Kingdom	Animalia
Phylum	Platyhelminthes
Class	Trematoda
Subclass	Digenea
Order	Echinostomiformes
Family	Fasciolidae
Genus	<i>Fasciola</i>
Species	<i>hepatica</i>

The morphology of *Fasciola hepatica* is typical for its taxonomical classification: it has a leaf-shaped appearance averaging in length and width from 18-50 x 7-14 mm respectively (Fig. 1a) (Eckert *et al.*, 2008). According to its endoparasitic mode of life the mouthparts are characterized by a pharynx for food ingestion and powerful suckers, which are located orally and ventrally. These organs support the efficient attachment within the definite host and the

invasion of tissues en route to its final destination, namely the liver and more specifically the bile ducts.

(<http://web.stanford.edu/class/humbio103/ParaSites2001/fascioliasis/diagrams.htm>)

Liver flukes are hermaphrodites; each individual has two testes, an ovary and a cirrus pouch (i.e., a copulatory organ equivalent to a penis). Thus, self-fertilization can take place. However, cross-fertilization and gynogenesis have also been reported (Fletcher *et al.*, 2004). The Mehlis gland is a spherical organ, which is essential for egg shell formation. Its cross section varies around 1 to 1.5mm. The other reproductive organs such as ovary ducts and the vitellarium end within the Mehlis gland areas. Vitellaria are necessary for secreting and producing yolk to ensure nutrition of eggs and egg formation (Thorsell *et al.*, 1965).

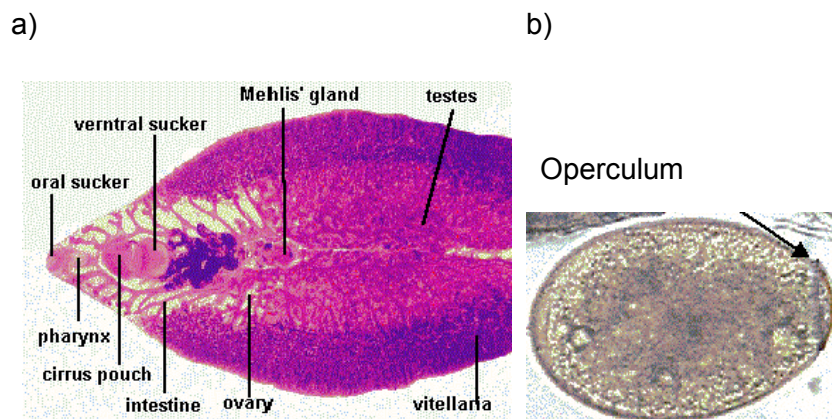


Figure 1 Adult *Fasciola hepatica* & egg

a) Representation of *Fasciola hepatica* to illustrate the morphology of adult *F.hepatica* including oral and ventral sucker up to reproduction organs. The presence of testes and ovary document the hermaphroditic nature of the fluke. b) *F.hepatica* egg with closed operculum labelled by arrow.

(<http://web.stanford.edu/class/humbio103/ParaSites2001/fascioliasis/diagrams.htm>)

1.1.2 Life Cycle

The life cycle of *Fasciola hepatica* includes free-living larval stages and developmental stages within an intermediate host (Fig. 2) (Dusak *et al.*, 2012): fertilized eggs (stage 1 in Fig. 2) leave the definite host via its faeces. On the soil, the miracidium (stage 3 in Fig. 2), the first free-living developmental stage of *F. hepatica* (length about 130 μm) escapes the egg through an operculum (Fig. 1b) with the help of its ocellum, a light-sensing organ: the recorded photon fluxes provides a signal to trigger hatching, which is only possible under wet

conditions. Once hatched, the miracidia rely on energy stores for surviving for 20 to 30 hours. They find their intermediate host, the water snail *Lymnaea (Galba) trunculata* (4 in Fig. 2) by chemotaxis. The snails prefer humid conditions and secrete glycoconjugates, which attract the miracidia. They attach to the epidermis of the intermediate host, which they actively penetrate by secreting proteolytic enzymes (Eckert *et al.*, 2008). In the snail, asexual reproduction and development proceeds from sporocysts via rediae to the infectious and mobile stage of cercariae (stages 4a, b and c, respectively, in Fig. 2), which are released from the digestive glands of the snail. Cercariae are endowed with a tail that propels them to find plants at the edge of the puddle, where they attach and encapsulate to form metacercariae (5 in Fig. 2). Metacercariae are ingested by ruminants when feeding on contaminated plants (6 in Fig. 2); humans are exposed to metacercariae by eating water cress (Sukhdeo *et al.*, 2003).

The low pH in the stomach triggers excystment of the metacercariae, which is completed in the duodenum: the released juvenile flukes (stage 7 in Fig. 2) invade the intestine wall, reach the peritoneal cavity and find the liver, where they start feeding on the parenchyma. After several weeks, the fluke eventually invades a bile duct and develops into the adult fluke (stage 8 in Fig. 2); the ensuing sexual reproduction completes the life cycle (Dusak *et al.*, 2012).

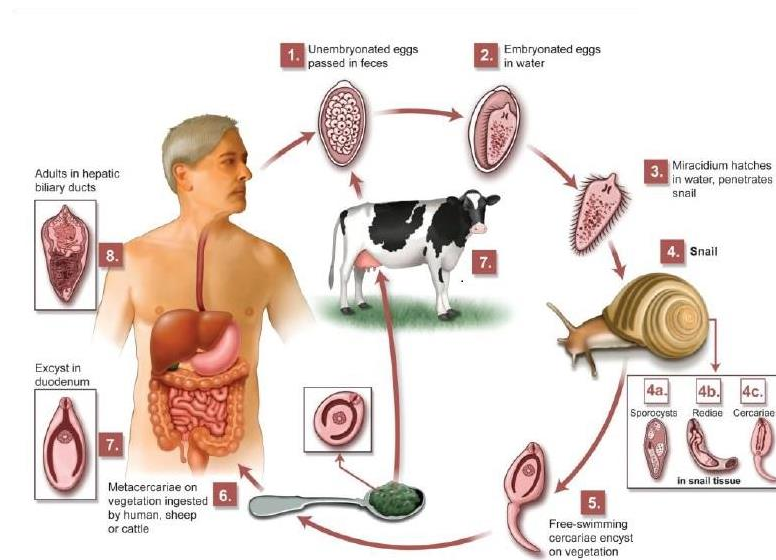


Figure 2 Life cycle of *Fasciola hepatica*:

Schematic view of the life cycle of *Fasciola hepatica* (Dusak *et al.*, 2012); for details see text.

1.1.3 Fascioliasis

Fascioliasis is the disease associated with *F. hepatica* infestation; the symptoms arise from the destruction of liver parenchyma and the inflammatory response triggered by the presence of worms in the bile ducts; they can vary from mild anemia to jaundice and cirrhosis.

Fascioliasis occurs mostly in cattle and sheep, but it also affects humans. Infestation of livestock has economic repercussions: financial losses result from a decrease in meat production and in milk output (Eckert *et al.*, 2008).

F. hepatica was known to have its original habitat in Europe but currently it can be found all over the world. This is presumably linked to the distribution of its main intermediate host. The range of the water snail *Lymnaea trunculata* is thought to have expanded at least in part due to changes in the global climate (Mas-Coma *et al.*, 2005).

Different species of this snail family can act as an intermediate host, but the mortality rates are high resulting in to a low number of shed cercariae. However, a high rate of livestock infestation was observed in France in the absence of the preferred intermediate host: this lead to the hypothesis that other snail species adapt to parasite load over several generations and thus act as the reservoir for infection; this conjecture was confirmed by experimental observations (Rondelaud *et al.*, 2014).

As reported by the WHO in 2006 the estimated number of human infections ranges from 2.4 up to 17 million cases worldwide. The disease is classified into different phases. The incubation phase is defined by the interval between ingestion of the metacercariae and the onset of symptoms. It is variable in length and can range from a few days up to months. As a result of the migration of juvenile flukes through the liver, holes and cavities are formed observed. The destruction of liver tissue can lead to intense internal bleeding, inflammation, abscesses and fibrosis which are defined as the acute phase of fascioliasis (Dusak *et al.*, 2012). Necrotic tissue eventually leads to scarring (Fig. 3a/b). Other symptoms, which are observed in patients within this acute phase, include abdominal pain, fever and jaundice lasting up to 2 to 4 months (WHO, 2006). The latent phase of infestation with *F. hepatica* corresponds to the colonization of the bile ducts by the flukes. It can be asymptomatic. Within the bile duct, flukes start to mature and start producing and laying eggs.

The manifestation of the disease is obviously determined by the dose of ingested metacercariae by the definite host, because the final parasite load with adult flukes is linked to the number of larvae that invade the intestinal wall (Eckert *et al.*, 2008). Interestingly, the host range of *F. hepatica* is limited. Many candidate end hosts, which come into contact with contaminated plants (e.g., pigs and dogs), are resistant. The mechanism for this naturally occurring resistance remains unclear.

The infestation is diagnosed non-invasively by detecting the eggs of *F. hepatica* eggs in the faeces or by immunological techniques such as enzyme-linked immunosorbent assays (ELISA) to detect anti-fluke antibodies (Eckert *et al.*, 2008) or to determine immunoglobulin E levels within the patient's plasma typical for worm infection (Trifina *et al.*, 2011).

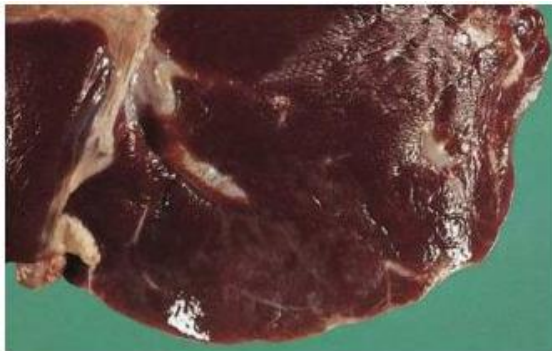
While juvenile stages migrate through liver parenchyma intracellular enzymes as Serum aspartate aminotransferase (AST), alanine aminotransferase (ALT) and glutamate dehydrogenase (GLDH) levels are increased within the patient's serum.

Adult stages of *F. hepatica* can be detected by increased serum levels of gamma-glutamyl transpeptidase (GGT) released in necrotic bile ducts.

Infestations of adult stages of *F. hepatica* are also characterized by decreased levels of erythrocytes and degradation of muscle protein. As a consequence, patients suffer from anemia and disorders in growth development (Eckert *et al.*, 2008; Dusak *et al.*, 2012).

Besides biochemical and immunological approaches, medical imaging techniques are further used in detection of *F. hepatica* infection in humans – ultrasonography (US), magnetic resonance imaging (MRI) computed tomography (CT) (Dusak *et al.*, 2012; Trifina *et al.*, 2011).

a)



b)



Figure 3 *Fasciola hepatica* infected liver of sheep or cattle

a) sheep liver with chronic fascioliasis showing thickened bile ducts and fibrosis of the liver parenchyma; b) chronic fascioliasis in cattle also showing thickened and necrotic bile ducts

1.1.4 Triclabendazole and increasing resistance

The drug of choice used in *F. hepatica* infection is Triclabendazole, marketed as Fasinex®. It has been used for therapy in cattle (12mg/kg bodyweight) and sheep (10mg/kg bodyweight) since the early 1980s successfully. Nowadays this anthelmintic drug plays a major role in treatment of humans. Triclabendazole enters the fluke via diffusion and is rapidly metabolized within the patient. Major advantage of this anthelmintic drug is the ability to affect all developmental stages of *Fasciola hepatica* occurring within the definite host – from the early immature, the juvenile and the adult stages (Fairweather, 2009).

Over the last years an increasing number of flukes resistant to Triclabendazole have been reported. Thus, it is important to address possible mechanism involved in increasing resistance to TCBZ and investigate appropriate modulators for it (Wilkinson *et al.*, 2012).

The parent drug Triclabendazole cannot be detected in plasma levels after oral medication within the treated patient (cattle or human). This phenomenon is linked to rapid metabolism into the compounds TCBZ sulfoxide and TCBZ sulfone (Fig.4) via the flavin monooxygenase (FMO) pathway (Barrera *et al.*, 2012; Brennan *et al.*, 2007).

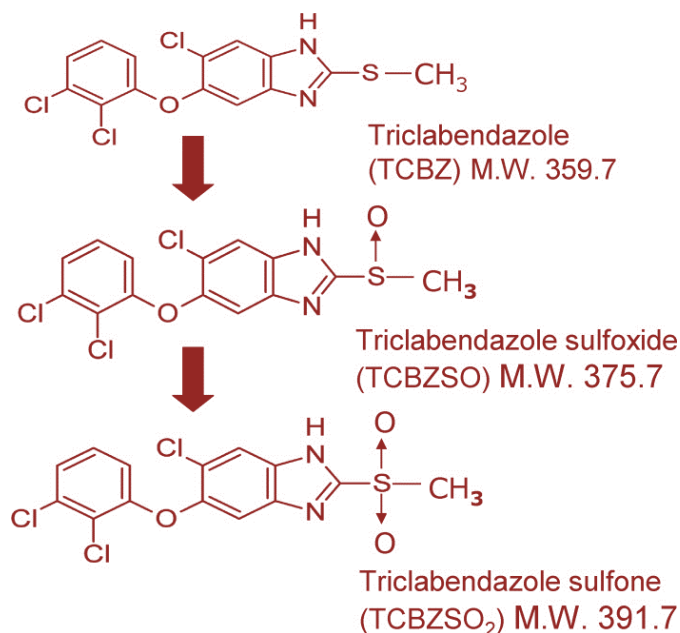


Figure 4 Triclabendazole and its metabolites.

Chemical structures of the parent drug triclabendazole (TCBZ) and the metabolites triclabendazole sulfoxide (TCBZ.SO) and triclabendazole sulfone (TCBZ.SO₂) including molecular weight (Barrera *et al.*, 2012).

FMO is the main enzymatic pathway involved in the sulfoxidation of triclabendazole. Metabolic studies were carried out on microsomal TCBZ and TCBZ.SO in the presence of appropriate enzyme inhibitors or substrates for either FMO or cytochrome P450. Thus, involvement of these two pathways in the biotransformation of TCBZ was investigated. Experimentally generated data were statistically analyzed. These results indicate FMO as the major key player in TCBZ metabolism. Nevertheless the cytochrome P450-dependent pathway also contributes to this metabolism ("ratio FMO/P450 = 3.83+/- 1.63 nM of metabolic products formed per min/mg") (Virkel *et al.*, 2006).

The proposed mechanism of anthelmintic action of TCBZ arises from its structural relation to other benzimidazoles. These are known to bind to β -tubulin and to interfere with microtubule formation (Brennan *et al.*, 2007). A microtubule-directed mode of action of TCBZ was substantiated by direct observations. TCBZ and TCBZ.SO disrupt and severely damage the tegumental layer and have an inhibitory effect on mitotic spindle apparatus (reviewed in: Wolstenholme *et al.*, 2004). The effect of TCBZ.SO on the tegumental layer has been investigated by transmission electron microscopy on either intact flukes or tissue-slices (Stitt *et al.*, 1994).

Over the years of treatment with TCBZ, resistant flukes have emerged. Drug resistance can be accounted for by mutations in the target proteins or by one or several of processes, which lead to reduced concentrations of the drug in the organism. Against expectations increase in resistance to TCBZ is not associated with mutations of β -tubulin encoding genes: susceptible and resistant fluke populations do not differ in the coding sequence (Wolstenholme *et al.*, 2004).

In contrast, there is circumstantial evidence for increased metabolism of the drug, decreased uptake or increased export (Jones *et al.*, 2005).

The influx/efflux rate of TCBZ was shown to be modulated by another antiparasitic drug, ivermectin. As this substance is a substrate of ABC transporters it is speculated that this family of proteins is involved in the development of resistances (Mottier *et al.*, 2006). A partial sequence of the cDNA of *F. hepatica* could be identified showing high homology to the MDR1 (multidrugresistance), a member of the B subfamily of ABC transporters (Reed *et al.*, 1998). Further, many different ABC transporter orthologues have been found in helminths. Circumstantial evidence indicates that this may be true in fasciolidae: adult flukes of *Fasciola gigantica* express proteins that cross-react with antibodies recognizing mammalian multidrug resistance-associated protein1 (MRP1), breast cancer resistance protein (BCRP) or bile salt export pump (BSEP) (Kumkate *et al.*, 2008). Experimental designs with overexpressed P-gP in *Trypanosoma brucei* supports the hypothesis that P-gP plays a crucial role in upcoming resistance (Kerboeuf *et al.*, 2003).

1.2 ATP-binding cassette (ABC) transporters

1.2.1 Introduction

The ATP (adenosine triphosphate) -binding cassette (ABC) transporter family is classified as one of the largest members of transmembrane transport proteins occurring in all species from microbe to man (Higgins, 2001).

These integral membrane proteins are able to transport specific substrates across the lipid bilayer in both directions. Energy necessary for this transport process is provided by the hydrolysis of ATP. While import function of ABC transporters is exclusively found in prokaryotic organism (Fig. 5 A), exporters are present in prokaryotes and eukaryotes (Fig. 5 B). Importers guarantee the uptake of essential nutrients, while exporters can detoxify the cell. This feature leads to issues in chemotherapeutic treatments (e.g. cancer therapy) as the human P-glycoprotein mediates multidrug resistance by export of drugs used in cancer treatment (Rees *et al.*, 2009).

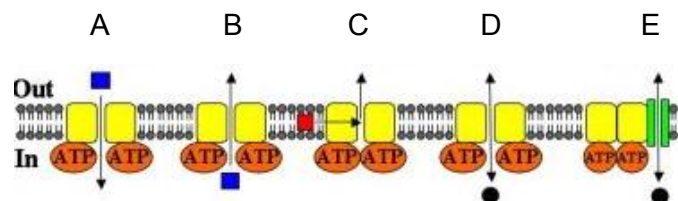


Figure 5 Schematic overview of ABC transporter function

A) Importers (only found in prokaryotes) B) Exporters C) direct export out of phospholipid membrane D) CFTR (Cystic Fibrosis Transmembrane Conductance Regulator) acting as ion channel E) SUR (sulphonyl urea receptor)-type: channel regulating function (Figure adapted by Loo *et al.*, 2008).

In humans 48 different ABC proteins have been identified which play an important role in physiological processes and are linked to different diseases (Loo *et al.*, 2008). Furthermore, they are supposed to be targets in medical and pharmacological implications (Higgins, 2001). The human proteins are divided into seven subfamilies from A to G based on phylogenetic analysis (Sharom, 2008). Classification is shown in the adapted Fig.6 including a prominent representative of each class.

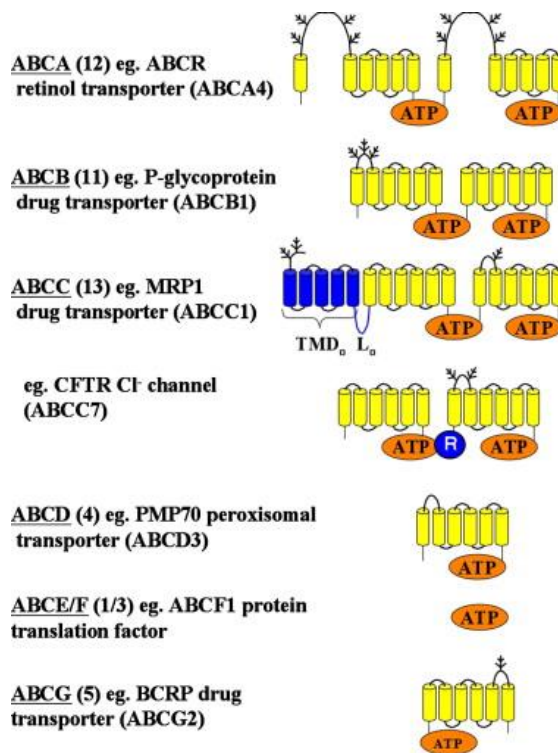


Figure 6 Structure based classification of the human ABC transporters.

7 classes of the human ATP-binding cassette transporter from A to G represented by one characteristic member and basic structure of each class; NBDs are outlined as orange ovals; the transmembrane spanning parts (TMDs) are shown via yellow cylinders. Additional domains are represented in blue (Figure adapted from Loo *et al.*, 2008).

Based on the first full-length sequence of the periplasmic histidine transporter of *Salmonella typhimurium*, which guarantees nutrient uptake, further investigations have been carried out to explore the physiological importance of this transport system (Higgins *et al.*, 1982). Simultaneously the maltose transporter (MalK) in *E. coli* was identified. Observed sequence similarities of these two transporters led to the hypothesis of a common mechanism and ancestor (Gilson *et al.*, 1982).

1.2.2 Basic structure & mode of action

Basic structure and mode of action of ABC exporters have been analyzed and studied based on the determined crystal structure of the isolated bacterial ABC transporter of *Staphylococcus aureus* termed as Sav1866 (Fig. 7). This bacterial ABC transporter shows significant sequence homology to human ABC multidrug transporters of the B subfamily including MDR1 (P-glycoprotein/ABCB1) (Dawson *et al.*, 2006).

ABC transporters consist of a typical core structure found in all families. This includes transmembrane domains (TMDs) consisting of 6 transmembrane spanning helices and nucleotide binding domains (NBDs). Transporters that possess two TMDs and NBDs are defined as full-transporters, those with just one NBD and TMD as half transporter. TMDs contribute to the binding and transport of substrates through the lipid bilayer (Higgins *et al.*, 2004). The variability of the TMDs within their primary sequence length and architecture indicates that these bilayer-spanning helical structures act as adjunct modulators in insertion and regulation rather than playing a crucial role in core function (Higgins, 2001).

The second core domain of ABC transporters is the eponymous cytoplasmic ATP-Binding-Cassette, also termed nucleotide-binding domain (NBD). This highly conserved region binds and hydrolyses ATP via characteristic encoded sequences (Loo *et al.*, 2008).

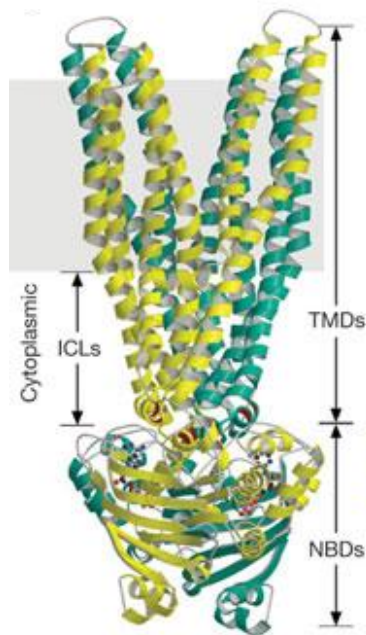


Figure 7 Sav1866 crystal structure

Backbone of the homodimeric ABC transporter Sav1866 (*Staphylococcus aureus*): subunits are represented in yellow/green; bound ADP is demonstrated via red dots (Figure adapted from Dawson *et al.*, 2006).

Detailed view on isolated crystal structures of NBDs - also known as the motor domains of this transporter family - demonstrate how ATP binding and hydrolysis are accomplished (Hollenstein *et al.*, 2007). The NBDs are arranged in a conserved head-to-tail fold showing

the conserved motif sequences at their shared interfaces. This formation results in the generation of two possible binding sites for ATP due to the interaction of the Walker-A motif (P-loop) of NBD1 and the LSGGQ signature sequence (C-loop) of NBD2. Once ATP is bound and keeps in touch with the ABC signature motif further processing can be performed. The Walker-B motif recognizes bound ATP and provides hydrolysis via a conserved glutamate residue by a “nucleophilic attack” of a water molecule. The Q-loop is further thought to be involved in contacting the TMD via its γ -phosphate of the functional group. Finally the main catalytic reaction is performed by the histidine group of the switch-motif (Hollenstein *et al.*, 2007).

1.2.3 P-glycoprotein / MDR1 / ABCB1

P-glycoprotein (P-gP)/MDR1/ABCB1 is a member of the ABC transporter B subfamily. The human B family consists of 11 genes encoding four full-transporters and seven half-transporters. It is involved in detoxification of cells and multidrug resistance (Vasilidou *et al.*, 2009).

P-glycoprotein was the first cloned and fully sequenced mammalian ABC transporter (Chen *et al.*, 1986) and is used as the prototype of this family. Due to low substrate specificity (e.g. transport of many cytostatic drugs), P-gP is a transporter of high clinical relevance.

The *mdr1* gene is located on chromosome 7q21, it consists of 28 exons and encodes 1,280 amino acids (aa). P-gP has a molecular weight of approximately 170 kDa (Sarkadi *et al.*, 2006).

Overexpression of P-gP in tumors correlates with multidrug resistance due to active efflux of chemotherapeutic drugs as anthracyclines (doxorubicin, daunorubicin), taxanes (paclitaxel) and vinca alkaloids (vincristine, vinblastine) (Dean *et al.*, 2001).

The ABC B family also includes transporters which are localized within the liver as ABCB4 and ABCB11 which is especially involved in bile acid secretion as the major bile salt export pump (BSEP) (Dean *et al.*, 2001).

1.3 Solute carrier 6A6 (Taurine transporter)

1.3.1 The taurine transporter (SLC6A6)

The solute carrier 6 gene family, or also termed as sodium/chloride (Na^+/Cl^-) dependent transporters, represents one of the largest groups of the solute carrier superfamily. Accordingly, the SLC6 family is subdivided into four classes based on sequence similarities and substrate specificity (Fig. 8) (Kristensen *et al.*, 2011): a) the monoamine transporter branch with the prominent representatives: dopamine (DAT), norepinephrine (NET) and serotonin (SERT) transporter, b&c) amino acid transporters I including glycine transporters (GlyT) and II, and d) the gamma-aminobutyric acid (GABA) transporters including the taurine transporter (TauT/SLC6A6) (Bröer *et al.*, 2012).

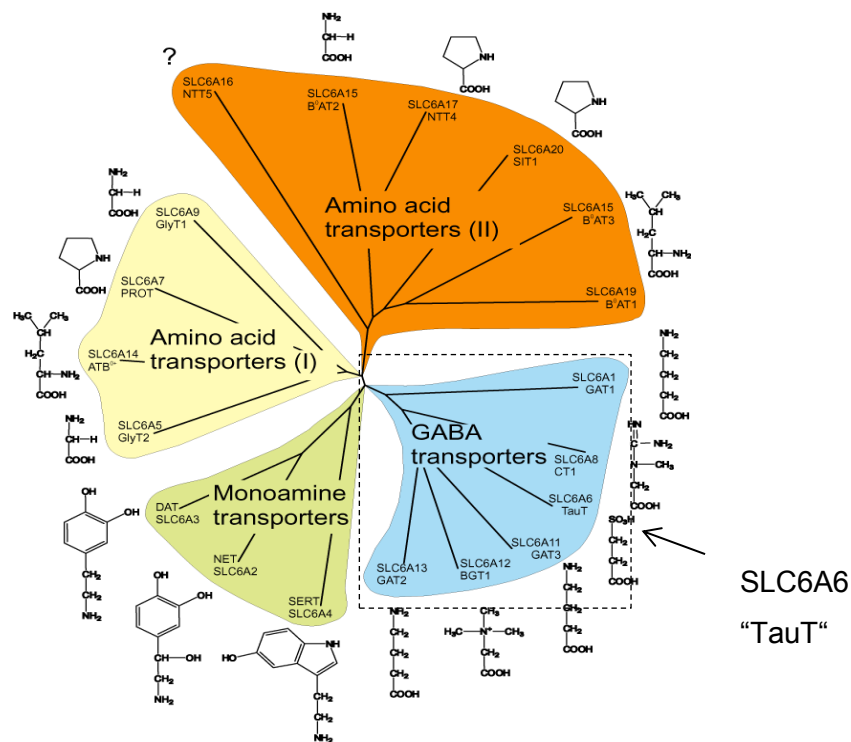


Figure 8 SLC6 transporter families and their sequence similarities

Schematic view on the 4 subfamilies of the SLC6 transporters : amino acid transporter I&II, monoamine transporters (DAT, NET, SERT) and GABA transporters outlined with the dashed square to point out the membership of SLC6A6 (taurine transporter) to this branch (Bröer *et al.*, 2012).

TauT is characterized as a high-affinity, low-capacity transporter that tends to be highly selective for β -amino acids (Anderson *et al.*, 2009) and is highly distributed throughout the tissue (Kristensen *et al.*, 2011).

The gene coding for the human taurine transporter is localized on chromosome 3 p24→p26. It encodes a 2864 bp long mRNA with a coding region of 1860 bp (Ramamoorthy *et al.*, 1994).

The taurine transporter shows the same structure as other Na^+/Cl^- coupled transporters of the SLC6 transporter family. It consists of 12 transmembrane spanning domains with intracellularly located N- and C-termini. Two potential N-glycosylation sites are present within the second extracellular hydrophilic loop. One potential phosphorylation site is present in the fourth intracellular loop and another four are located at the C-terminus (Fig. 9) (Uchida *et al.*, 1992).

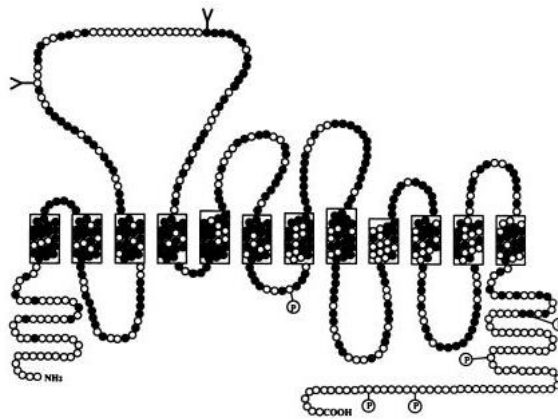


Figure 9 Schematic membrane topology of hTauT

This adapted figure is a proposed model of the membrane topology of the human taurine transporter. It consists of 12 transmembrane spanning domains; N- and C-terminus are located intracellularly. Each black dot represents amino acids, which are identical to betaine and GABA transporters. Y represents N-glycosylation sites and P potential phosphorylation sites (Uchida *et al.*, 1992).

Similar to other members of the SLC6 transporter family which display electrogenic transport, the transport mediated by TauT is also electrogenic and coupled to Na^+ and Cl^- (Miyasaka *et al.*, 2001). Translocation of one taurine is associated with the transport of two Na^+ and one Cl^- molecule across the plasma bilayer (Fig. 10) (Han *et al.*, 2006; Zelikovic *et al.*, 1989).

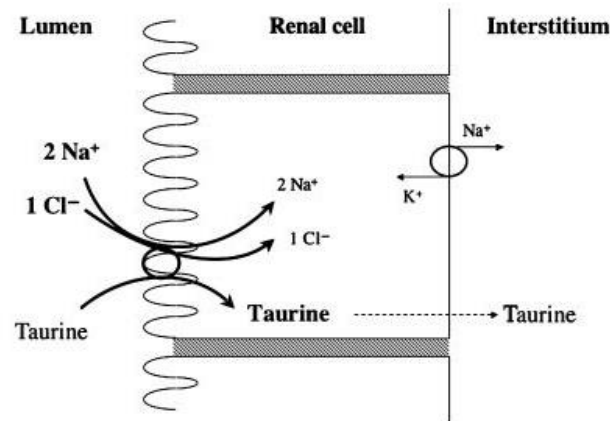


Figure 10 Schematic model of taurine transport and indicated Na⁺/Cl⁻ exchange.

This schematic representation shows a tubular epithelial cell of the kidney, where the taurine transporter resides in the apical (=luminal) membrane: the translocation of one taurine is accompanied with 2 Na⁺ and one Cl⁻ molecule (Figure adapted from Zelikovic *et al.*, 1989).

1.3.2 Taurine

Historically the first discovery of taurine dates back from findings of Tiedemann and Gmelin where they describe a newly isolated compound of ox (*bos taurus*) bile initially termed as bile-asparagine (Jacobsen *et al.*, 1968).

Taurine (2-aminoethane-sulfonic acid) is characterized as one of the most abundant β -amino acids or organic osmolytes found in a wide range within the whole body and is found in a non-bound state within intracellular water (Han *et al.*, 2006). It is involved in many physiological processes such as maintenance of osmolarity, membrane stabilization or detoxification (Satsu *et al.*, 2003). Taurine also plays a crucial role in other physiological processes as conjugation of bile salts and in developmental processes in ocular tissues. Biosynthesis of endogenous derived taurine is performed from bioconversion of the amino acids methionine or cysteine. Initially cysteine dioxygenase (CDO) provides transformation of cysteine to cysteine sulphinic acid (CSA) followed by a decarboxylation of CSA to hypotaurine which is mediated by CSA decarboxylase. In a final step, taurine is obtained non-enzymatically by oxidation of the precursor hypotaurine (Fig. 11 B) (Tsuboyama *et al.*, 1996).

Not all mammals are capable of synthesizing enough taurine by themselves. Cats are not able to synthesize appropriate amounts of taurine. Therefore, the dietary uptake has to be guaranteed. Taurine deprived diet of cats leads to severe damage on photoreceptors and retinal pigment epithelium (Schmidt *et al.*, 1976).

Taurine is also known as non-essential or semi-essential amino acid as, for example, newborn mammals lack in the ability of biosynthesis of taurine from cysteine or methionine on their own. Thus, dietary supplementation is necessary. Human infants obtain their intake by human breast milk, which provides a high level in taurine (40 μ mol per 100ml) (Lambert *et al.*, 2014).

The complete mammalian taurine level is a balanced composition of taurine bioconversion of cysteine and/or methionine, dietary uptake and either absorption or reabsorption via intestine or kidney respectively (Lambert *et al.*, 2014).

Taurine lacks the carboxyl group characteristic for proteinogenic amino acids. It is therefore not involved in protein biosynthesis (Ripps *et al.*, 2012). A sulfonate group (Fig. 11 A) substitutes the missing carboxyl group (Ripps *et al.*, 2012). This sulfonate group is characterized by strong acidity. The acidic dissociation constant (pKa) of 1.5 of taurine is equivalent to the pKa of hydrochloric acid (Huxtable, 1992).

Within the liver, primary bile salts as cholate or chenodeoxycholate derived from cholesterol are conjugated with either taurine or glycine. Due to this conjugation, micelles can be formed which is important for providing secretion of these conjugated bile salts to the bile (Silbernagl *et al.*, 2003)

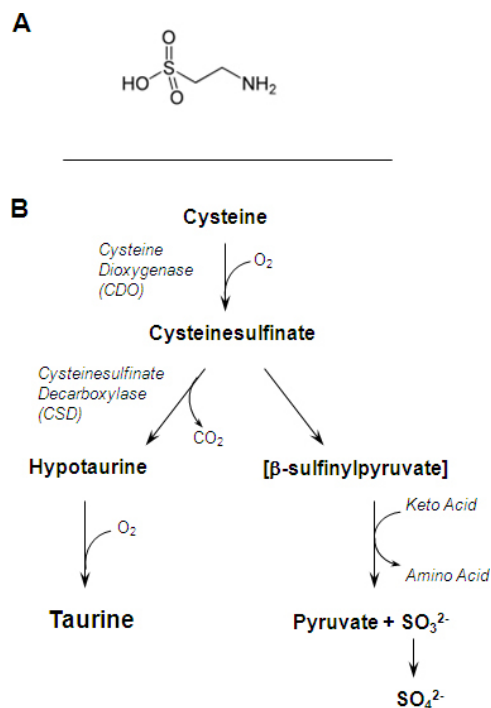


Figure 11 Structure and biosynthesis of taurine.

A) Chemical structure of Taurine; B) Conversion of cysteine to hypotaurine is provided enzymatically; hypotaurine is oxidized to taurine. Further details: see text (Figure adapted by Ripps *et al.*, 2012).

1.4 Aim of the study

The liver fluke *Fasciola hepatica* is one of the most important parasites affecting livestock's health all over the world, causing the liver fluke disease fascioliasis. During recent years it became a major risk factor in humans as well. Nowadays *Fasciola hepatica* and the linked disease can be found worldwide due to a high distribution of the intermediate host *Lymnaea trunculata*.

Triclabendazole (TCBZ) is for unknown reasons the only anthelmintic drug specifically acting against *Fasciola hepatica* infection. The flukicidal effect on all developmental stages which occur in the definite host is the major benefit of this drug.

During the last decades an emerging number of resistant flukes have evolved. Accordingly many hypotheses were put forth on putative modulators and key players in increasing resistance to Triclabendazole. Based on a published partial ABC transporter sequence in *Fasciola hepatica*, which shows high homology to the human multidrugresistance transporter MDR1 (or P-glycoprotein), this transport system seemed to be the most promising key player. ABC transporters are known to provide active export of complex macromolecules. Thus, it was suggested that the *F. hepatica* MDR is able to actively efflux triclabendazole (TCBZ) leading to resistances of the flukes.

Recently, anthelmintic drugs were shown to interact with homologues of P-glycoprotein/MDR1/ABCB1 in other helminthic parasites e.g., the anti-schistosomal drug praziquantel with SMDR2, a homologue of ABCB1 (Kasinathan *et al.*, 2010).

Different ABC transporters were also identified by immunoblot using human antibodies in *Fasciola gigantica*, which is a close relative to *Fasciola hepatica* (Kumkate *et al.*, 2008).

Due to little information about the mechanisms of ABC transporters in *Fasciola hepatica*, it was therefore interesting to obtain and characterize the full-length cDNA of FhMDR for further cloning, expression and functional analysis.

I also identified and amplified a full-length cDNA of a second transmembrane transporter which shows high homology to the SLC6 superfamily, specifically to the human taurine transporter (SLC6A6). Although multidrug resistance to TCBZ is not supposed to be linked to the taurine transporter, it might represent an alternative drug target for the treatment of fascioliasis.

The aim of this study was to obtain the full-length sequences of two transmembrane transporters of *Fasciola hepatica* (FhMDR and FhepSLC6) and their functional characterization:

- Obtain and amplify full-length cDNA sequences (FhMDR/FhepSLC6).
- Establishment and expression of transporters within a mammalian model system (HEK293 cells).
- Verification of localization within the model system by fluorescence microscopy.
- Functional analysis of FhMDR by established assays for human P-gP (FACS based rhodamine123 assay) in order to test a putative interaction with triclabendazole
- Characterization of FhepSLC6 using general pharmacological assays (Uptake and inhibition assays).

2 Material and Methods

2.1 Materials

2.1.1 Standard solutions/buffers

TSS buffer (chemical competent <i>E. coli</i>)	
Trypton	1 %
Yeast Extract	0.5 %
NaCl ₂	100 mM
Polyethylenglycol (PEG)	10 %
DMSO	5 %
MgCl ₂	50 mM
pH	6.5

LysoGeny Broth medium (LB)	
NaCl ₂	10 %
Peptone	10 %
Yeast extract	5 %
ddH ₂ O	appr.vol

50x Tris acetate EDTA buffer (TAE)	
TRIS	2 M
Acetic acid	1 M
EDTA	50 mM
ddH ₂ O	appr.vol

RIPA (Radio-Immunoprecipitation Assay) buffer	
Tris-HCl (pH 7.4)	10 mM
NaCl ₂	150 mM
EDTA	1 mM
Triton-X 100	1%
SDS	0.1 %

1x SDS sample (loading) buffer (SB)	
Tris pH 6.8	62.5 mM
SDS	2 %
Glycerol	10 %
Betamercaptoetanol	5 %
Bromophenol Blue	0.01 %

10x SDS Page Running Buffer	
TRIS	250 mM
Glycine	1920 mM
EDTA.Na ₂	1 mM
SDS	1.75 mM

10x Tris Buffered Saline (TBS) / 0.1 %T	
TRIS	200 mM
NaCl ₂	1500 mM
(Tween-20)	1g/l [0.1%]

10x electron transfer buffer (TB²)	
TRIS	250 mM
Glycine	1920 mM

1x Krebs-HEPES Buffer (KHP)	
HEPES	10 mM
NaCl ₂	120 mM
KCl (Merck)	3 mM
CaCl ₂ x 2 H ₂ O (Merck)	2 mM
MgCl ₂ x 6 H ₂ O (Merck)	2 mM
α-D-(+)-Glucose-monohydrate (Roth)	20 mM
pH	7.3

5x Poly-D-lysine	
Poly-D-lysine (Sigma)	25 mg
ddH ₂ O	ad 100 ml

1x PBS (Phosphate Buffered Saline)	
KCl	2.7 mM
KH ₂ PO ₄	1.5 mM
NaCl	137 mM
Na ₂ HPO ₄ x 2H ₂ O	4.3 mM
pH	7.3

2.2 Methods

2.2.1 Cloning

2.2.1.1 RNA Isolation from tissue and cells using TRI Reagent[®]

Liver flukes were isolated from livers of slaughtered cows by Dipl-TA Mag. Franz Plank at "Schlachthof Berger" (Eschenau, Austria). RNA was extracted from whole fluke tissue using TRI Reagent[®] (Sigma-Aldrich), according to the manufacturer's recommendations.

Fluke tissue was homogenized in TRI Reagent[®] (1ml per 100mg tissue) at 4°C using an ultra-turrax dispersing instrument (Janke&Kunkel IKA-WERK). Samples were kept at room temperature (RT) for 5 minutes to allow the complete dissociation of nucleoprotein complexes. 0.2 ml CHCl₃ per 1 ml of TRI Reagent[®] were added and mixed gently for 15 seconds. After an additional incubation of 2-15 minutes at RT the mixture was centrifuged for 15 minutes at 12,000 x g at 4°C (Centrifuge 5415R Eppendorf). The solution was separated via this centrifugation step into three different phases. The upper (aqueous) phase containing RNA, the interphase DNA and the red (organic) phase protein.

The aqueous, RNA containing, phase was carefully transferred to a new reaction tube and 0.5 ml of 2-propanol per 1 ml of TRI Reagent[®] were added to precipitate the RNA. After additional 10 minutes incubation at RT the sample was centrifuged at 12,000 x g, for 10 minutes at 4°C. The precipitated RNA became visible as a slightly white or even transparent pellet depending on the purity of the RNA precipitate.

The remaining supernatant was removed and the pellet was washed once with 1 ml 75% EtOH per 1 ml TRI reagent[®] used in tissue preparation.

After vortexing and centrifuging at 7,500 x g for another 5 minutes at 4°C the remaining RNA pellet was completely air dried and finally dissolved in an appropriate volume of double distilled (dd) H₂O.

RNA content was measured using NanoPhotometer (Implen GmbH). Final RNA preparation should be free of DNA and protein indicated by a A_{260}/A_{280} ratio higher than 1.7.

In addition to fluke tissue, RNA was also isolated from monolayer cells, according to the manufacturer's recommendations as well.

2.2.1.2 Rapid amplification of cDNA ends (RACE)

Rapid amplification of cDNA ends was performed using either 5'/3' RACE Kit, 2nd Generation[®] (Roche Diagnostics GmbH) for 5' RACE or Transcriptor High Fidelity cDNA Synthesis Kit (Roche Diagnostics GmbH) for 3' RACE according to the manufacturer's recommendations.

Primer design was based on published (partial) sequences of *Fasciola hepatica* MDR and *Fasciola hepatica* SLC6 (Fh_contig15063) respectively (see Table 2/Table 3). Primers were synthesized by Microsynth (Balgach, Switzerland). The procedure was repeated until full-length sequences of the transporters were identified. Full-length cDNAs of the open reading frames (ORF) were generated by PCR and cloned into mammalian expression vectors (see section 2.2.1.6).

Table 2 3' and 5' primers for RACE for full-length sequence of FhMDR

RACE of FhMDR was performed in both directions using the listed primers. Name of primers are adapted from their storage name; Primer design by Dr.Oliver Kudlacek and generated by Microsynth.

5'/3' RACE primers FhMDR	
FHepATP RACE 1	5' - CAG CTT GTG CCA GTT CCG -3'
FHepATP RACE 2	5' - AAC GCG ACC GCG ATC C -3'
FhepATP RACE 3	5' - AAC CAC AAT GCG ATC AGC -3'
RACE4	5' - TTG AAA GAA TGA TTC TGG TTT C -3'
RACE5	5' - GAC ACT TGT CAA CTG GAG G -3'
RACE6	5' - CAA TGA TTT CAA AAA CAT GAT G -3'
RACE7	5' - AAT GAG ACA TCT TGA AAC CG -3'
RACE8	5' - AAG GAA CAT GCT GCC AAT G -3'
RACE9	5' - AGG AAT ACC AGA ATG ACA G -3'
RACE 10	5' - AGT ACC GGC ATC ATA TTC G -3'
RACE 11	5' - CTT CTT CAG CAA TAG CAC TA -3'
RACE 12	5' - TAA GCG AGA GAT TCT TTT CTG -3'
RACE 13	5' - CTG AAG TAA CGT GTC AAA CC -3'
RACE 14	5' - CCA CCG AAT GAA CCG AAT G -3'

Table 3 3' and 5' primers for RACE for full-length sequence of Fh_contig15063

3' and 5' RACE was performed via listed primers (name adapted from their storage names) on isolated fluke RNA. Primer design was performed by Dr. Oliver Kudlacek and generated by Microsynth.

5'/3' RACE primers Fh_contig15063 (FhepSLC6)	
TaurinRace1	5'- CTGCTCGAACCAATAGGA -3'
TaurinRace2	5'- CTGGTTGCTGTCACATAC -3'
TaurinRace3	5'- CCGGACGTTTTGATCCC -3'
TaurinRace4	5'- TAGCTTGTTTTCTTGTTGG -3'
TaurinRace5	5'- GGTCACAGAGGGTGGTA -3'
Tau Trace 6	5'- TTG AAA ATA CAA AGG AAC -3'

2.2.1.3 Polymerase Chain Reaction (PCR)

Polymerase Chain Reaction was performed using Expand High Fidelity^{PLUS} PCR System, dNTPack[®] (Roche Diagnostics GmbH) or High Fidelity Enzyme Mix[®] (Fermentas). Both kits contain all components necessary to set up PCR reactions except for the forward and reverse primers which were designed according to the amplicon of interest. Primer design was performed by Dr. Oliver Kudlacek and synthesized by Microsynth.

PCR enables smallest amounts of specific DNA sequences to be enzymatically amplified using complementary DNA oligo.

PCR is performed in three repeated steps, including denaturation, hybridization of the primers (annealing) and DNA synthesis (elongation) using a Thermal Cycler (model:TC-34/H(b) provided by BIOER technology co, LTD or Multigene (model: multigene gradient) by Labnet International, Inc).

Standard PCR reactions include 50 to 100 ng of dsDNA, 250nM of forward and reverse primer, 1x PCR buffer, dNTP mix [200µM each] and a heat stable polymerase to synthesize the new strand of the DNA helix. The standard reaction conditions were optimized for each reaction by varying MgCl₂ concentrations or adding DMSO to increase reaction efficiency. Annealing temperature and elongation time were calculated for each reaction. Annealing temperature is related to the length and the GC content of designed primers while the elongation time correlates to the size of the amplicon and velocity of the polymerase (usually 0.5-1 min per kb).

2.2.1.4 Amplification of full-length cDNA

After identification of full-length sequences, cDNA was amplified in order to clone the coding region of the various transporters into mammalian expression vectors. Reverse transcription was performed using “Transcriptor High Fidelity cDNA Synthesis Kit (Roche Diagnostics GmbH)”, according to the manufacturer’s recommendations. 1 µg of RNA and oligo-dT primers were used. FhMDR was cloned in two steps and restriction sites were introduced via specific primers.

Primers used:

For FhMDR: 5' fragment: MDR fw YFP-N1 (5'- GCG CAA GCT TCG ATG CGA TGG AAA CGT CC-3') and MDR KspI rv (5'- AAT GCC ATA ATC CCC GCG G -3').

For 3' fragment: Fhep ATP YFP rv (5'- GCG CGG ATC CTA CAG CTC ATT AGC TTG-3') and Fhep ATP YFP fw (5'- GCG CAA GCT TCG ATG GTC GCG CAT CGT TTG TC-3')

For FhepSLC6: Taurin ATG fw (5'- GCG CCT CGA GCC ATG CGC CAG GAA TTC AGT TTC -3') and Taurin stop rv (5'- GCG CGG TAC CTA ATT CAA ATT ATT TGA TGT TGA -3')

For human taurine transporter (hTauT): hTAUTfw (5'- GCG CAA GCT TCG ATG GCC ACC AAG GAG AAG -3') and hTAUTrv (5'- GCG CGG ATC CTC ACA TCA TGG TCT CCA CA - 3').

For the fusion of C-terminal fluorescent proteins, primers removing the Stop-codon were used as reverse primers MDR fw YFP-N1 (5'- GCG CAA GCT TCG ATG CGA TGG AAA CGT CC-3') for PCR.

The PCR products were cloned to the expression vectors using the introduced restriction sites: FhMDR HindIII, KspI and BamHI, FhepSLC6 XhoI and KpnI and hTauT HindIII and BamHI.

Amplification was performed running 10 cycles at 55°C (to add the new restriction sites) and 40 cycles at 58°C annealing temperature. Elongation time was set up to 2'30 sec according to the ability of the polymerase to synthesize 1 kb within 1 minute.

2.2.1.5 PCR product clean-up and agarose gel extraction

PCR products were separated according to their size via agarose gel electrophoresis. Concentration of agarose, dissolved in 1x TAE, was dependent on the size of the of DNA fragments. The DNA fragments were either visualized and documented using “molecular analyst” software or purified from the gel by NucleoSpin® Plasmid QuickPure Kit (Marcherey-

Nagel) according to the manufacturer's recommendations. This kit was also used for purification of PCR products without prior loading on an agarose gel.

2.2.1.6 Ligation

Purified PCR fragments were ligated either in frame to fluorescent proteins (CFP, YFP) using the respective plasmids obtained from Clontech (Mountain View, CA) (Fig. 12), or to other mammalian expression vectors. Ligation was performed using Fast-Link™ DNA Ligation Kits® (Epicentre Technologies Corp.) according to the manufacturer's recommendations with modifications in vector:insert ratio and incubation time. The reaction was set up according to Table 4 including a negative control without insert to estimate the number of self-ligated or uncut vectors.

Table 4 Ligation reaction

Standard setup for the ligation reaction (Fast-Link™ DNA Ligation Kits, Epicentre® Technologies Corp.)

Components	Volume
10x Fast-Link Ligation Buffer (330 mM Tris-acetate [pH 7.5], 660mM potassium acetate, 100 mM magnesium acetate and 5 mM DTT)	1.5 µl
ATP (10mM)	1.5 µl
Fast-Link DNA Ligase (2U/µl)	1 µl
Vector (50 ng/µl)	1 µl
Insert (0µl negative control & two reactions with a vector/insert ratio (Moles open ends) of 1:5 and 1:10)	variable µl
ddH ₂ O	ad 15µl

The reaction was incubated for 30 minutes at RT. Fast-Link DNA ligase was inactivated at 70°C for 15 minutes as remaining activity of the ligase could cause problems in transformation efficiency.

5µl of the 15µl reaction was used for transformation of competent *E. coli* bacteria (see 2.2.1.7). Bacteria were grown over night at 37°C on LB-agar dishes supplemented with antibiotics according to resistance gene encoded on the plasmid.

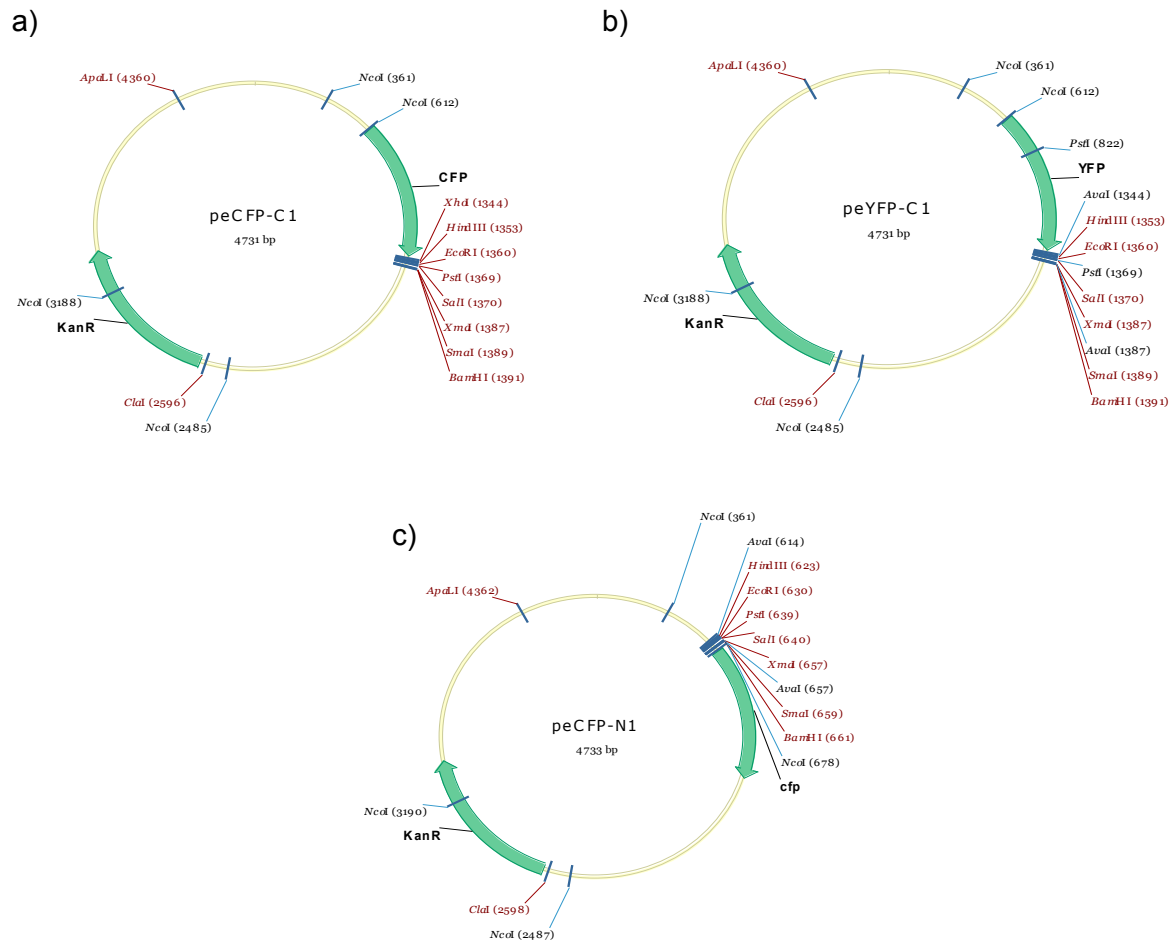


Figure 12 peCFP-C1 / peYFP-C1/peCFP-N1 schematic vector maps.

a) peCFP-C1 and b) peYFP-C1 for adding fluorescent protein to the N-terminus of a protein; c) peCFP-N1 for adding the fluorescent protein to the C-terminus of a protein;

2.2.1.7 Generating competent *E. coli* bacteria

Chemically competent *E. coli* cells were prepared following an established protocol. 10ml LB medium containing 10µg/ml tetracyclin was inoculated with a bacterial *E. coli* colony (XL10) from a tetracyclin supplemented agar plate. After cultivation at 37°C while shaking overnight, 2ml of this preculture were transferred to sterile Erlenmeyer-flask containing 200 ml prewarmed LB medium. The flask was again incubated on 37°C until OD₅₅₀ of 0.5 was reached, which corresponds to exponential growth of the bacteria. The flasks were transferred on ice (10 minutes) and the bacteria harvested by centrifugation (15 minutes, 4°C 1500g). Pellets were resuspended in 20ml of ice-cold TSS (see materials) buffer. Afterwards

5ml glycerol was added and competent bacteria were aliquoted in sterile Eppendorf-tubes at the appropriate volume, immediately frozen in liquid nitrogen and stored at -80°C.

2.2.1.8 QuikChange Site-Directed Mutagenesis[®]

For introducing a specific mutation into a double-stranded DNA in vitro the QuikChange Site-Directed Mutagenesis kit from Agilent Technologies (Santa Clara, CA) was used.

The mutagenesis is performed by using two complementary primers harboring the desired mutation. As template a plasmid coding for the gene of interest is used (Table 5). By running a PCR (Table 6) both strands of the plasmid are amplified introducing the desired mutation. After PCR has been performed the samples are treated with the endonuclease DpnI for 30 minutes at 37°C. DpnI which uses 5'-Gm6ATC-3' as target sequence only digests methylated and hemimethylated parental DNA. As DNA from PCR reactions is not methylated, it is resistant to this enzyme. Therefore only mutated DNA is supposed to stay intact.

These mutated plasmids were transformed into competent bacteria, which were grown over night on LB agar dishes selected with antibiotics according to the antibiotic resistance on the plasmid.

Table 5 QuikChange reaction pipetting.

10µl of generated dsDNA "megaprimer" was used as it provides function of sense and antisense primer based on the double stranded sequence (QuikChange Site-Directed Mutagenesis Kit by Agilent Technologies).

Components	Volume
10× reaction buffer [(100mM KCl, 100mM(NH ₄) ₂ SO ₄ , 200mM Tris-HCl (pH 8.8), 20mM MgSO ₄ , 1% Triton® X-100, 1mg/ml nuclease-free BSA)]	2.5 µl
dsDNA template	5-50 ng
dNTP mix	0.5 µl
Quick Solution	0.75 µl
Primer	10 µl
PfuTurbo DNA polymerase (2.5 U/ µl)	1µl
ddH ₂ O	ad 25 µl

Table 6 QuikChange PCR protocol

Temperature (°C)	Time	Cycles
95	2 min	1x
95	20 sec	20x
58	20 sec	
68	4 min 30 sec	
72	5 min	1x
4	Endless	1x

2.2.1.9 Transformation

For amplifying plasmids, they were transformed into chemically competent bacteria XL10, using the so called “heat shock” protocol. 100µl of competent cells (2.2.1.7) were thawed on ice, 5µl of DNA was added and gently mixed. After an incubation time of 20 minutes on ice, a heat shock (45 seconds on 42°C) was performed, followed by an additional incubation time of 2 minutes on ice. During these steps the plasmid DNA can enter the competent bacterial cells. 1 ml of Lysogeny Broth (LB) medium was added and the transformed bacteria were incubated for one hour at 37°C while shaking. Within this incubation time, bacteria had time to express the plasmid encoded gene for antibiotic resistance. After one hour of incubation the bacteria were centrifuged for 5 minutes at 10,000 rpm (MiniSpin by Eppendorf), the supernatant was poured off and the pellet was resuspended in the remaining medium. Cells were then plated on agar plates containing antibiotics for selection and the bacteria were grown over night.

In order to reduce the risk of contaminations, working with bacteria was always performed under aseptic conditions.

2.2.1.10 DNA/Plasmid Isolation

For qualitative analysis, DNA was isolated from 2ml overnight LB cultures (Mini Prep), using NucleoSpin® Plasmid QuickPure Kit (Marcherey-Nagel) following the manufacturer’s recommendations. After lysis of bacteria, proteins and genomic DNA gets precipitated and the plasmid of interest can be isolated by binding to and eluting from a membrane.

DNAs from “mini preps” were used for diagnostic restriction digest and sequencing. Correct plasmids were transformed again and larger amounts of plasmid were isolated using 250ml LB cultures (Midi Prep).

Therefore, bacteria were harvested by centrifugation (3000 x g, 4°C, 20 minutes) using GS-3 or GSA rotor in a Sorvall™ centrifuge and plasmids were isolation using NucleoBond® Extra Midi Plus (Marcherey-Nagel).

2.2.2 Cell culture

2.2.2.1 Cultivation

Media, Trypsin, serum and antibiotics used for cell culture were purchased from Sigma-Aldrich, (St. Louis, MO), cell culture dishes were purchased from Sarstedt (Germany).

Standard cultivation of HEK293 cells was performed in Dulbecco’s modified eagle’s medium (DMEM) High Glucose (4.5 g/L) containing 10%(w/v) FCS and additional antibiotics 1% Penicillin/Streptomycin (10,000 units penicillin/10mg/ streptomycin/ml) on polystyrene culture dishes. Cells were kept in an incubator (CO₂ Incubator CB, Binder) under optimal temperature (37°C) and CO₂ (5 %) conditions.

To allow for optimal growth conditions of the cells, they were split upon confluency of 80-90%.

For this cultivation, medium was soaked up by aspiration via a pump and the cells were washed once with 1x phosphate buffered saline (PBS) to get rid of remaining medium and dead, not attached cells and cell debris. Afterwards 1 ml of prewarmed Trypsin/EDTA (0.5g trypsin/0.2g EDTA; Sigma-Aldrich) was added to detach the cells from the culture dish.

Proper detachment was confirmed by light microscopy and trypsin was inactivated by adding 8 ml of prewarmed cultivation medium. Detached cells were collected in a 50 ml tube (Greiner) and harvested by centrifugation for 5 minutes at 1000 rpm.

After aspiration of the supernatant, the pelleted cells were resuspended in 10 ml fresh cultivation medium and transferred to new culture dishes, normally 1ml of cell suspension plus 9 ml of cultivation medium.

2.2.2.2 Cell counting/seeding

Cells were detached by adding Trypsin/EDTA (1ml per 10ml cultivation medium), harvested by centrifugation and resuspended in fresh cultivation medium as described before. Cells were counted using a Neubauer improved counting chamber. 10 to 15 µl of the cell suspension is added to the object slide consisting of 9 large squares further subdivided into

16 smaller squares each. The larger squares have an area of 1mm^2 with the coverslip 0.1mm above resulting in a total volume of 0.1mm^3 ($=0.1\mu\text{l}$) / square. The number of cells counted in this field has to be multiplied with 1×10^4 in order to calculate the number of cells per ml.

2.2.2.3 Transfection

Introducing DNA of interest into a mammalian cell system like HEK293 (transfection) cells can be performed using different methods. Transfection reagents, which are based on the formation of lipid complexes (Fig. 13) and by a precipitate which is adhering to the cells (Calcium phosphate transfection) are two of those.

Transfection reagents such as LipofectAMINE PLUS[®] (Invitrogen Life Technologies[™]) or jetPrime[®] promote the formation of cationic lipids consisting of a positively charged head group and hydrocarbon chains. As the surface of these liposomes is charged positively, they are able to interact with the negatively charged cell surface and enter the cell through endocytosis. Once entered the negatively charged DNA binds spontaneously to the positively charged liposomes.

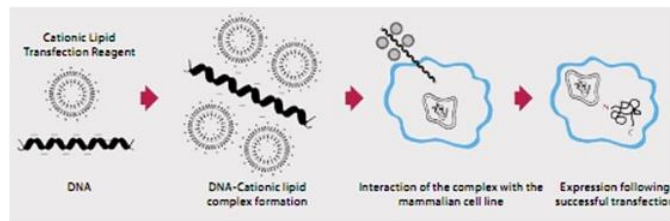


Figure 13 Transfection by cationic lipid transfection reagent

(www.lifetechnologies.com/at/en/home/life-science/cell-culture/transfection/transfection-methods/lipid-transfection.html)

jetPrime[®] DNA Transfection (Polyplus transfection)

HEK293 cells were seeded at 2.5×10^6 cells per 10cm^2 the day before transfection. The seeded cell number depends on the cell line used. Therefore confluency should be around 70% on the day of transfection to guarantee optimal conditions for the transfection using jetPrime[®] (Fig. 14).

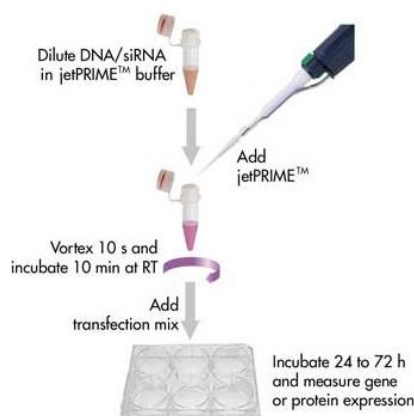


Figure 14 jetPrime® DNA Transfection

Schematic view on standard jetPrime transfection procedure

(http://www.polyplus-transfection.com/wp-content/uploads/2009/08/CPT_114_jetPRIME_VI.pdf)

LipofectAMINE PLUS™ Reagent (Invitrogen by Life Technologies)

The day before transfection, cells of interest were seeded to reach a confluency of 60-80% the next day.

According to the manufacturer's recommendations DNA was diluted with PLUS Reagent in serum and antibiotic free DMEM (Starving medium) and the mixture was incubated at RT for 15 minutes. Meanwhile LipofectAMINE Reagent was diluted in starving medium as well. After this incubation time, pre-complexed DNA was added to diluted LipofectAMINE reagent, mixed, centrifuged shortly and for the formation of complexes incubated for another 15 minutes at RT. Meanwhile the cellular cultivation medium was replaced by starving medium and DNA-PLUS-LipofectAMINE Reagent complexes were finally added to the dishes. After incubation on 37°C at 5% CO₂ for 3 hour the transfection medium was replaced by standard cultivation medium to guarantee optimal growth of the cells.

Lipofectamine™ RNAiMAX (Invitrogen by Life Technologies)

For generating a specific knockdown cell line, siRNAs were obtained from Invitrogen. In order to reach a confluency of 60-80%, cells were seeded at a density of 0.25-1x10⁶ cells per well of a 6-well plate to in antibiotic free cultivation medium as recommended by the manufacturer (Fig. 15).

9 µl Lipofectamine® RNAiMAX reagent were diluted in 150µl Opti-MEM® Medium (GIBCO™). A second tube contains 150µl Opti-MEM® Medium and 3µl of a 10µM siRNA (final: 30pmol) (one reaction -6well). Diluted siRNA was added to the Lipofectamine RNAiMAX reagent in Opti-MEM Medium, mixed well and incubated for 5 minutes at RT to ensure siRNA lipid

complex formation. Afterwards complexes were added to the cells and incubated at 37°C with 5% CO₂. Transfected cells were used for experiments one to three days post transfections.

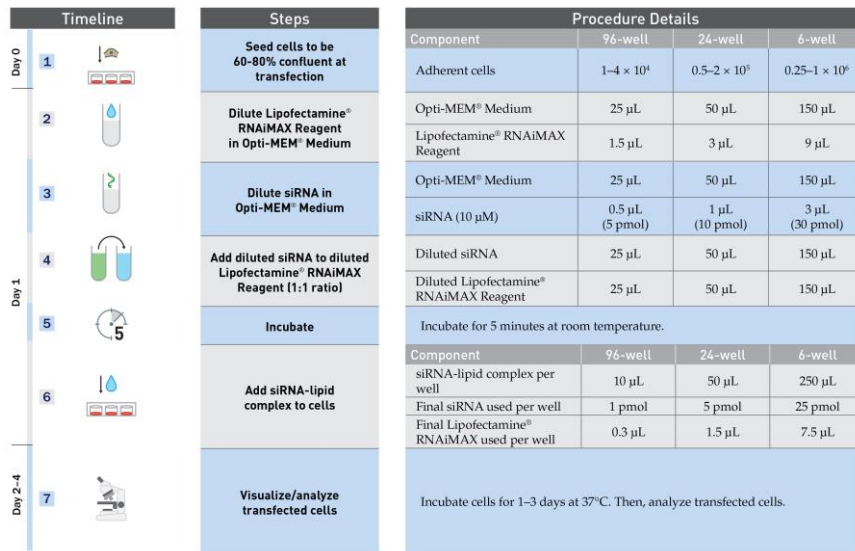


Figure 15 RNAiMAX transfection procedure

Overview of RNAiMAX transfection procedure and detailed view on components in order to amount and necessary equipment.

(http://tools.lifetechnologies.com/content/sfs/manuals/Lipofectamine_RNAiMAX_Reag_protocol.pdf).

2.2.2.4 Stable cell line

Generating a stable cell lines is based on the fact that plasmids harbor, beside a gene of interest, coding regions for antibiotic resistance. After transfection plasmids might get integrated into a chromosome. In this rare event the transfected DNA is segregated during cell division to the daughter cells. HEK293 cells and RNAi cells were transfected as described before. The day after the transfection, cells were exposed to antibiotics in order to generate selection pressure for cells carrying an integrated plasmid. As cells regularly lose plasmids during cell division, only cells in which the rare event of chromosomal integration of the plasmid occurred can survive. Transporters cloned into a pcDNA3.1zeo vector were selected via zeozin™ (InvivoGen) using [300µg/ml]. Transporters cloned into YFP/CFP expressing vectors were selected using Geneticin/G418 [50µg/ml] (Biochrom).

The medium was replaced every second day to remove dead cells and as single colonies were visible they were transferred to 6 well dishes (3cm in diameter; Greiner bio-one) for getting monoclonal subclones. Final evaluation was performed by fluorescent microscopy and further by functional assays.

Once generated and cultivated, antibiotic pressure has to be kept all the time as cells have the ability to exclude the plasmid after longer cultivation periods. Therefore 50µl per 10ml [25µg/ml] of medium G418 or 15µl of zeozin™ per 10ml [150µg/ml] medium had to be added.

2.2.3 Western Blot

Western Blot, or immunoblot analysis is a special technique used for the detection of specific proteins within tissue-lysate. Therefore, an SDS-PAGE has to be performed to denature and separate proteins by mass. In a second step, separated proteins are transferred to a special membrane. Incubating these membranes with specific antibodies allows detection of the desired proteins.

2.2.3.1 Protein preparation

To get a total protein lysate from cells, they were seeded on a 100mm dish and cultivated upon confluency. Cell lysis was performed on ice. The dishes were washed twice with ice cold 1x PBS and cells were lysed by addition of 1ml of RIPA Buffer (see materials) containing 1x protease Inhibitor cocktail (cOmplete Tablets EASYpack; Roche), followed by an incubation of 30 min at 4°C under continuous agitation.

Cell lysates were collected in Eppendorf-tubes and centrifuged with 16,000 x g for 20 minutes at 4°C. Cell debris and damaged tissue material is pelleted and the supernatant containing only solubilized proteins was transferred to a fresh reaction tube.

2.2.3.2 Protein concentration measurement (Bradford reagent)

Protein concentration was measured by using Bradford reagent provided by BioRad. 2 µl of protein solution were mixed with 1 ml of Bradford reagent (diluted 1:5 in ddH₂O) and absorbance was measured in duplicates at 595nm using the U-2001 spectrophotometer (Hitachi).

Protein concentration was then calculated via the standard formula (Fig. 16) in µg/µl.

BRADFORD REAGENT ADVANCED
 assay 1cm @ 595nm; 100µl Sample & 1ml Reagent 1:5
 22NOV'13 tetraplicates helmut facit

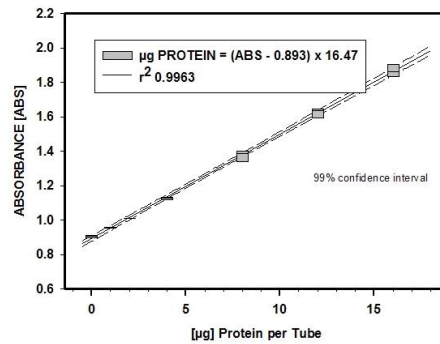


Figure 16 Bradford reagent advanced standard curve

Curve was generated by defined BSA concentrations;

2.2.3.3 SDS-page and blotting

SDS-PAGE was performed using 10% resolving and 5% stacking gel as listed in Table 7.

Table 7 Resolving gel/Stacking gel recipe

Standard recipe for 10% Resolving gel and 5% Stacking Gel for SDS-page. Percentage is based on size of proteins loaded onto the gel.

Resolving Gel	10% [ml]	Stacking Gel	5% [ml]
1.5M TRIS pH 8.8	2.5	0.5M TRIS pH 6.8	1.25
10% SDS (Sigma-Aldrich)	0.1	10% SDS	0.05
Aqua Dest. MQ	3.96	Aqua Dest. MQ	2.81
30%-0.8% Acryl-Bisacryl (BioRad)	3.33	30%-0.8% Acryl-Bisacryl	0.84
10% Ammonium per sulfate (APS) (Sigma-Aldrich)	0.1	10% Ammonium per sulfate (APS)	0.05
TEMED (Merk)	0.01	TEMED	0.005

Casting frames were built up to a sandwich using glass plates with integrated 1mm spacer provided by BioRad.

A 10% resolving gel was filled up within this chamber until optimal height and overlaid with isopropanol to avoid air bubbles and drying out during polymerization. Once polymerized,

isopropanol could easily be discarded. The resolving gel was overlaid with 5% stacking gel and a 10 or 15 well comb was inserted immediately afterwards.

After polymerization, gels were placed into a clamping frame which consisted of an electrode assembly and transferred into the running chamber containing 1x SDS-Page running buffer (see materials). Proteins, which were denatured by 1 x SDS loading buffer, were loaded into the wells and electrophoresis was run for about 10 minutes on 100 V, followed by approximately 1 hour on 170 V. In the first step, proteins were collected to a sharp band within the stacking gel before separation within the running gel. This protocol guaranteed clearer bands.

After separation of proteins the actual blot could be performed. Therefore the proteins, which were separated in the polyacrylamide gel, were now transferred to a nitrocellulose membrane (Amersham™ Hybond ECL; GE Healthcare Life Sciences) using a semi-dry blotter (BioRad). Due to hydrophobic interactions and hydrogen bonds between the membrane and the proteins, these macromolecules get covalently bound.

Transfer was performed using the semi-dry technique. Therefore sheets of Whatman filter paper (Protran) and the nitrocellulose membrane were equilibrated in 1x electrotransfer buffer concentrate (TB²) (see materials). Three filter papers were placed on the slightly wetted semidry apparatus bottom, overlaid with the equilibrated nitrocellulose membrane, next the gel, containing the proteins and as a last step the pile is covered by another three in TB² transfer buffer equilibrated filter papers.

After one hour of blotting at constant 25 Volts the membrane was shortly incubated in PonceauS (Sigma-Aldrich) solution to control the transfer. PonceauS reversibly stains membrane bound proteins.

The membranes were incubated for 1 hour at room temperature in 0.1% TBS-T (see materials), supplemented with 5% Bovine Serum Albumine (GE Healthcare), to avoid unspecific binding of the primary antibody by blocking binding sites at the membrane. Afterwards membranes were washed twice for 10 minutes and once for 5 minutes with 0.1% TBS-T to get rid of the remaining blocking solution which could interfere with the primary antibody. Optional a last washing step was performed with only 1x TBS for 5 minutes lacking of Tween-20 as this detergent may also interfere with the antibody.

The membrane was incubated with primary antibodies (Table 8) overnight at 4°C followed by washing steps as described before.

Membranes were incubated with the appropriate fluorescent secondary antibody (Table 8) for one hour on RT in the dark. Analysis was performed on the LI-COR® Odyssey® CLx system and the related software Image Studio™.

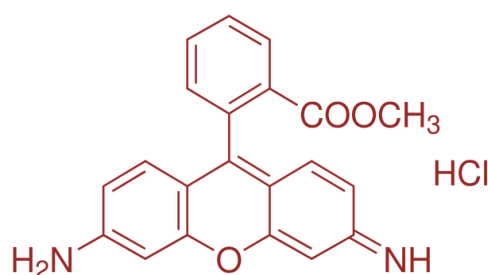
Table 8 Antibodies used for Western Blot

Primary and secondary antibodies used in Western Blot including dilution factor.

Primary AB	Dilution (in 0.1% TBS-T)	Secondary AB	Dilution (in 0.1% TBS-T)
Rabbit Anti GFP	1:5000	IRDye® 800CW Donkey anti-Rabbit (LI-COR®)	1:5000
Rabbit Anti K5 (FhMDR)	1:1000		

2.2.4 Rhodamine123 uptake via FACS

To determine functional activity of CFP tagged FhMDR rhodamine123 uptake was analyzed by fluorescent-activated cell sorting (FACS) on a BD Accuri™ C6 flow cytometer (BD Bioscience). This method is well established for human MDR using the mitochondrial specific fluorescent dye rhodamine123 (2-(6-Amino-3-imino-3H-xanthen-9-yl)benzoic acid methyl ester) (Sigma-Aldrich). Rhodamine123 (Fig. 17) is known to be a potent substrate for human P-gP and is commonly used within flow cytometry.

**Figure 17 Chemical structure of rhodamine123**

(<http://www.sigmaaldrich.com/catalog/product/sigma/83702?lang=de®ion=AT>)

Based on the homology of FhMDR to the human P-gP, this method was chosen to measure rhodamine123 accumulation in transiently transfected “RNAi” cells. RNAi cells are HEK293 cells stably expressing a shRNA to knock-down endogenous P-glycoprotein (kindly provided by Ao. Univ.-Prof. Dr. Peter Chiba’s laboratory). As CFP is not interfering with the excitation and emission spectra of rhodamine123 (433 and 475nm vs 488 and 534nm, respectively), this fluorescent tagged version of the FhMDR plasmid was used for the experiment. RNAi cells were cultured in standard DMEM cultivation medium plus additionally 2µg/ml puromycin

to ensure stability of P-gP knock-down within these cells. Three days post transfection, cells were checked under the microscope to guarantee expression of the ABC transporter and its localization at the plasma membrane.

Transfected cells were washed once with PBS, detached from the culture dishes by trypsin and counted. Approximately 1×10^6 or 1.5×10^6 cells per FACS tube (sample) were used and each data point was measured in triplicates. An additional washing step was performed by adding 2 ml PBS followed by centrifugation at 500 x g (Eppendorf 5403 centrifuge). The remaining supernatant was aspirated. Afterwards the pellet was resuspended in 2 ml of loading medium containing DMEM +10% FCS+25mM HEPES (Sigma-Aldrich)+ 0.2g/ml [0.53 μ M] rhodamine123 pH 7.8 and incubated at 37°C in a waterbath under continuous agitation to load cells with the fluorescently labelled dye.

Different ABC transporter blockers (tariquidar [1 μ M], the propafenone analogue GPV031 [1-(2-(2-(3-(4-(4-fluorophenyl)-3-phenyl)piperazin-1-yl)-2-hydroxypropoxy)phenyl)-3-phenylpropan-1-one]) [5 μ M]) (both provided by Ao. Univ.-Prof. Dr. Peter Chiba; Institute for Medical Chemistry) were added to the loading medium. To test the function of tricloabendazole as a potential substrate/blocker of FhMDR this was added at a final concentration of 10 μ M.

ABC transporters provide active efflux on 37°C. Therefore rhodamine123 should be transported out of the cell. The loading process was terminated by chilling samples on wet ice which immediately stops the activity of ABC transporters. To guarantee inactivation all further steps were performed on wet ice.

Samples were washed once with pre-cooled washing medium containing DMEM+2%FCS+25mM HEPES (pH 7.4) to remove the remaining rhd123 within the loading medium. After centrifugation (500 x g, 6 min, 4°C) the samples were resuspended for measurements in 0.5 ml washing medium.

Measurement and analysis were performed via fluorescence-activated cell sorting (FACS). The basic principle of this method is the measurement of fluorescence intensities of loaded viable cells. Viability of the cells is characterized by their size and granularity defined by scattered and emitted light when excited by a laser beam. These light signals are further transformed into electronic pulses which can be processed by computer software.

Fluidics, optics and electronics are the major parts of this method.

Some parameters within this method are essential for later analysis of FACS data. Cell populations, after excitement of the laser beam, show different forward scattered (FSC) and side scattered (SSC) light. As FSC is determined to the proportionality to the measured cell

surface area also or size, SSC is the unit of cell granularity. According to the scattered light different cell populations can be distinguished (Fig. 18) (BD Bioscience, 2000).

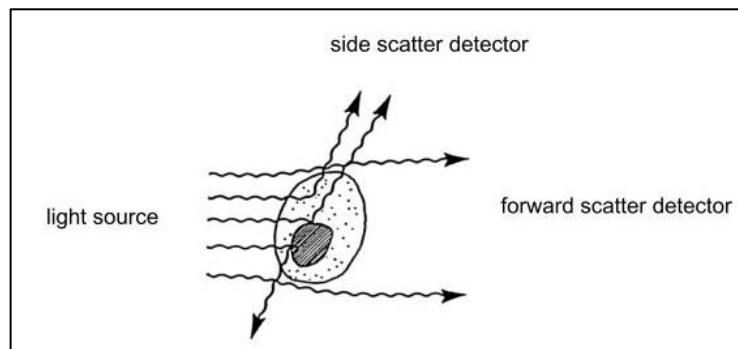


Figure 18 Schematic few of FSC and SSC.

This schematic drawing shows forward and side scatter of a single cell, which is emitted after excitement by a light source and detection via specific detectors. (BD Bioscience, 2000)

Via their FSC and SSC properties intact cells are chosen for further analysis. After this “gating” process the intensity of rhodamine123 emission was measured for every single cell. This emitted light stands for the amount of rhodamine123 in the cell and is regulated by the export via ABC transporters. For each condition 20,000 cells were analyzed. The exact SOP of this rhodamine123 accumulation assay was performed at the Institute of Medical Chemistry (MUW) in the working group of Ao. Univ.-Prof. Dr. Peter Chiba.

2.2.5 Uptake

Functional activity of the taurine transporter was analyzed via uptake assays using tritiated substances. The substrates used are listed in the table below. Methyl-4-phenylpyridinium iodide (MPP^+) was from ARC (American Radiolabeled Chemicals Inc.), the remaining [3H] compounds from PerkinElmer (Table 9).

Table 9 List of [3H] substances

List of tritiated substances and specific transporter blockers used in uptake assay including specific activity and final concentrations.

[3H] substance	Spec. activity [Ci/mmol]	Final conc [μM]	Blocker final conc [μM]
[2,2- $^3H(N)$]-Taurine	22.7	0.05/0.1	β -alanine [1mM]
[2,3- $^3H(N)$]- γ Aminobutyric acid (GABA)	35	0.06	Nipecotic acid [1mM]
5-[1,2- $^3H(N)$]- Hydroxytryptamine creatinine sulphate (5HT)	28.7	0.1	<ul style="list-style-type: none"> • Clomipramine • Cocaine • Paroxetine [100 μM]
L-[3,4- 3H]-Glutamic acid	51.1	0.1	L-trans-pyrrolidine-2,4-dicarboxylic acid (PDC) [100 μM]
[2- 3H]-Glycine	56.4	0.05	Sacrosine [100 μM]
3,4-, [ring-2,5,6- 3H]-Dihydroxyphylethylamine (Dopamine)	52.8	0.1	<ul style="list-style-type: none"> • Desimipramine • Nisoxetine • Mazindol [100 μM]
Methyl-4-phenylpyridinium iodide (MPP^+)	80	0.015	<ul style="list-style-type: none"> • Clomipramine • Cocaine • Paroxetine [100 μM]

If not indicated otherwise uptake experiments were performed at 37°C.

Following the standard protocol, transfected cells or stable cell lines were seeded on Poly-D-Lysine (PDL purchased by Sigma-Aldrich) coated 48well cultivation dishes. 0.1×10^6 cells per well were seeded in a final volume of 500 μ l standard cultivation medium and incubated overnight at 37°C and 5% CO₂.

On the following day the cultivation medium was replaced by 750 μ l prewarmed Krebs-HEPES Buffer pH 7.3 (see materials). Cells were then incubated with 100 μ l of the uptake solution, which contained a fixed concentration of the tritiated substance and different amounts of the unlabeled substance. Incubation time was dependent on the predicted transport rate of the individual transporter. Uptake experiments were performed for 10 minutes (YFP FhepSLC6) or for 5 minutes (CFP hTauT). Uptake was stopped by washing the cells with 750 μ l ice cold PBS. Afterwards cells were lysed by adding 500 μ l 1% (w/v) SDS and the solution was transferred to mini-vials and 2 ml of scintillation cocktail (Rotisint[®] eco plus LSC-Universalcocktail; Roth) was added. The scintillation cocktail absorbs emitted energy produced by the disintegration of the radioisotopes and re-emits it as flashlight. These signals can be detected and measured in a β -counter (TRI-CARD 2300 RT (Packard)).

Unspecific uptake was determined in the presence of a blocker (see Table 9). After determination of the cell number, it was possible to calculate the transport rate in pmol/Mio cells/min for every data point.

Data were analyzed using GraphPadPrism5.0 software. Non-linear regression curve fitting allowed the calculation of K_m and V_{max} values.

K_m value or Michaelis-Menten constant is defined as the substrate concentration at which the reaction rate is half of the maximal rate (defined as V_{max}). To characterize enzyme reactions it is important to refer to the K_m value as, half of reactive binding sites for the substrate are occupied which is linked to the concentration of the substrate needed for considerably performing catalytic reaction (Stryer *et al.*, 2007).

2.2.6 Inhibition

Basic principle of this method is to test the potency of a substance (antagonist or second substrate) to inhibit the transport of a standard substrate. This potency is characterized by the IC₅₀ value which is defined as the concentration of the substance needed for 50 % of inhibition of substrate transport.

Inhibition assays were performed using the same procedure as in uptake experiments. Different substances working as putative blockers for the *F. hepatica* taurine transporter were tested to evaluate their inhibitory potency on human and fluke transporter (Table 10). Uptake was performed at 37°C using identical uptake times as described in 2.2.5. Substrate concentration was kept constant using a final concentration of 0.2µM [2,2-3H(N)]-Taurine [22.7 Ci/mmol]. Blockers were used at increasing concentrations according to expected IC₅₀ values. After 10 or 5 minutes incubation reaction was stopped by washing with ice cold KHP, cells were lysed by 1% SDS and the remaining radioactivity was measured by liquid scintillation counting. Inhibition curves were fitted as non-linear regression curve standardized by S.E.M (standard error of mean). Graphs were analyzed and IC₅₀ values were calculated via GraphPadPrism5.0. Graphs were blotted in % of uptake of the radio-ligand versus the applied concentration of antagonist.

Table 10 Blocking substances including serial dilution used for inhibition.

Blocker	Final dilution range [µM]
β-alanine (Sigma-Aldrich)	0-1000 µM
GABA (Sigma-Aldrich)	0.001-100,000 µM
Guanidinoethyl sulfonate (Santa Cruz Biotechnology)	0.001-10,000 µM
Tiagabine (Sanofi)	0-100 µM

3 Results & Discussion

3.1 *Fasciola hepatica* MDR

3.1.1 Cloning and localization

The first (partial) sequence of an ABC transporter from *F. hepatica* was published by Reed *et al.* (1998). This sequence information was used as a starting point for the identification of the full-length sequence by rapid amplification of cDNA ends (RACE). Therefore RNA was extracted from total fluke tissue using TRI Reagent[®]. 5' and 3' RACE was performed using RACE specific primers FhepATP RACE1-14 (see 2.2.1.2). The full-length sequences (see section "sequences") displayed an open reading frame of 3,786 bp encoding 1,261 amino acids with a calculated mass of 140 kDa. Database search of the newly identified nematode transporter revealed highest homology to an ABC transporter of *Schistosoma mansoni*, which belongs to the B-family of the ABC transporters.

The full-length cDNA was amplified from fluke RNA by RT-PCR (see 2.2.1.4.). The first five cycles were run at 52°C annealing temperature followed by 40 cycles at 68°C. Elongation time was 4.30 minutes. The 5' and 3' fragments of FhMDR (Fig. 19) were visualized by 1.5% agarose gel electrophoresis and the desired bands were excised and purified using NucleoSpin[®] Gel and PCR Clean-up gel extraction kit (see 2.2.1.5).

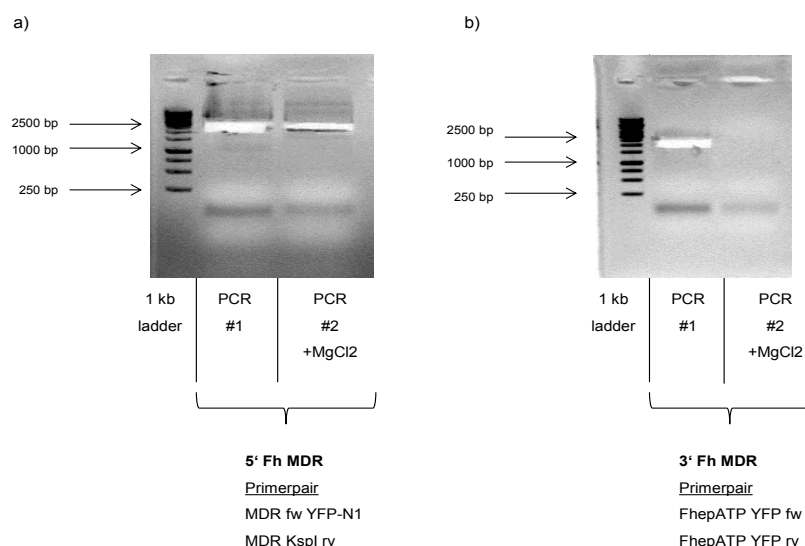


Figure 19 5'/3' cDNA fragments FhMDR

Amplicons of the N-terminal a) and C-terminal fragment of FhMDR (b) PCR samples were loaded onto 1.5% agarose gels and bands with predicted size were excised.

Both fragments were separately ligated into peCFP-C1 and peCFP-N1 vectors (5': HindIII/KspI; 3':KspI/BamHI).

Cloned full-length FhMDR was verified via XhoI digest resulting in expected bands of 4,9 kb and 3,5 kb (Fig. 20). Positive plasmids were sent for sequencing for final verification (see vector map Fig. 21).

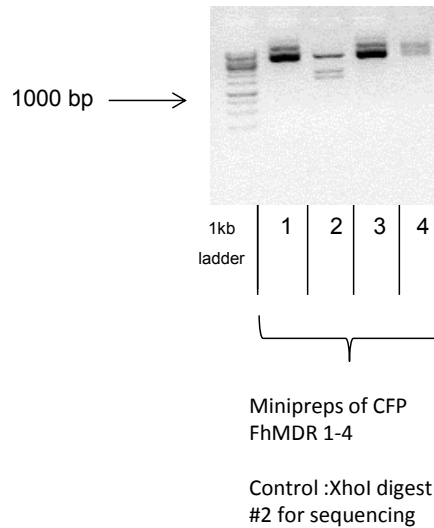


Figure 20 CFP FhMDR full-length XhoI control digest

Control digest of minipreps by the restriction enzyme XhoI; expected full-length sequence should reveal 2 fragments at 4,9kb and 3,5kb. Sample 2 was sent for sequencing.

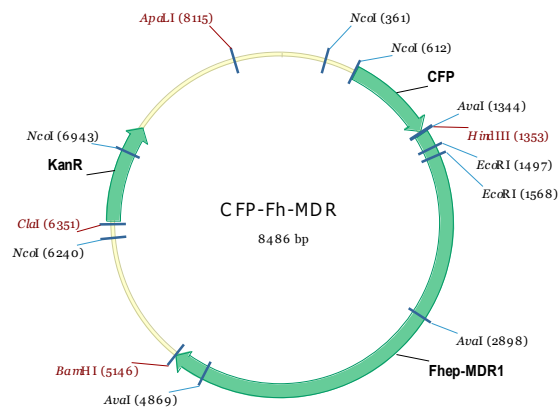


Figure 21 Vector map CFP FhMDR

Vector map of CFP FhMDR showing restriction sites HindIII and BamHI;

The cloned transporters (N- or C- terminally CFP tagged) were transiently expressed in HEK293 cells or for further experiments in RNAi cells. RNAi cells do not express endogenous human P-glycoprotein through a stable knock-down. The localization of the fluorescently labelled transporter was determined by epifluorescent microscopy using a Zeiss Axiovert 200 microscope (Fig. 22). The N-terminal tagged version (CFP FhMDR) of the transporter was localized at the cell membrane (Fig. 22a), while the C-terminally tagged one (FhMDR CFP) was found in an intracellular compartment (Fig. 22b). The full-length ABC transporters of family B, as known from the four human isoforms (ABCB1, 4, 5 and 11) are expressed at the plasma membrane, while the half-transporters localize in the endoplasmatic reticulum (ABCB2 & 3), lysosomes (ABCB9) or mitochondria (ABCB6, 7, 8 and 10). Sequence analysis predicted different probabilities for the localization of *F. hepatica* MDR: plasma membrane 65% probability (PSORT) (<http://psort.hgc.jp/>) or mitochondria 64% probability (Target P) (Emanuelsson *et al.*, 2000). The exact localization of the C-terminally tagged transporter (FhMDR CFP) was identified to be the mitochondria by counter-stainings with various organelle specific dyes (Fig. 22 c/d).

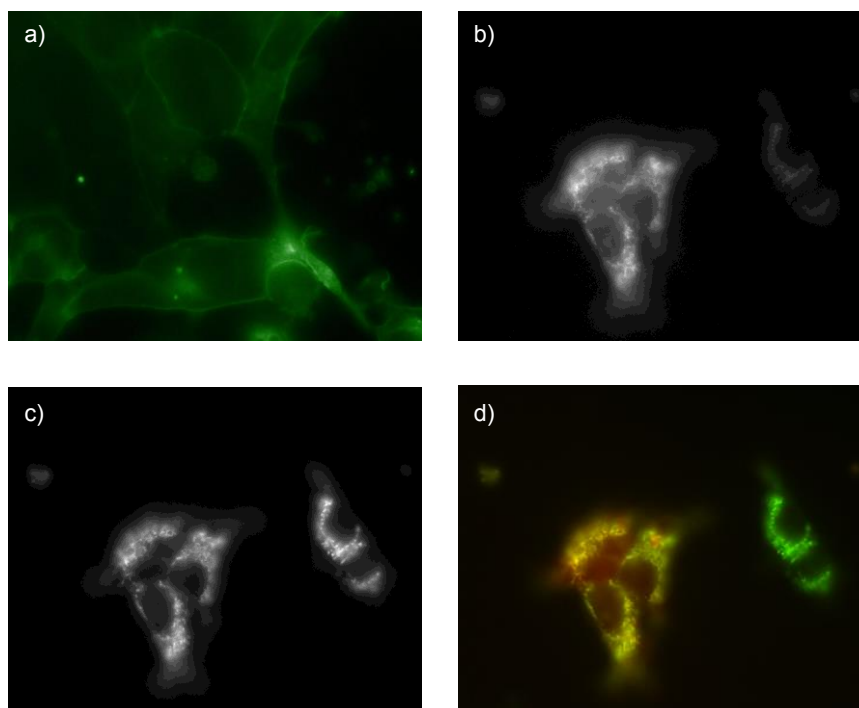


Figure 22 N- or C-terminal CFP tagged FhMDR expressed in RNAi cells.

Epifluorescent pictures of HEK 293 cells heterologously expressing the N-terminally tagged FhMDR (a) (colour optimization performed on AdobePhotoshop) or C-terminally CFP tagged version of FhMDR(b) .c) staining with YFP-mitotracker to verify exact localization d) overlay FhMDR CFP (red) and mitotracker staining (green) shows colocalization (yellow) of the C-terminal tagged FhMDR in mitochondria.

In order to verify that the transporter is expressed in its full-length form in HEK293 cells Western Blot analysis was performed.

Cells expressing N-terminally CFP tagged FhMDR or untransfected “empty” HEK293 cells were therefore lysed, proteins were separated by SDS-page and immediately blotted to a nitrocellulose membrane (see 2.2.3). Detection of the protein using the polyclonal antibody K5, binding the highly variable linker region of the first nucleotide binding domain, showed the expected band at 170 kDa (CFP around 30 kDa and FhMDR predicted to be around 140 kDa).

These findings were additionally confirmed using an anti GFP antibody targeting the CFP tag (Fig. 23).

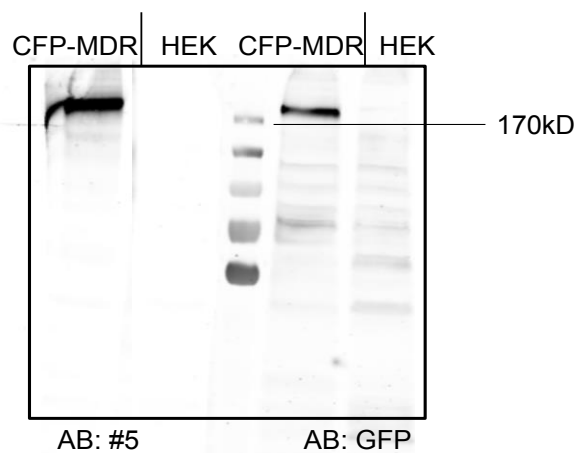


Figure 23 Western Blot with primary antibody against FhMDR.

20µg total tissue protein lysate were loaded onto a 10% polyacrylamide gel and transferred to a nitrocellulose membrane by semidry transfer. CFP-MDR: expressing the CFP tagged version of FhMDR. HEK: non-transfected HEK293 cells; AB#5: rabbit polyclonal antibody against FhMDR; AB: GFP rabbit polyclonal anti-GFP antibody. Middle lane: protein length standard; Fluorescently labelled secondary antibodies were used for analysis using the LI-COR system.

3.1.2 Functional analysis via rhodamine123 accumulation

The functional activity of FhMDR and its proposed interaction with triclabendazole (TCBZ) was tested by a rhodamine123 (rhd123) accumulation assay using fluorescent-activated cell sorting (FACS). Rhd123 is known to be a high affinity substrate for human P-glycoprotein (hPgP) (Lee *et al.*, 1994) and other ABC transporters.

In our setup this assay was dedicated to show reduced rhd123 uptake in cells expressing an ABCB1 transporter (FhMDR or hPgP). Therefore, RNAi cells transiently expressing hPgP, N-

terminally tagged FhMDR (CFP FhMDR) or C-terminally tagged FhMDR (FhMDR CFP), were included in the experiment. Empty RNAi cells served as negative control.

FhMDR CFP expressing cells were chosen to discriminate specific from unspecific efflux, due to alterations in the plasma membrane after liposomal based transfection. Referring to the intracellular localization, it was not expected that FhMDR CFP is able to provide active efflux of rhd123.

Cells were loaded with rhd123 and measured in the presence or absence of candidate blockers for ABC transporters (Table 11). Tariquidar and GPV31 are known blockers of hPgP and tricloabendazole was used as a putative interactor (substrate) of FhMDR.

Table 11 Sample preparation for rhodamine123 accumulation assay.

Table represents samples used in rhd123 accumulation assay with final concentrations of specific blockers added to loading medium.

Cell	Additive blocker
RNAi	<ul style="list-style-type: none"> • no blocker • Tariquidar [1µM] • GPV31 [5µM] • Tricloabendazole [10µM]
CFP hPgP	<ul style="list-style-type: none"> • no blocker • Tariquidar [1µM] • GPV31 [5µM] • Tricloabendazole [10µM]
CFP FhMDR	<ul style="list-style-type: none"> • no blocker • Tariquidar [1µM] • GPV31 [5µM] • Tricloabendazole [10µM]
FhMDR CFP	<ul style="list-style-type: none"> • no blocker • Tariquidar [1µM] • GPV31 [5µM] • Tricloabendazole [10µM]

Rhd123 uptake into cell lines as mentioned above was terminated by removing media and transferring the cells on ice, as MDRs are not active at low temperature. Rhd123 accumulation in single cells was measured by a FACS based approach (see 2.2.4). Cell debris were excluded from viable cells by setting the gate P1 (Fig.24). Measurements were processed and analyzed by using the evaluation software of Becton Dickinson (BD Accuri C6).

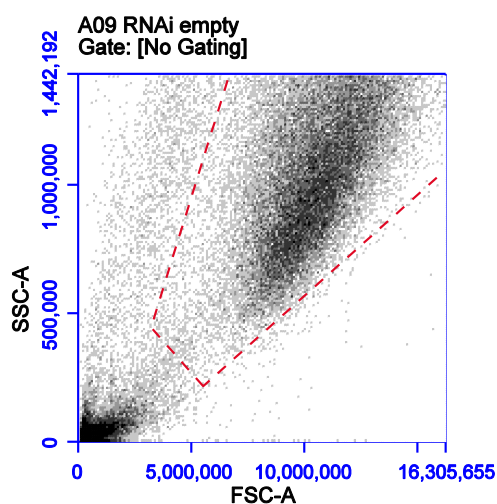


Figure 24 Viable cells gated in P1.

P1 was set according to FCS and SSC. Viable cells were excluded from cell debris or dead cells (outlined in red).

Cells devoid of any transporter will be highly loaded with rhd123. In contrast, cells expressing ABC transporters should be capable of exporting rhd123 resulting in reduced fluorescence. Therefore basic uptake and efflux levels were determined first. Figure 25 displays rhd123 accumulation levels in the absence of blockers in the different cell lines. RNAi cells (black) show the main population with the expected high fluorescence. Cells expressing CFP hPgP (blue) show one population comparable to the RNAi cells and one broad population with less fluorophore accumulated. This is the expected result for transiently transfected cells, as not all cells express the efflux pump, giving rise to the two populations based on the transfection efficiency. Looking at FhMDR, similar results were expected for cells transfected with CFP FhMDR. The presence of CFP FhMDR (red) causes an efflux of rhd123, although the effect is not as pronounced as for hPgP. The second population emerges as a left shifted shoulder. This can be interpreted as a slower export of rhd123 by FhMDR compared to hPgP, fitting the observation that it was not possible to calculate an efflux rate significantly different from diffusion in preliminary efflux experiments

(data not shown). The fact that cells expressing the intracellularly located C-terminally tagged version of the transporter (FhMDR CFP (green)), are indistinguishable from non-transfected cells rules out that the effect visible with CFP FhMDR is due to alterations in the plasma membrane after transfection. In order to verify the hypothesis that FhMDR is responsible for rhd123 efflux fluorescent values should increase if cells were incubated with medium containing blockers of the respective ABC transporter.

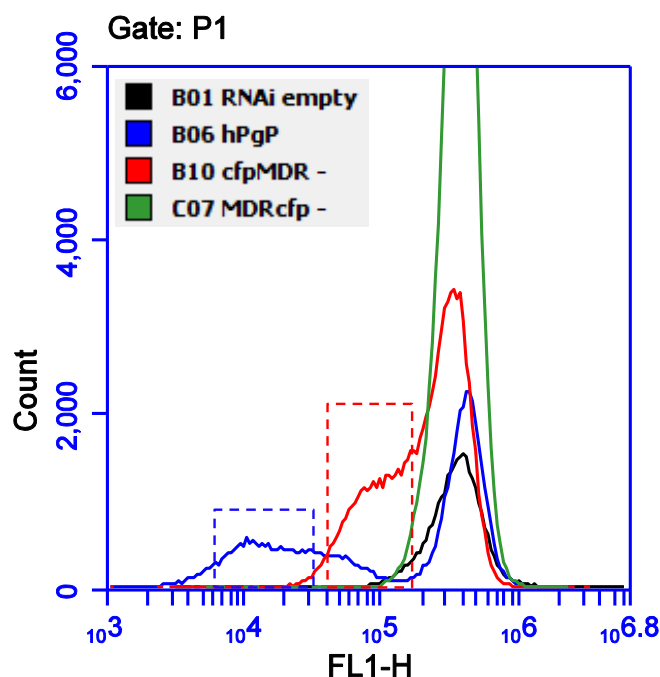


Figure 25 Rhd123 accumulation

Rectangles highlight populations with reduced fluorescence, standing for increased efflux and therefore reduced uptake. Blue: CFP hPgP; red: CFP FhMDR; black: untransfected RNAi cells; green: FhMDR CFP;

By addition of blockers an increase in rhd123 accumulation comparable to levels of empty RNAi cells and a disappearance of the low fluorescent population was expected for hPgP. Previous studies have shown that both, tariquidar and GPV31, are inhibitors of hPgP. Tariquidar and GPV31 were both able to block the transporter mediated rhd123 efflux as shown in Figures 26a und b respectively. A shift towards higher fluorescent intensities was also detected for CFP FhMDR, which leads to the assumption that this helminthic ABCB1 homologue is blockable by tariquidar and GPV31 as well. TCBZ in contrast showed a comparable effect only on cells expressing CFP FhMDR but not hPgP. The observed reduction of transport activity can be explained by two possible mechanisms; i) a full blocker which would blunt the transport or ii) a second substrate which could compete with the

measured substrate for the transporter. While tariquidar was for a long time thought to be a blocker of P-gP, it turned out to be a slow transported substrate (Bankstahl *et al.*, 2013). This could be an indication that TCBZ is transported by CFP FhMDR but not by hPgP. All efforts to treat drug resistances by blockade of ABC transporters (e.g. in cancer therapy) have failed so far, because of severe side effects of the tested compounds on the patients. Therefore, it will not be possible to use compounds like tariquidar or GPV31 to revert resistance to TCBZ in *F. hepatica* as they will be toxic for the animals and the patients respectively. The fact that TCBZ is transported by FhMDR, but not by hPgP is a first indication that it could be possible to develop substance recognizing fluke transporters but not mammalian ones, being a necessity to circumvent resistance.

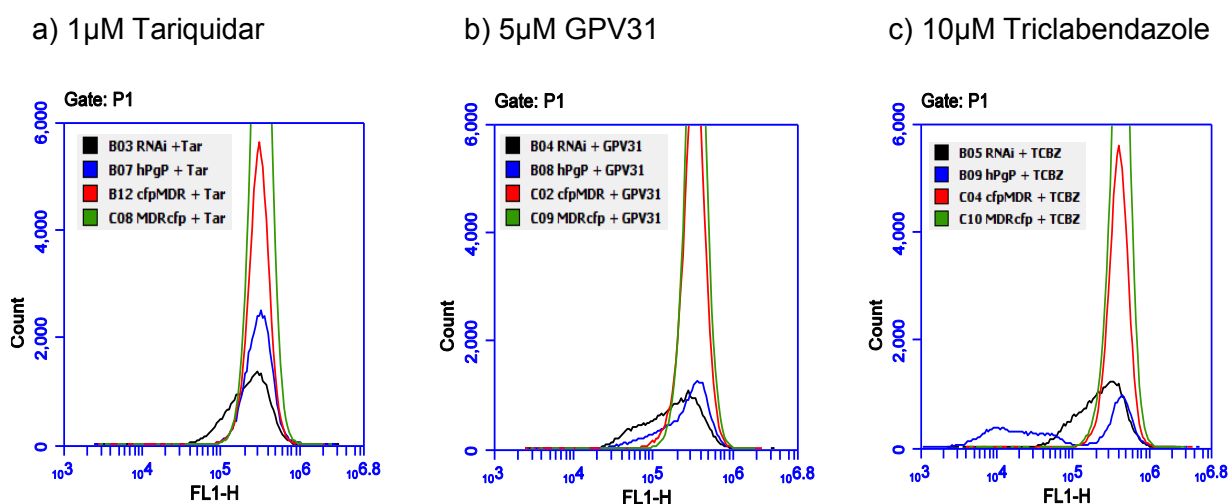


Figure 26 Rhd123 accumulation +Tar/GPV31/TCBZ

Blockers were added during loading of cells with rhd123 on 37°C –untransfected RNAi cells, transiently transfected hPgP, CFP FhMDR and FhMDR CFP a) additional tariquidar [1µM] b) additional GPV31 [5µM] c) additional Triclabendazole [10µM]. Measurement was performed on ice.

Results from Figures 25 and 26 relevant for CFP FhMDR were summarized in Figure 27 to show in detail the accumulation intensity of rhd123 in CFP FhMDR expressing cells. Main focus was set on the most promising results related to the unblocked sample showing less intracellular accumulation to TCBZ blocked CFP FhMDR as indicated by arrows.

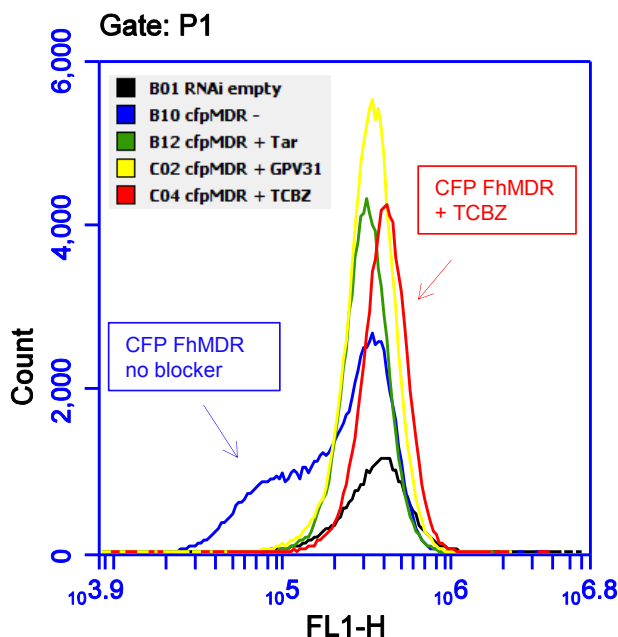


Figure 27 Rhd123 accumulation of CFP FhMDR +/- blocker

CFP FhMDR samples either with additional tariquidar [1 μ M], GPV31 [5 μ M] or TCBZ [10 μ M]; effluxing population was tagged by blue arrow whereas blocked TCBZ sample is illustrated with red arrow.

As these first preliminary data were promising the experiments will be repeated with a cell line stably expressing the transporter.

3.2 FhepSLC6/Taurine transporter and the human orthologue hTauT

3.2.1 Cloning-strategy and verification of localization via fluorescence microscopy

3.2.1.1 FhepSLC6

So far, knowledge about biochemical pathways playing an important role in the life of *Fasciola hepatica* is limited. In order to identify new fluke proteins, parasite sequence databases were evaluated (bioinfosecond.vet.unimelb.edu.au (Gasser laboratory)). Searching against the human transporter for the neurotransmitter serotonin, partial sequences of putative orthologue transporters were found. The highest similarities were

found to a putative taurine transporter in *Fasciola hepatica* (Fh_contig15063). Starting from these 839 bp sequence, primers were designed (Taurin Race 1-6) for final identification of C- and N- terminal sequences using RACE. With this method we could determine the full-length sequence of the transporter and named it FhepSLC6. Full-length cDNA was generated using the primer pair Taurin ATG fw and Taurin stop rv (Fig. 28a) and cloned into peYFP-C1 vector via restriction enzymes XhoI and KpnI, for further expression in mammalian cells. Verification of the full-length sequence of YFP FhepSLC6 was provided by a control digest using BamHI. This enzyme cuts within the cloned YFP FhepSLC6 resulting in an expected band around 1.4 kb, which was visualized by gel electrophoresis. Within the N-terminally tagged CFP version no positive sample could be found. After sequencing, YFP FhepSLC6 sample#3 was verified for containing the matching sequences (Fig. 28b).

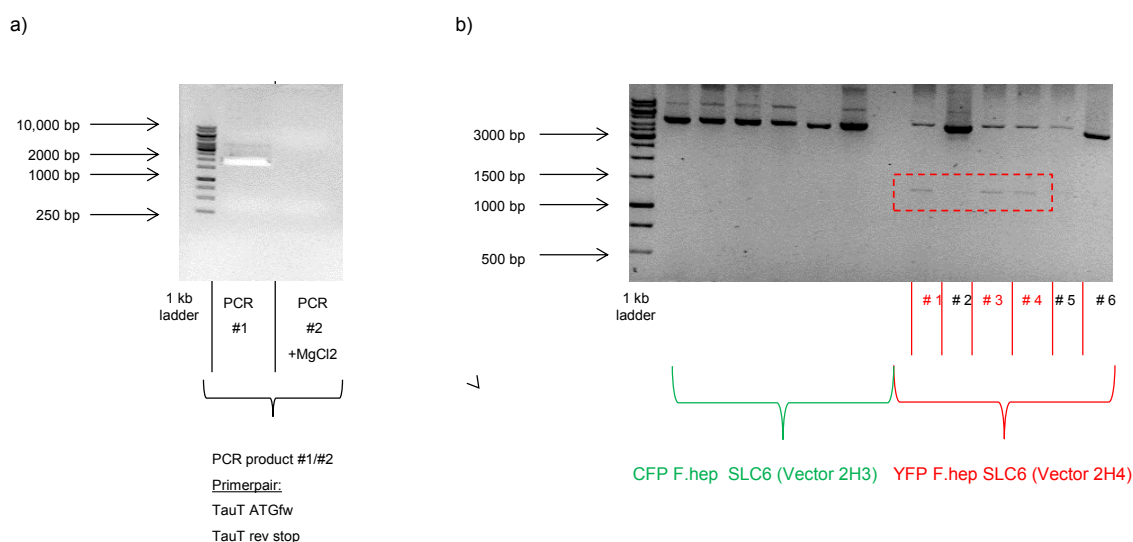


Figure 28 Amplification and cloning of FhepSLC6

a) PCR products either with or without additional $MgCl_2$ generated by amplification via primerpair TauT ATG fw and TauT rev stop); PCR #1 was cut out, purified and restriction digest was performed using enzymes XhoI/KpnI. b) Control digest by restriction enzyme BamHI after insertion to peCFP-C1 and peYFP-C1. Dotted red square showing weak bands at expected height of 1.4 kb in sample #1/#3/#4;

The hence generated YFP FhepSLC6 DNA sequence was missing a 26 bp fragment as compared to the original one, most likely due to the formation of a hairpin loop of the mRNA during cDNA synthesis. To insert the missing sequence, flanking primers (RACE6 and TauT repair fw) were used to generate a double stranded 180 bp DNA fragment including the missing 26 bp out of fluke cDNA. After amplification of this short double stranded DNA sequence, the fragment was directly loaded onto a 3% (w/v) agarose gel, the desired band at 180 bp was cut out and purified (Fig. 29). The product was immediately used as primer (due

to its length termed as megaprimer) for mutagenesis to introduce the missing sequence by “QuikChange site directed mutagenesis Kit[®]”.

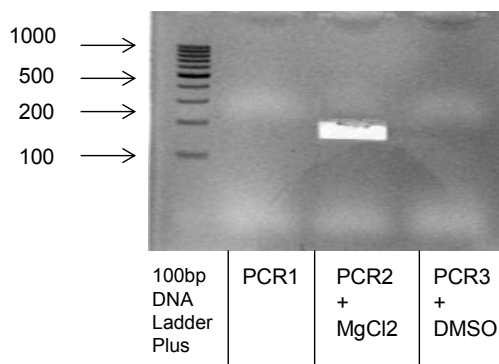


Figure 29 Taurine dsMegaprimer for QuikChange (Mutagenesis)

dsPrimer to introduce missing sequence amplified via PCR by using template from reverse transcriptase (from fluke RNA) and primers Taurine RACE6 and TauTrepair fw 250nM each; PCR1/PCR2/PCR3: number is according to additional components as MgCl₂ or DMSO to PCR reaction; PCR reactions were loaded onto 3% agarose gel. PCR2 was cut out and purified.

Mutated plasmids were isolated and subjected to diagnostic restriction digest using Bsu15I/ClaI and EcoRI (Fig. 30).

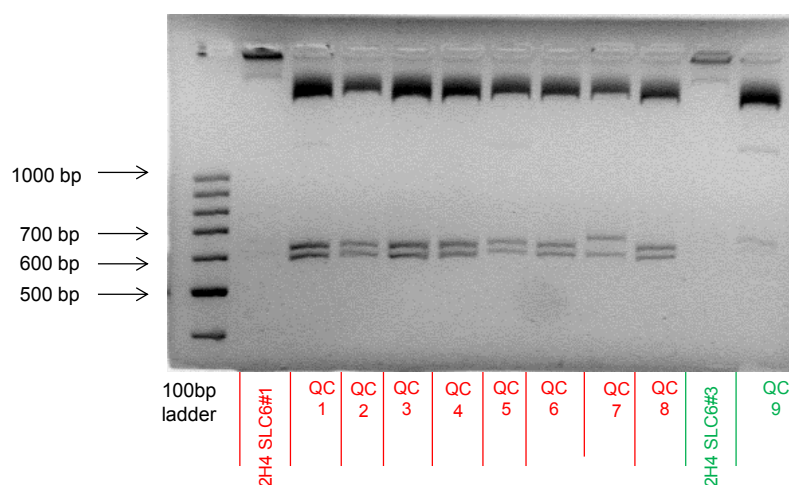


Figure 30 Bsu15I/ClaI and EcoRI control digest after mutagenesis.

Introduction of missing 26bp fragment was performed via QuikChange mutagenesis using a “megaprimer”. Control restriction digest was performed using restriction enzymes Bsu15 (CLaI) and EcoRI 2H4 SLC6#1= N-terminally tagged YFP SLC6 DNA clone#1 (colour code red) control digest of plasmid before QC; numbers QC1-8 indicates the sample of the miniprep. 2H4 SLC6#3=N-terminally YFP tagged SLC6 DNA clone#3 (colour code green) control digest of plasmid before mutagenesis.

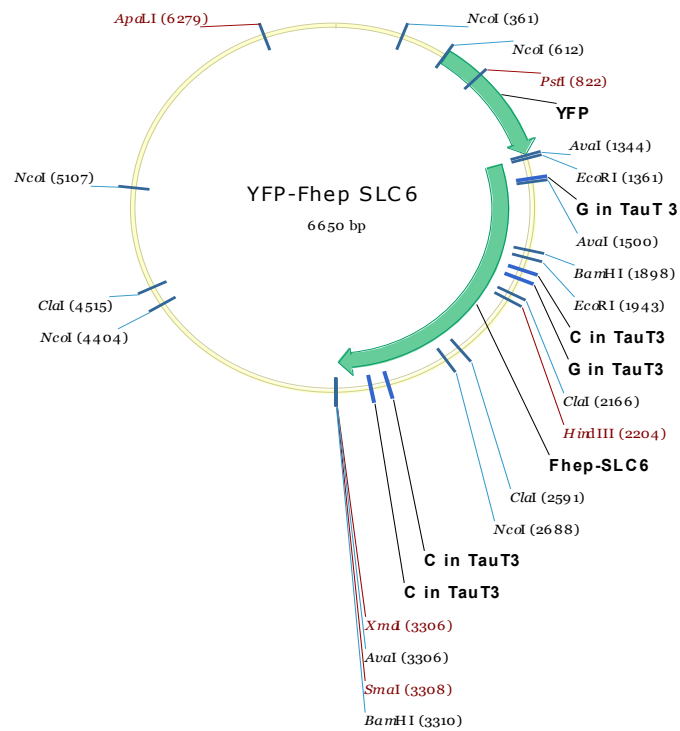


Figure 31 N-terminally YFP tagged FhepSLC6

YFP FhepSLC6 was cloned via EcoRI and BamHI restriction sites into peYFP-C1 vector. Polymorphisms of two sequenced clones are indicated.

The N-terminally YFP tagged version of the taurine transporter (YFP FhepSLC6, Fig. 31) was transfected into HEK293 cells using jetPrime[®] transfection reagent. Three days post transfection the localization of the transporter was evaluated by microscopy. YFP FhepSLC6 is expressed mainly at the plasma membrane (Fig. 32).

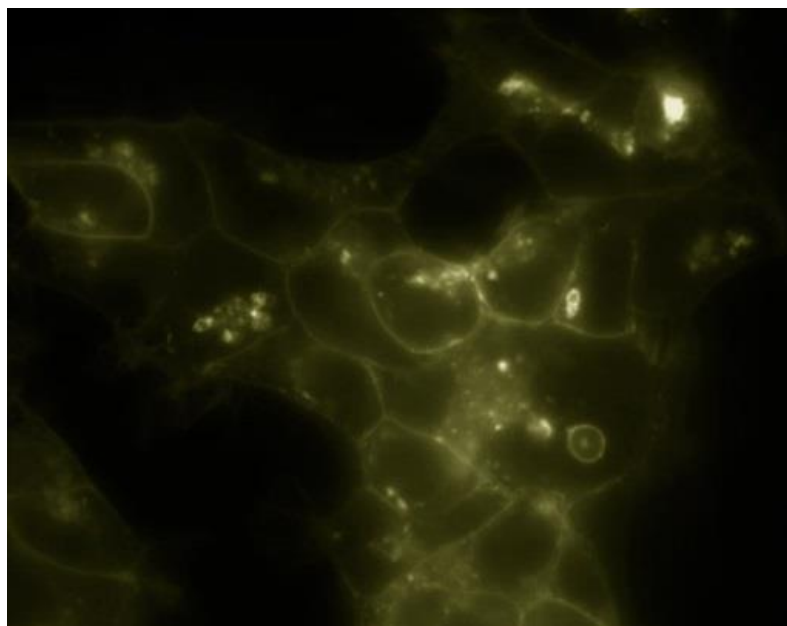


Figure 32 YFP FhepSLC6

HEK293 cells transiently expressing YFP FhepSLC6 were visualized via epifluorescence microscopy to confirm localization of the taurine transporter of *Fasciola hepatica* (modified in color by AdobePhotoshop).

The same results could be observed in an established stable cell line which was selected under the influence of the antibiotic G418, a neomycin derivative.

Based on an encoded neomycin resistance cassette in the plasmid, only transfected cells could survive the antibiotic treatment.

3.2.1.2 Human taurine transporter hTauT

The human orthologue of FhepSLC6 (taurine transporter, hTauT) was cloned from HEK293 cells as an appropriate control for functional analysis. HEK293 cells are known to express the human taurine transporter at low levels. Therefore it was amplified from isolated RNA from HEK293 cells using specific sense and antisense primers (see 2.1.1.4). Resulting fragments were digested using BamHI and HindIII and cloned into peCFP-C1 and peYFP-C1 vectors cut with the same enzymes. Amplification of hTauT was performed as described in section 2.2.1.4 and the PCR product was loaded onto a 1.5% agarose gel (Fig. 33 a/b).

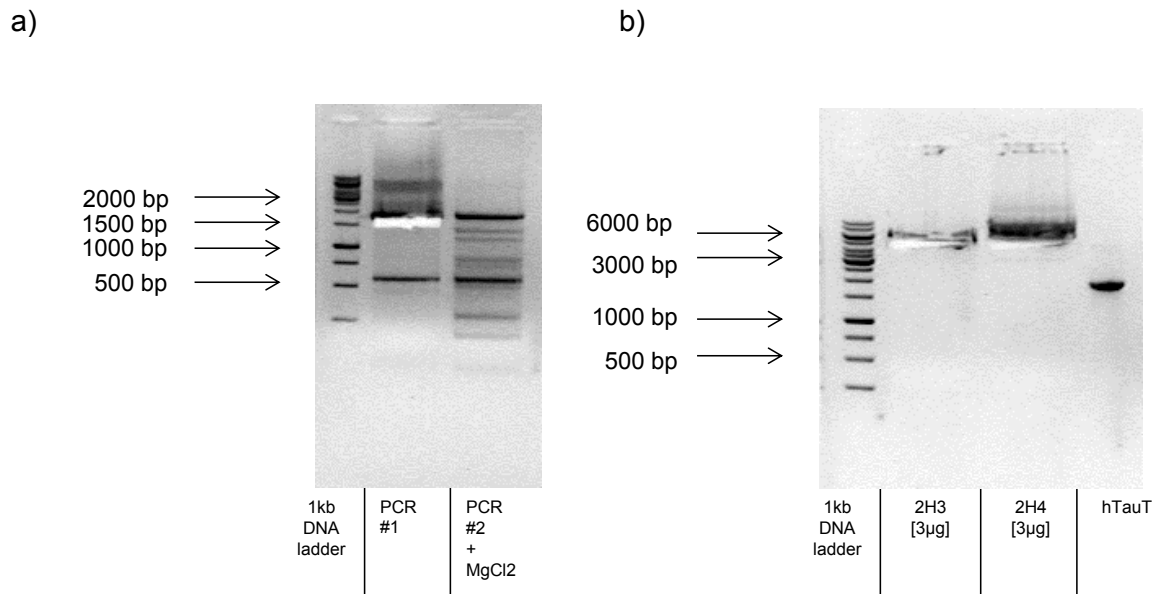


Figure 33 Amplification and cloning of hTauT

a) PCR amplification of hTauT from cDNA of HEK293 cells via primerpair hTauT fw and hTauT rev. PCR#2 contains additional $MgCl_2$ within PCR reaction; b) Restriction digest by BamHI and HindIII of 2H3=peCFP-C1, 2H4=peYFP-C1 using $3\mu g$ each and as a control digested hTauT PCR sample.

Cloned hTauT cDNA (1863bp) was verified by sequence analysis (Fig. 34).

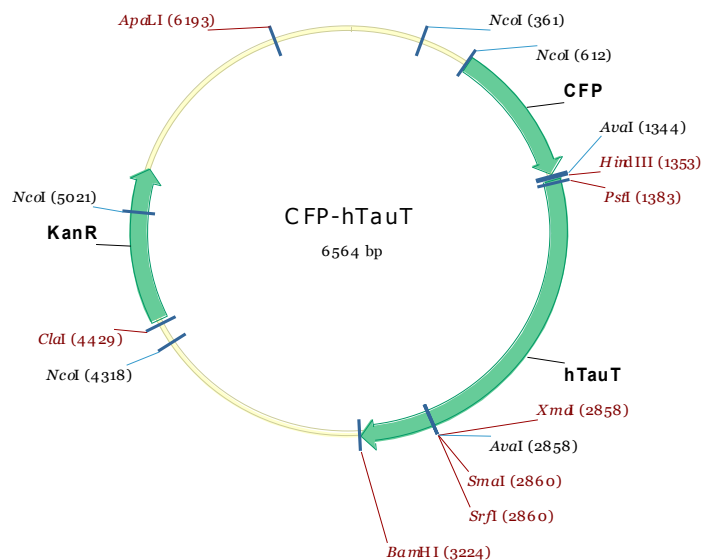


Figure 34 Vector scheme of CFP hTauT.

Map of N-terminally CFP tagged version of the human taurine transporter (6564 bp). Single-cutting sites are pictured in brown and other restriction enzyme sites in black.

HEK293 cells were transfected with CFP hTauT using jetPrime. Expression levels and cellular localization of the transporter were analyzed by epifluorescence microscopy (Fig. 35). N-terminally tagged CFP hTauT is expressed at the plasma membrane in HEK293 cells.

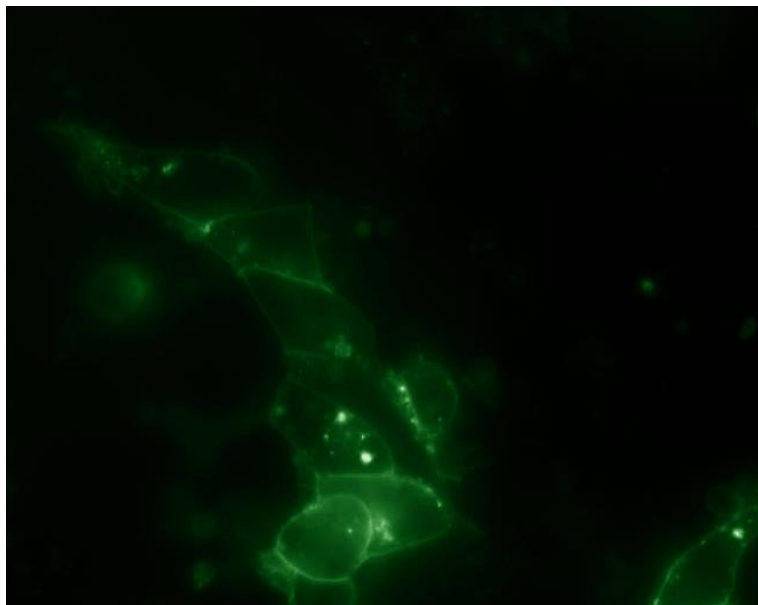


Figure 35 hTauT expressed in HEK293 cells

Analysis of transfected HEK293 cells expressing CFP hTauT at the plasma membrane via epifluorescence microscopy (Picture was optimized in color by AdobePhotoshop).

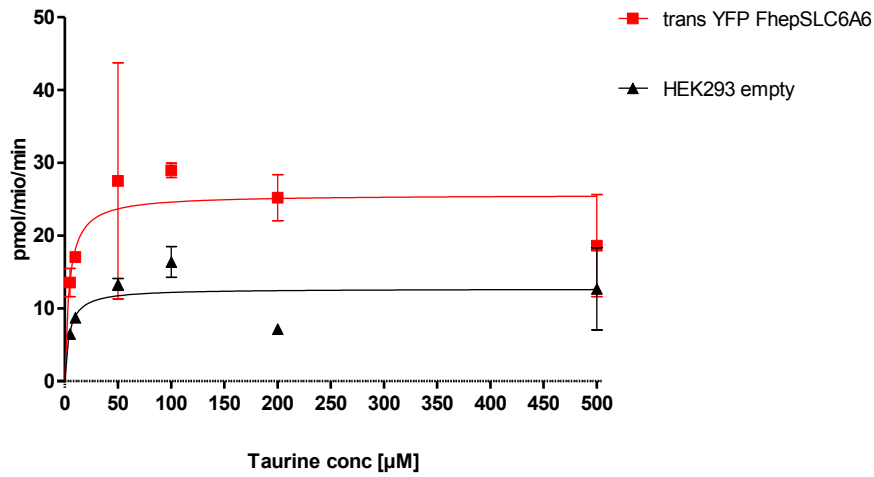
A stable cell line for CFP hTauT was established in HEK293 cells mediated by jetPrime[®] transfection and selection with G418 as described for YFP FhepSLC6.

3.2.2 Functional activity

3.2.2.1 Uptake: Substrate specificity

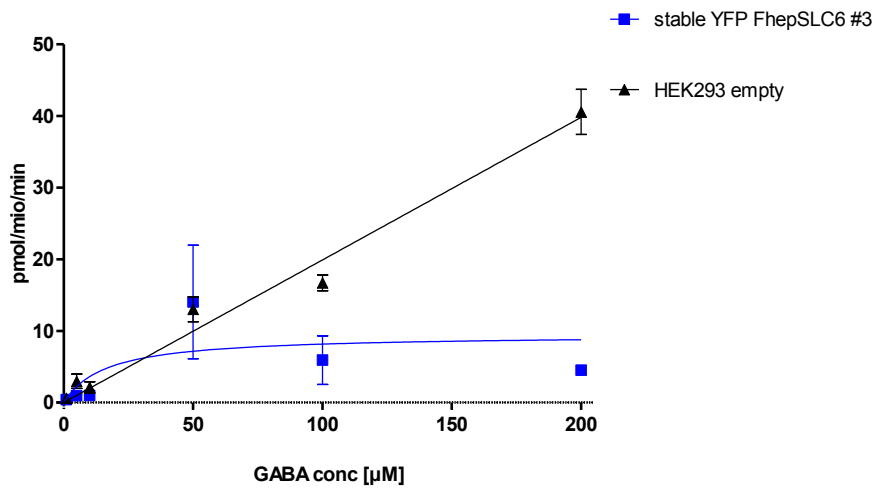
In order to analyze the transport properties of the newly identified transporter (FhepSLC6), HEK293 cells expressing the transporter were exposed to various radioactively labelled compounds. In the first round of experiments the amino acids taurine, GABA, glycine and glutamate were tested (Fig. 36a-d). For these experiments cells were exposed to increasing concentrations of the substrate (see 2.2.5). Non-specific uptake (termed background) was determined in the presence of appropriate blockers. Obtained uptake rates and substrate affinities were calculated using GraphPadPrism5.0, and further compared to the transport rate of non-transfected HEK293 cells acting as negative control.

a)

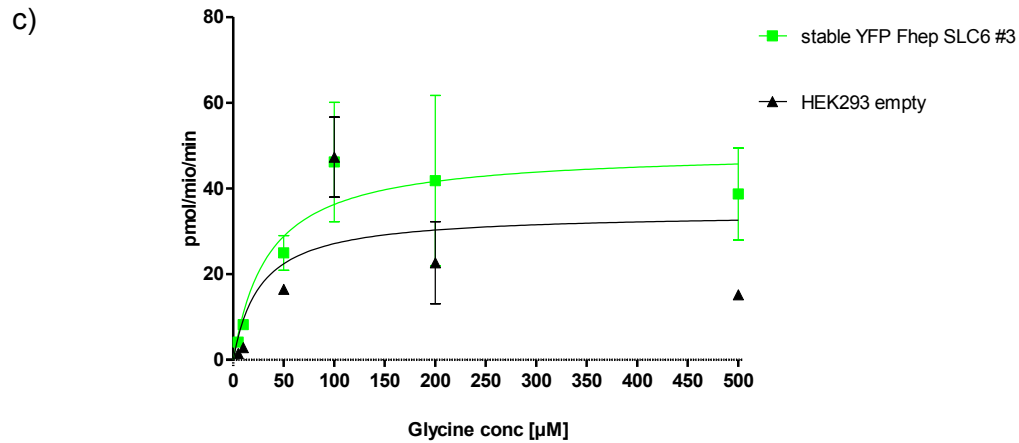


	YFP Fhep SLC6	HEK293 empty
One site binding (hyperbola)		
Best-fit values		
Bmax	25.61	12.69
Kd	4.068	4.117

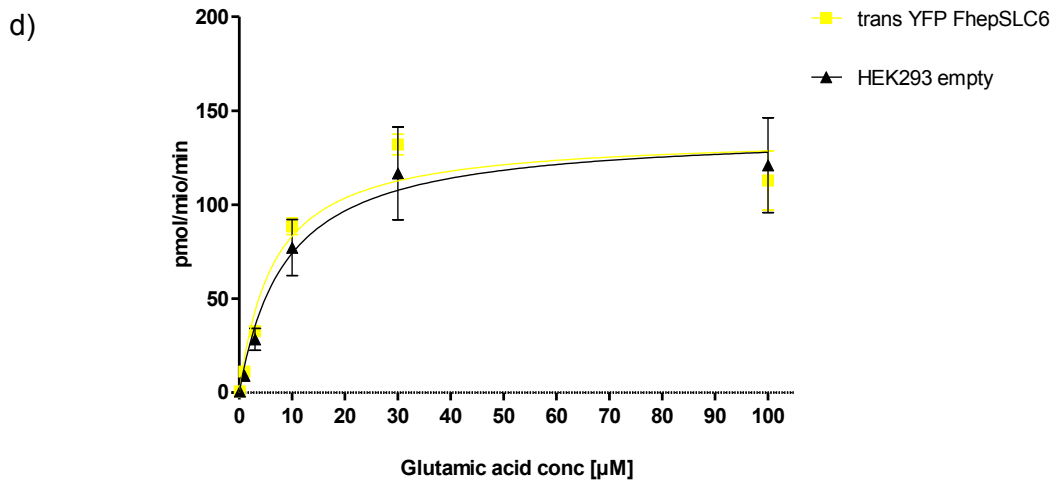
b)



	stable YFP FhepSLC6 #3	HEK293 empty
One site binding (hyperbola)		Ambiguous
Best-fit values		
Bmax	9.488	$\sim 2.749\text{e}+015$
Kd	16.23	$\sim 1.381\text{e}+016$



	stable YFP Fhep SLC6 #3	HEK293 empty
One site binding (hyperbola)		
Best-fit values		
Bmax	48.87	34.31
Kd	34.71	26.48



	trans YFP FhepSLC6	HEK293 empty
One site binding (hyperbola)		
Best-fit values		
Bmax	136.9	139.1
Kd	6.446	8.758

Figure 36 [^3H]-Taurine/[^3H]-GABA/[^3H]-Glycine/[^3H]-Glutamic acid uptake;

Representative dose-response-curves of tritiated a) taurine; b) GABA; c) Glycine; d) Glutamic acid to verify substrate specificity of FhepSLC6. YFP FhepSLC6: HEK293 cells expressing the *F. hepatica* transporter; HEK293 empty: non transfected HEK 293 cells.

Although HEK293 cells expressing YFP FhepSLC6 showed uptake of glycine and taurine slightly above background levels, rates were much lower than expected.

Therefore, YFP FhepSLC6 was exposed to different substrates of other transporters of the SLC6 family carried out as single-point uptake experiment.

[³H]-dopamine, [³H]-5HT and [³H]-MPP⁺ which are known to be transported by DAT (dopamine transporter), SERT (serotonin transporter) or NET (norepinephrine transporter) were tested using appropriate blockers in a final concentration of 100μM (Table 12). As anticipated, none of the tested substances showed specific uptake via the expressed FhepSLC6. Raw measurement data were ranging within the background or did not indicate a transport potential to the exposed substrates (data not shown).

Table 12 [³H]-Dopamine, [³H]- 5HT, [³H]- MPP⁺ one point uptake.

Final concentrations of [³H] substances and associated blockers including appropriate preincubation and uptake times.

Substrate [μM]	Blocker [100μM]	Preincubation / uptake time
[³ H]-Dopamine [0.1μM]	Desimipramine	5' / 1'
	Nisoxetine	
	Mazindol	
[³ H]-5HT [0.1μM]	Clomipramine	5' / 1'
	Cocaine	
	Paroxetine	
[³ H]-MPP ⁺ [0.015μM]	Clomipramine	5' / 3'
	Cocaine	
	Paroxetine	

So far it was not possible to confirm transport properties or substrate specificities of the cloned FhepSLC6. Comparison to empty HEK293 cells revealed no significant difference in the active transport of any tested substance.

It is known that HEK293 cells endogenously express taurine transporters which could interfere with or mask data of the *Fasciola hepatica* taurine transporter.

To overcome this problem, a siRNA knockdown for human taurine transporter was performed in native HEK293 and FhepSLC6 expressing cells. This knockdown was performed using

two different siRNAs purchased from Invitrogen, followed by [³H]-taurine uptake according to standard protocols.

Validation of these dose response curves (Fig. 37) show a reduced uptake of taurine after knock-down, without leading to a difference in cells expressing the *Fasciola hepatica* transporter and empty cells.

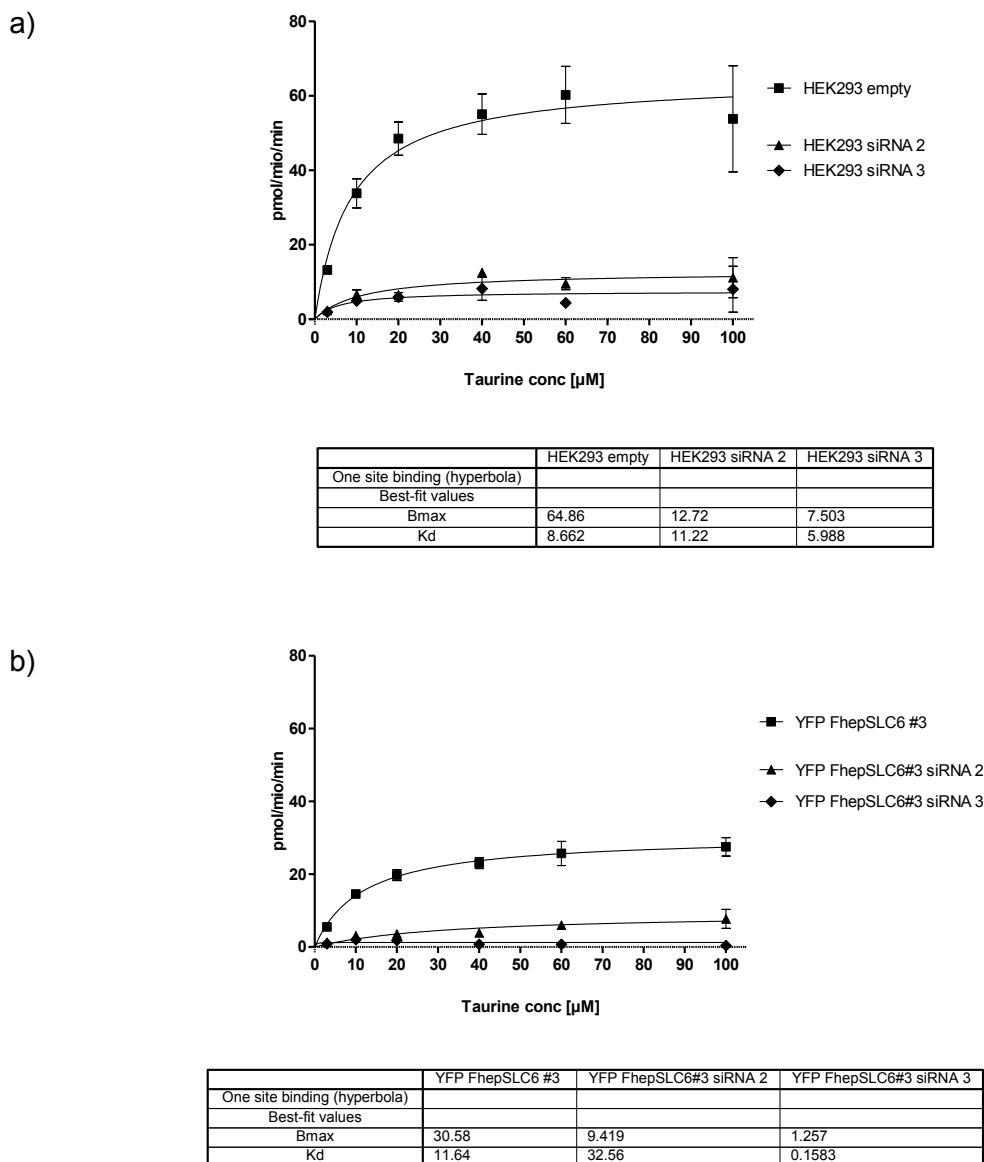


Figure 37 Saturation of [³H]-Taurine uptake in siRNA knockdown cells.

Endogenously expressed taurine transporter of HEK293 cells was knock downed by siRNAs #2/#3; a) [³H]-taurine uptake by HEK293 cells, which had been transfected with the indicated siRNAs and - as a control – untransfected HEK293 cells ; squares: untransfected HEK293, triangles: siRNA#2 transfected HEK293, rhombus: siRNA#3 transfected HEK293 b) [³H]-taurine uptake by YFP FhepSLC6 (stable cell line in HEK293) transfected with siRNA #2/#3 and- as a control untransfected YFP FhepSLC6 cells. squares: untransfected YFP FhepSLC6, triangles: siRNA#2 transfected YFP FhepSLC6, rhombus: siRNA#3 transfected YFP FhepSLC6;

Due to these findings, functional activity of the transporter still remained unclear or rather indicated a non-evaluable transporter function of YFP FhepSLC6.

To broaden the spectrum of controls within these functional assays a positive control was introduced - the human taurine transporter (hTauT). After amplification of the full-length sequence the N-terminally CFP tagged version of termed CFP hTauT was stably expressed in HEK293 cells and compared to the fluke transporter. Results gave a K_m value of 5-18 μ M for hTauT implicating a high affinity for the substrate taurine.

3.2.2.2 Uptake: temperature dependency of FhepSLC6

First uptake experiments with hTauT did not reveal transport rates clearly distinguishable from native HEK293 cells (data not shown). The next step within characterization and validation of taurine transporter function was to optimize the temperature conditions of our assay.

Although it is known that transmembrane transporters have an optimum function on 37°C all experiments were performed at room temperature so far. Previous experiments on other SLC6 transporters in the lab perfectly worked out at room temperature. Based on literature about taurine uptake experiments on human or mouse taurine or GABA transporters (Zhou *et al.*, 2012; Satsu *et al.*, 2003) we suggested that this transporter could show a higher dependency on temperature than other SLC6 transporters.

To support this theory a [³H]-taurine uptake assay on FhepSLC6 at three different temperatures was performed: I) 37°C, expected to be the ideal condition II) 18°C, chosen as lowest reasonable room temperature and III) wet ice, which should completely inactivate transport function (hTauT served as a positive control)

Dose response curves were fitted via GraphPadPrism5.0 showing an enormous increase in uptake ability on 37°C (Fig. 38).

This assay supported our hypothesis that the cloned taurine transporter of *Fasciola hepatica* is functionally active but is highly temperature dependent.

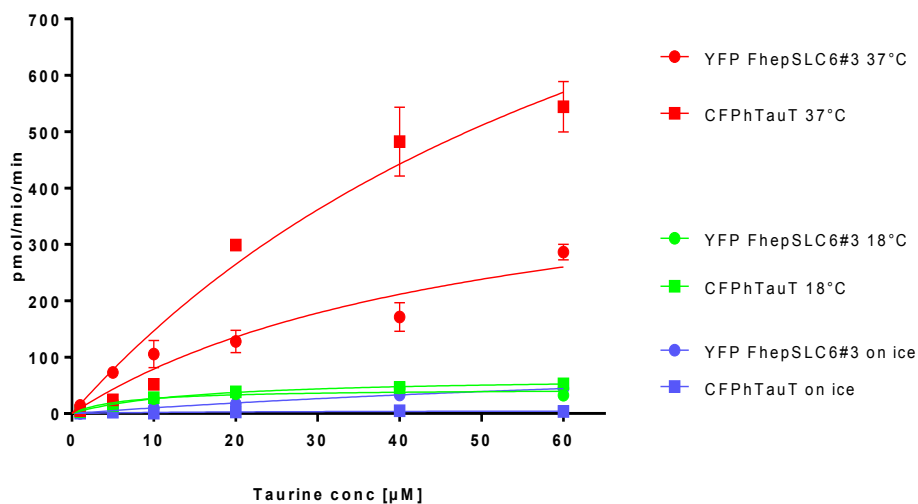


Figure 38 [³H]-Taurine uptake related to temperature

Dose-response curves of [³H]-taurine uptake to demonstrate dependency on temperature of either *Fh* or *h* TauT. red: uptake experiment on 37°C. In green: uptake performed on 18°C. In blue: uptake performed on ice. circles: Fhep SLC6; squares: hTauT

3.2.2.3 Uptake: time dependency of FhepSLC6

So far, I evaluated substrate specificity and temperature dependency of the taurine transport, the next step within the characterization of FhepSLC6 was based on the determination of the transport velocity.

Therefore either FhepSLC6 or empty HEK293 cells were exposed to [³H]-taurine for different time points including 1/3/6/10/15/20/30/45 minutes. Time points were standardized to non-specific uptake by measuring the uptake in the presence of the taurine transporter blocker β -alanine [1mM].

Curves (Fig. 39a) show either non-specific uptake (background), total uptake or specific uptake under subtraction of background.

For further optimization of the experiments, it was crucial to define an uptake time showing a high signal to noise ratio, without reaching saturation. Referring to generated data 5 to 10 minutes uptake time turned out to be optimal for FhepSLC6. Uptake time for hTauT was set to 3-5 min.

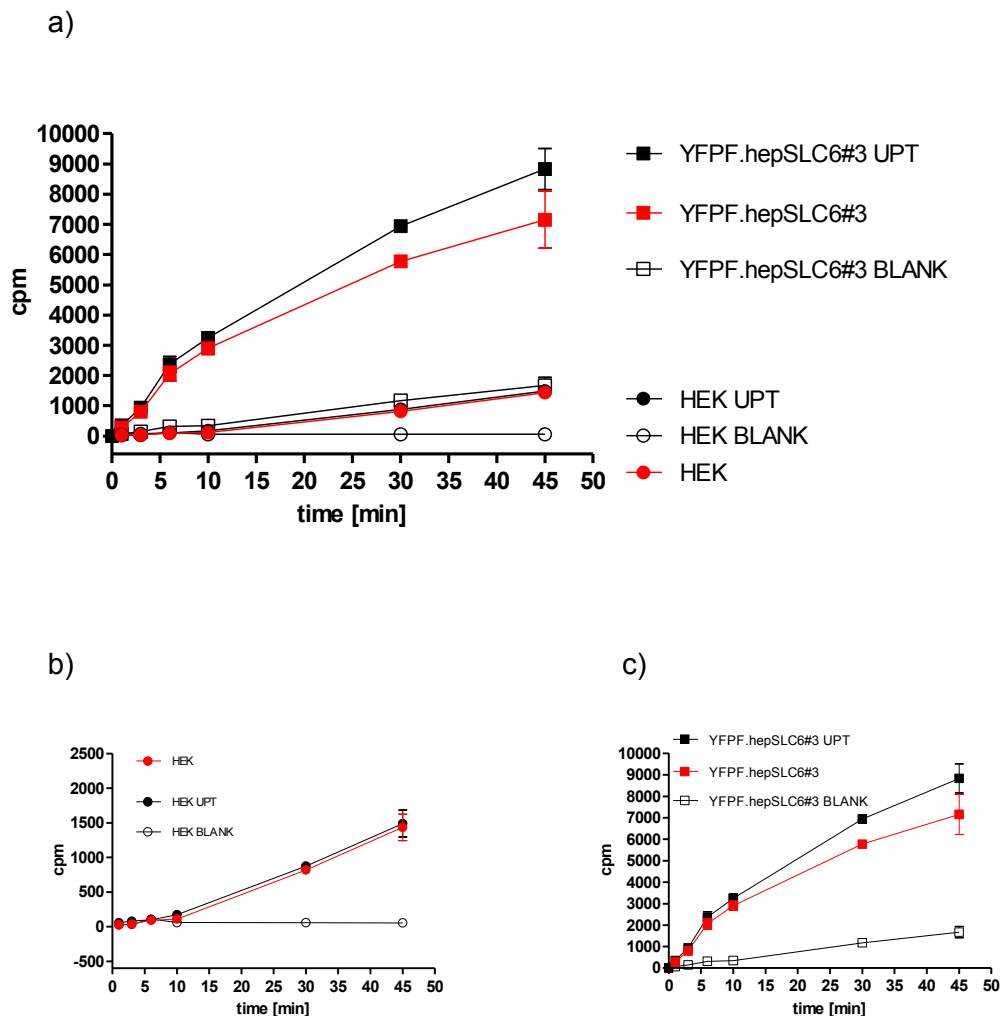
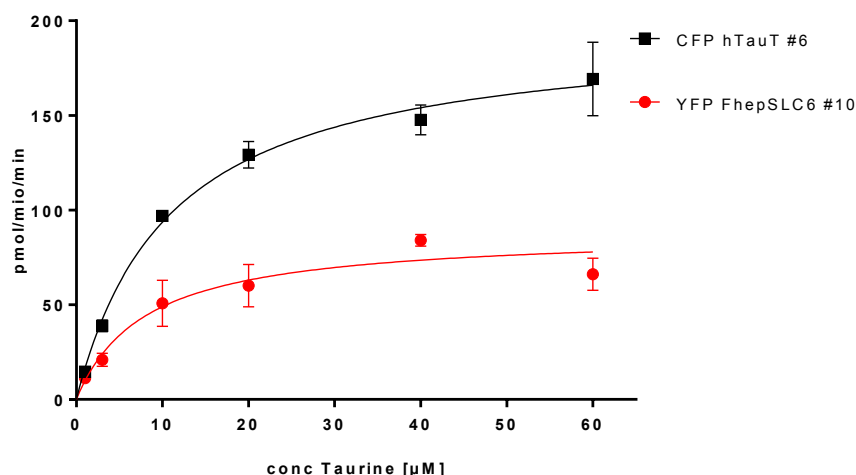


Figure 39 Time dependent [³H]-Taurine uptake

Uptake was performed on 37°C at 6 different time points (1/3/6/10/30/45 minutes) ; YFP FhepSLC6 clone#3 (squares) HEK 293 cells expressing the *F. hepatica* transporter; HEK293 (circles) non transfected HEK293 cells.. Samples were plotted cpm versus time [min] a) fitted curves on all samples b) single view of HEK293 cells c) single view on YFP FhepSLC6 #3; Blank(open symbols) is representing background according(β -alanine 1mM final concentration) total uptake(black filled symbols) [³H] taurine uptake in the absence of a blocker; Red curves: specific uptake

Uptake performed under optimized conditions showed comparable affinities of the human and the *F. hepatica* transporter for taurine (K_m 8 and 10 μ M respectively) as shown in Fig. 40. Differences in the V_{max} values are most likely due to either faster transport of taurine via the human transporter or higher expression levels of the human transporter in the stable cell lines.



	YFP FhepSLC6 #10	CFP hTauT #6
One site binding (hyperbola)		
Best-fit values		
Bmax	88.30	196.2
Kd	8.032	10.95

Figure 40 [³H]-Taurine uptake referring to optimal conditions

Experimental design was performed under optimal conditions for YFP FhepSL6 and hTauT as a reference. Uptake time was set up to 5 minutes for FhepSLC6 and 3 minutes for CFP hTauT on 37°C.

3.2.2.4 Inhibition

The next steps within functional characterization of FhepSLC6 were inhibition experiments. In order to evaluate the affinity of different blockers for FhepSLC6 (displayed by corresponding IC_{50} values) a pharmacological inhibition assay was performed based on related uptake results. The unit IC_{50} is defined by the concentration of antagonist which inhibits half of the maximum transport of substrate. Using GraphPadPrism5.0 as analyzing software, agonist function was plotted at the y-axis in % of uptake against logarithmic concentration of blocker. For these assays, cells were exposed to one constant concentration of the substrate (taurine) and increasing concentrations of putative blockers or other substrates.

Bröer *et al* recently characterized blockers of the human taurine transporter including β -alanine with a calculated IC_{50} of about 100 μ M and guanidinoethyl sulfonate (GES) with a predicted IC_{50} value of 50 μ M (Bröer *et al.*, 2012). Furthermore GABA was tested as it is known to act as a low affinity substrate (K_m 1.5mM) on the taurine transporter (Zhou *et al.*, 2012). Detailed experimental design is shown in 2.2.6.

Inhibition assays were performed by exposing FhepSLC6 and hTauT to the high affinity antagonist β -alanine or the low affinity substrate GABA within a serial dilution of 0-1mM or 0.001-10mM respectively under constant [3 H]-taurine concentration. Referring to the dose response curves fitted in Fig. 41a/b we were able to support the hypothesis that β -alanine is a high affinity blocker for taurine uptake either within FhepSLC6 or CFP hTauT. IC_{50} values were in a similar range of 59 and 117 μ M, respectively (Fig. 41a).

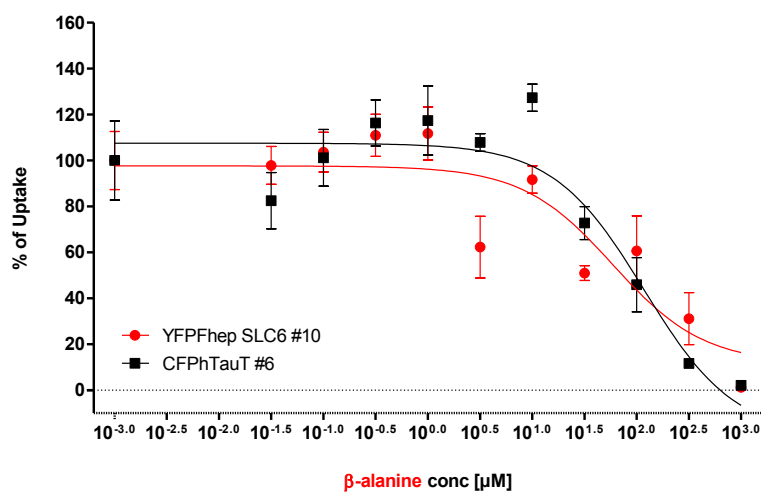
GABA was reported to be transported via taurine transporters and vice versa. Therefore the taurine transporter is also known as a low affinity GABA transporter with reported affinity of 1.5mM for GABA. GABA blunted taurine transport with an IC_{50} value of 0.6mM for FhepSLC6 and 1.4mM for hTauT (Fig. 41b) which fits to reported affinities for GABA for the hTauT of 1.2mM. To test whether GABA has a statistically significant higher affinity for the *F. hepatica* compared to its human counterpart further experiments have to be performed.

Guanidinoethyl sulfonate (GES) as a taurine analogue is another known inhibitor of the taurine transporter (Sergeeva *et al.*, 2002).

Data shown in Fig. 41c supported the hypothesis of GES being a competent blocker for hTauT resulting in an IC_{50} around 135 μ M. Nevertheless; it did not act within the same affinity on FhepSLC6 displayed by an IC_{50} value almost 20 times higher (2.3mM) when compared to hTauT. This led to the assumption of GES being a rather low affinity blocker for FhepSLC6 resulting in high doses of blocker needed for complete inhibition.

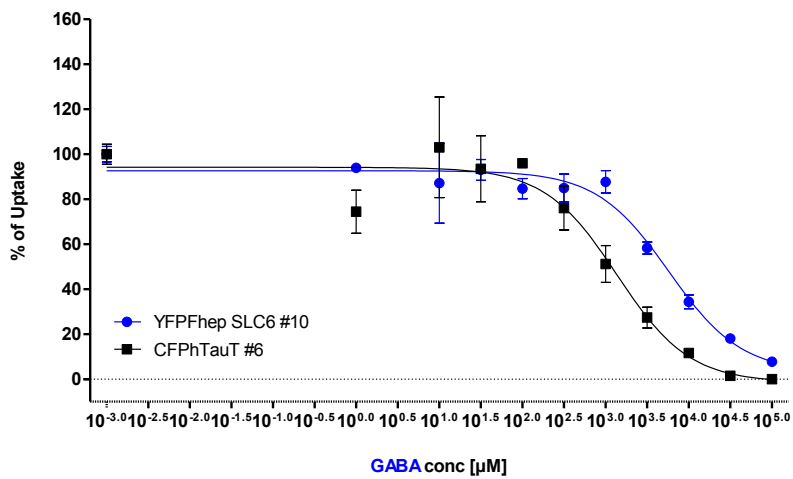
The anticonvulsive drug tiagabine is a blocker of GABA transporter (GAT) with a reported affinity in the range of 50-100nM. As taurine and GABA transporters are highly homologous the effect of tiagabine on the taurine transporter was tested. No effect, neither on FhepSLC6 nor on hTauT, could be observed even in concentrations as high as 100 μ M as visualized in Fig. 41d.

a)



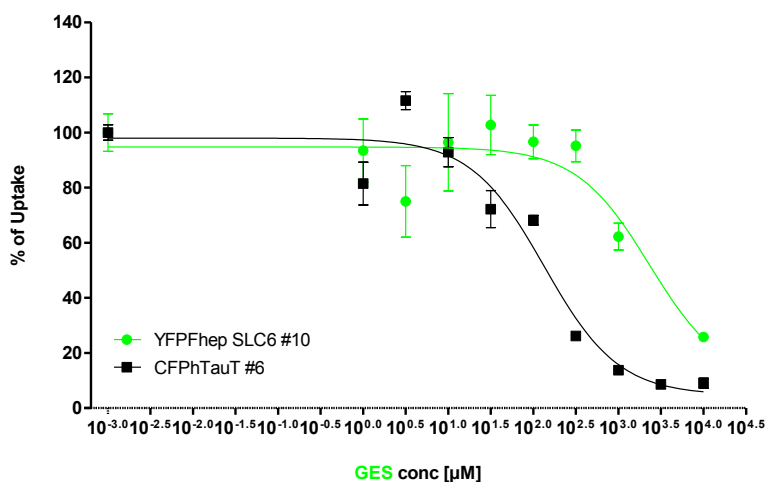
	YFPFhep SLC6 #10	CFPhTauT #6
One site competition		
Best-fit values		
Bottom	11.59	-20.00
Top	97.63	107.5
LogEC50	1.772	2.070
EC50	59.12	117.4

b)



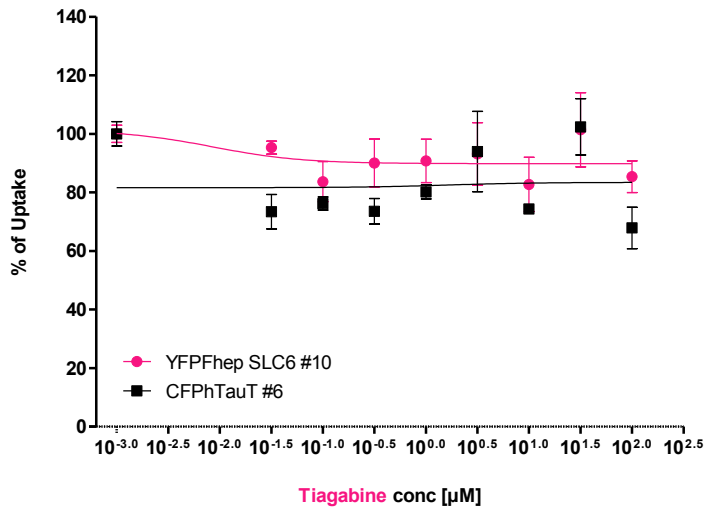
	YFPFhep SLC6 #10	CFPhTauT #6
One site competition		
Best-fit values		
Bottom	3.003	-1.503
Top	92.66	94.19
LogEC50	3.762	3.138
EC50	5774	1373

c)



	YFPFhep SLC6 #10	CFPhTauT #6
One site competition		
Best-fit values		
Bottom	8.874	4.660
Top	94.74	97.98
LogEC50	3.369	2.130
EC50	2338	135.0

d)



	YFPFhep SLC6 #10	CFPhTauT #6
One site competition		
Best-fit values		
Bottom	89.81	83.43
Top	101.3	81.61
LogEC50	-2.070	0.2120
EC50	0.008505	1.629

Figure 41 Inhibition curves of different blockers

Inhibition curves and related IC₅₀ values generated by using different substances to block uptake of 0.2 µM [³H]-taurine. coloured curves show inhibition for YFPFhepSLC6 ;CFPhTauT is shown in black a) β-alanine inhibition 0-1mM b) GABA 0-100mM, c) guanidinoethyl sulfonate 0.001µM-1mM d) Tiagabine 0-100µM

The aim of these studies was to find chemical compounds that in future can be used to treat *F. hepatica* infection. The affinity for taurine is almost identical for *F. hepatica* and human taurine transporters. The same holds true for the inhibitory potency of β -alanine and GABA. Differences in the affinity of GES to hTauT and FhepSLC6 indicated the first promising trend towards a possible species-specific distinction of substances.

Development of new anthelmintic drugs could therefore be based on these findings. Although in this case the substance has a higher affinity for the human than for the *F. hepatica* transporter.

4 Conclusion & Outlook

During my master thesis I have cloned the first two full-length transmembrane transporters of the common liver fluke, *Fasciola hepatica*, named FhMDR and FhepSLC6.

The main focus of this work was set on the identification and functional characterization of ABC transporters of *Fasciola hepatica*. These proteins are thought to play a major role in the development of resistance of the liver fluke to the anthelmintic drug Triclabendazole. The first of the newly identified transporters, FhMDR, belongs to the B family of ABC transporters. Transporters of this family are responsible for cellular detoxification processes in many organisms and are therefore mediators of drug resistance.

A prerequisite for the functional analysis of a transporter was its successful heterologous expression in a cell culture system. After transfection of a plasmid harboring the cDNA of FhMDR I could show localization of this transporter at the plasma membrane in HEK293 cells. Furthermore I could demonstrate an, although weak, active transport of the fluorescent dye rhodamine123 in a FACS based accumulation assay. This experimental setup is well established to analyze other proteins of the ABC transporter family, like the prototypical human P-glycoprotein (h-Pgp, ABCB1). In these experiments triclabendazole indeed reduced the transport via FhMDR, whether as a blocker or as an alternative substrate was not clear. This was the first hint that FhMDR could play a role in the onset of triclabendazole resistance. To identify the transport properties of FhMDR in more details it will be necessary to establish more robust transport assays, e.g. using a different fluorescent substrates or using membrane vesicles. The vesicle based approach would allow the measurement of the transport of substances into the vesicles and not out of cells. One of these assays could then be used to identify substances capable of blocking this transporter. These drugs would be a way to counteract a transporter mediated drug resistance.

The second transporter (FhepSLC6) belongs to the family of Na⁺/Cl⁻ dependent solute carrier transporters. FhepSLC6 displays high homologies to the group of GABA transporters of this family, the highest to the taurine transporter (SLC6A6).

I also succeeded in the heterologous expression of FhepSLC6 in HEK293 cells. In these cells I could subsequently demonstrate a highly specific, temperature sensitive transport of taurine. The transport via FhepSLC6 was comparable to the transport via its human orthologue (hTauT) albeit known blockers of hTaut showed slightly different affinities for the transporter of *Fasciola hepatica*. In many animals taurine acts as an osmolyte and is used for the conjugation of, the otherwise toxic, bile acids. The question whether *Fasciola hepatica*

needs taurine as an osmolyte, whether it is needed to detoxify the fluke from surrounding bile acids, or if taurine can be used by the fluke as nutrition has to be solved.

Although FhepSLC6 is for sure not responsible for the evolution of drug resistances, understanding its role and the necessity of taurine for the fluke still could lead to the identification of new drug targets and therefore to the development of new anthelmintic drugs, providing an alternative to Triclabendazole.

References

- (n.d.). Retrieved June 22, 2013, from <http://web.stanford.edu/class/humbio103/ParaSites2001/fascioliasis/diagrams.htm>
- Anderson, C. M., Howard, A., Walters, J. R., & Ganapathy, V. (2009). Taurine uptake across the human intestinal brush-border membrane is via two transporters: H⁺-coupled PAT1(SLC36A1) and Na⁺- and Cl⁻-dependent TauT (SLC6A6). *J. Physiol*, *587*(4), pp. 731-744.
- Bankstahl, J. P., Bankstahl, M., Römermann, K., Wanek, T., Stanek, T., Windhorst, A. D., et al. (2013). Tariquidar and Elacridar Are Dose-Dependently Transported by P-Glycoprotein and Bcrp at the Blood-Brain Barrier: A Small-Anial Positron Emission Tomography and In Vitro Study. *Drug Metab Dispos*, *41*, pp. 754-762.
- Barrera, B., Otero, J. A., Egido, E., Prieto, J. G., Seelig, A., Álvarez, A. I., et al. (2012). The Anthelmintic Triclabendazole and Its Metabolites Inhibit the Membrane Transporter ABCG2/BCRP. *Antimicrob. Agents Chemother*, *56*(7), pp. 3535-3543.
- BD Biosciences. (2000, April). Introduction to Flow Cytometry: A learning guide. *Manuel Part Number:11-11032-01*.
- Brennan, G. P., Fairweather, I., Trudgett, A., Hoey, E., McCoy, McConville, M., et al. (2007). Understanding triclabendazole resistance. *Experimental and Molecular Pathology*, *82*, pp. 104-109.
- Brian, K. E. (1999). *Taxonomic classification*. Retrieved July 2014, from <https://www.msu.edu/course/zol/316/fheptax.htm>
- Bröer, S., & Gether, U. (2012). The solute carrier 6 family of transporters. *British Journal of Pharmacology*, *167*, pp. 256-278.
- Chen, C., Chin, J. E., Kazumitsu, U., Clark, D. P., Pastan, I., Gottesman, M. M., et al. (1986). Internal Duplication and Homology with Bacterial Transport Proteins in the *mdr1* (P-Glycoprotein) Gene from Multidrug-Resistant Human Cells. *Cell*, *47*, pp. 381-389.
- Chiba, P., Ecker, G., Schmid, D., Drach, J., Tell, B., Goldenberg, S., et al. (1996). Structural requirement for activity of propafenone-type modulators in P-glycoprotein-mediated multidrug resistance. *Mol Pharmacol*, *49*, pp. 1122-1130.
- Dawson, R. J., & Locher, K. P. (2006). Structure of a bacterial multidrug ABC transporter. *Nature*, *443*, pp. 180-185.
- Dean, M., Rzhetsky, A., & Allikmets, R. (2001). The Human ATP-Binding Cassette (ABC) Transporter Superfamily. *Genome Res*, *11*, pp. 1156-1166.
- Dusak, A., Onur, M., Cicek M, Firat, U., Ren, T., & Dogra , V. S. (2012). Radiological Imaging Features of Fasciola hepatica infection-A Pictorial Review. *J Clin Imaging Sci*, *2*(2).
- Eckert, J., Friedhoff, K. T., Zahner, H., & Deplazes, P. (2008). *Lehrbuch der Parasitologie für die Tiermedizin*. Enke Verlag Stuttgart.
- Emanuelsson, O., Nielsen, H., Brunak, S., & von Heijne, G. (2000). Predicting subcellular localization of proteins based on their N-terminal amino acid sequence. *J.Mol.Biol.*, *300*, pp. 1005-1016.
- Fairweather, I. (2009). Triclabendazole progress report, 2005-2009: an advancement of learning? *Journal of Helminthology*, pp. 83; 139-150.

- Fletcher, H. L., Hoey, E. M., Orr, N., Trudgett, A., Fairweather, I., & Robinson, M. W. (2004). The occurrence and significance of triploidy in the liver fluke, *Fasciola hepatica*. *Parasitology*, *128*(1), pp. 69-72.
- Gilson, E., Higgins, C. F., Hofnung, M., Ames, G. F., & Nikaido, H. (1982). Extensive homology between membrane-associated components of histidine and maltose transport systems of *Salmonella typhimurium* and *Escherichia coli*. *J. Biol. Chem.*, *257*, pp. 9915-9918.
- Han, X., Patters, A. B., Jones, D. P., Zelikovic, I., & Chesney, R. W. (2006). The taurine transporter: mechanisms of regulation. *Acta Physiol*, *187*, pp. 61-73.
- Higgins, C. F. (2001). ABC transporters: physiology, structure and mechanism - an overview. *Res. Microbiol.*, *152*, pp. 205-210.
- Higgins, C. F., & Linton, K. J. (2004). The ATP switch model for ABC transporters. *Nature structural & molecular biology*, *11*, pp. 918-926.
- Higgins, C. F., Haag, P. D., Nikaido, K., Ardeshir, F., Garcia, G., & Ferro-Luzzi Ames, G. (1982). Complete nucleotide sequence and identification of membrane components of the histidine transport operon of *S. typhimurium*. *Nature*, *298*, pp. 723-727.
- Hollenstein, K., Dawson, R. J., & Locher, K. P. (2007). Structure and mechanism of ABC transporter proteins. *Current Opininion in Structural Biology*(17), pp. 412-418.
- Huxtable, R. J. (1992). Physiological Actions of Taurine. *Physiological Reviews*, *72*(1), pp. 101-163.
- Jacobsen, J., & Smith, L. H. (1968). Biochemistry and Physiology of Taurine and Taurine Derivatives. *Physiological Reviews*, *48*(2), pp. 424-511.
- Jones, P. M., & George, A. M. (2005). Multidrug resistance in parasites: ABC transporters, P-glycoproteins and molecular modelling. *International Journal for Parasitology*, *35*, pp. 555-566.
- Kasinathan, R. S., Goronga, T., Messerli, S. M., Webb, T. R., & Greenberg, R. M. (2010). Modulation of a *Schistosoma ansoni* multidrug transporter by the antischistosomal drug praziquantel. *FASEB J*, *24*(1), pp. 128-135.
- Kerboeuf, D., Blackhall, W., Kaminsky, R., & von Samson-Himmelstjerna, G. (2003). P-glycoprotein in helminths: function and perspectives for anthelmintic treatment and reversal of resistance. *International Journal of Antimicrobial Agents*, *22*, pp. 332-346.
- Kristensen, A., Andersen, J., Jorgensen, T., Sorensen, L., Eriksen, J., Loland, C., et al. (2011). SLC6 Neurotransmitter Transporters: Structure, Function, and Regulation. *Pharmacological reviews*, *63*(3), pp. 585-640.
- Kumkate, S., Chunchob, S., & Janvilisri, T. (2008). Expression of ATP-binding cassette multidrug transporters in the giant liver fluke *Fasciola gigantica* and their possible involvement in the transport of bile salts and anthelmintics. *Mol Cell Biochem*, *317*, pp. 77-84.
- Lambert, I. H., Kristensen, D. M., Holm, J. B., & Mortensen, O. H. (2014). Physiological role of taurine - from organism to organelle. *Acta Physiologica*.
- Lee, J. S., Paull, K., Alvarez, M., Hose, C., Monks, A., Grever, M., et al. (1994). Rhodamine efflux patterns predict P-glycoprotein substrates in the National Cancer Institute drug screen. *Mol Pharmacol.*, *46*(4), pp. 627-638.
- Life Technologies. (n.d.). Retrieved July 7, 2014, from Lipid Transfection: www.lifetechnologies.com/at/en/home/life-science/cell-culture/transfection/transfection-methods/lipid-transfection.html

-
- Life Technologies. (n.d.). [www.lifetechnologies.com](http://tools.lifetechnologies.com/content/sfs/manuals/Lipofectamine_RNAiMAX_Reag_protocol.pdf). Retrieved 2014, from http://tools.lifetechnologies.com/content/sfs/manuals/Lipofectamine_RNAiMAX_Reag_protocol.pdf
- Loo, T. W., & Clarke, D. M. (2008). Mutational analysis of ABC proteins. *Archives of Biochemistry and Biophysics*, 476, pp. 51-64.
- Mas-Coma, S., Bargues, M. D., & Valero, M. A. (2005). Fascioliasis and other plant-borne trematode zoonoses. *International Journal for Parasitology*, 35, pp. 1255-1278.
- Miyasaka, T., Kaminogawa, S., Shimizu, M., Tatsuhiro, H., Reinach, P., & Miyamoto, Y. (2001). Characterization of Human Taurine Transporter Expressed in Insect Cells Using a Recombinant Baculovirus. *Protein Expression and Purification*, 23, pp. 389-397.
- Mottier, L., Alvarez, L., Fairweather, I., & Lanusse, C. (2006). Resistance-induced changes in triclabendazole transport in *Fasciola hepatica*: ivermectin reversal effect. *J Parasitol.*, 92(6), pp. 1355-1360.
- Polyplus Transfection. (n.d.). <http://www.polyplus-transfection.com/>. Retrieved July 2014, from http://www.polyplus-transfection.com/wp-content/uploads/2009/08/CPT_114_jetPRIME_VI.pdf
- Ramamoorthy, S., Leibach, F. H., Mahesh, V. B., Han, H., Yang-Feng, T., Blakely, R. D., et al. (1994). Functional characterization and chromosomal localization of a cloned taurine transporter from human placenta. *Biochem J*, 300(3), pp. 893-900.
- Reed, M. B., Panaccio, M., Strugnelli, R. A., & Spithill, T. W. (1998). Developmental expression of a *Fasciola hepatica* sequence homologous to ABC transporters. *International Journal for Parasitology*, 28, pp. 1375-1381.
- Rees, D. C., Johnson, E., & Lewinson, O. (2009). ABC transporters: The power to change. *Nat Rev Mol Cell Biol.*, 10, pp. 218-227.
- Ripps, H., & Shen, W. (2012). Review: taurine: a "very essential" amino acid. *Molecular Vision*, 18, pp. 2673-86.
- Rondelaud, D., Titi, A., Vignoles, P., Mekroud, A., & Dreyfuss, G. (2014). Adaptation of *Lymnaea fuscus* and *Radix balthica* to *Fasciola hepatica* through the experimental infection of several successive snail generations. *Parasites and Vectors*, 7(296).
- Sarkadi, B., Homolya, L., Szakács, G., & Váradi, A. (2006). Human Multidrug Resistance ABCB and ABCG Transporters: Participation in a Chemoimmunity Defense System. *Physiol.Rev*, 86, pp. 1179-1236.
- Satsu, H., Terasawa, E., Hosokawa, Y., & Shimizu, M. (2003). Functional characterization and regulation of the taurine transporter and cysteine dioxygenase in human hepatoblastoma HepG2 cells. *Biochem. J.*, 375, pp. 441-447.
- Schmidt, S. Y., Berson, E. L., & Hayes, K. C. (1976). Retinal degeneration in cats fed casein. I. Taurine deficiency. *Invest Ophthalmol.*, 15(1), pp. 47-52.
- Sergeeva, O., Chepkova, A. N., & Haas, H. L. (2002). Guanidinoethyl sulphonate is a glycine receptor antagonist in striatum. *British Journal of Pharmacology*, 137(6), pp. 855-860.
- Sharom, F. J. (2008, Januar). ABC multidrug transporters: structure, function and role in chemoresistance. *Pharmacogenomics*, 9, pp. 105-127.
- Sigma-Aldrich. (2014). Retrieved August 2014, from www.sigmaaldrich.com: <http://www.sigmaaldrich.com/catalog/product/sigma/83702?lang=de®ion=AT>

-
- Silbernagl, S., & Despopoulos, A. (2003). *Taschenatlas der Physiologie* (Vol. 6 (corrected)). Thieme.
- Stitt, A. W., & Fairweather, I. (1994). The effect of the sulphoxide metabolite of triclabendazole ("Fasinex") on the tegument of mature and immature stages of the liver fluke, *Fasciola hepatica*. *Parasitology*, *108*, pp. 555-567.
- Stryer, L., Berg, J. M., & Tymoczko, J. L. (2007). *Biochemie* (Vol. 6.). (S. A. Verlag, Ed.) ELSEVIER.
- Sukhdeo, M. V., & Sukhdeo, S. C. (2003). Trematode behaviours and the perceptual worlds of parasites. *Can. J. Zool.*, *82*, pp. 292-315.
- Thorsell, W., & Björkman, N. (1965). One the fine structure of the mehlis gland cells in the liver fluke *Fasciola hepatica* L. *Z.f. Parasitenkunde*, *26*, pp. 63-70.
- Trifina, E., Spenger, J., Zandieh, S., Haller, J., Auer, H., Österreicher, C., et al. (2011). Multiple Leberherde und Eosinophilie-ein Fallbericht einer *Fasciola hepatica*-Infektion. *Wiener Med Wochenschr*, *161*(17-18), pp. 448-454.
- Tsuboyama, N., Hosokawa, Y., Totani, M., Oka, J., Matsumoto, A., Koide, T., et al. (1996). Structural organization and tissue-specific expression of the gene encoding rat cysteine dioxygenase. *Gene*, *181*, pp. 161-165.
- Uchida, S., Moo Kwon, H., Yamauchi, A., Preston, A., Marumo, F., & Handler, J. S. (1992). Molecular cloning of the cDNA for an MDCK cell Na⁺-and Cl⁻-dependent taurine transporter that is regulated by hypertonicity. *Proc Natl Acad Sci U S A*, *89*, pp. 8230-8234.
- Vasiliou, V., Vasiliou, K., & Nebert, D. W. (2009). Human ATP-binding cassette (ABC) transporter family. *Human Genomics*, *3*(3), pp. 281-290.
- Virkel, G., Lifschitz, A., Sallovitz, J., Pis, A., & Lanusse, C. (2006). Assessment of the main metabolism pathways for the flukicidal compound triclabendazole in sheep. *J.vet.PPharmacol. Therap.*, *29*, pp. 213-223.
- WHO. (2006, October 17-18). *www.who.int*. Retrieved August 8, 2014, from Report of the WHO Informal Meeting on use of triclabendazole in fascioliasis control: http://www.who.int/neglected_diseases/preventive_chemotherapy/WHO_CDS_NTD_PCT_2007.1.pdf?ua=1
- Wilkinson, R., Law, C. J., Hoey, E. M., Fairweather, I., Brennan, G. P., & Trudgett, A. (2012). An amino acid substitution in *Fasciola hepatica* P-glycoprotein from triclabendazole-resistant and triclabendazole-susceptible populations. *Mol Biochem Parasitol.*, *186*(1), pp. 69-72.
- Wolstenholme, A. J., Fairweather, I., Prichard, R., von Samson-Himmelstjerna, G., & Sangster, N. C. (2004). Drug resistance in veterinary helminths. *TRENDS in Parasitology*, *20*(10), pp. 469-476.
- Zelikovic, I., & Chesney, R. W. (1989). Sodium-coupled amino acid transport in renal tubule. *Kidney Int.*, *36*(3), pp. 351-359.
- Zhou, Y., Holmseth, S., Caiying, G., Hassel, B., Höfner, G., Huitfeldt, H. S., et al. (2012). Deletion of the γ -Aminobutyric Acid Transporter 2 (GAT2 and SLC6A13) Gene in Mice Leads to Changes in Liver and Brain Taurine Contents. *J.Biol.Chem.*(287), pp. 35733-35746.

Sequences

FhMDR

DNA sequence

atgcatggaacgtcccactgagcaacaggtgaacaatgttcagtcgcagaaaaatgcaaccagagataataccgtgaggtt
tacagatctgttcgttacgctacacctccgagaagtaatgatcacttcgggaattctccttagttcattgctgggtgaggcttcccgt
tcgcaatgtgttcgactaattgtaacgaattcatcaacgggtggttcattggatgatcgcactgcccgtgtacagcacctcactgtg
gttcgaggatgccttatgacggtttatgtgcattgcccagtgccctcgtggaatatcgtcgttacgtcaggctgaacgtat
tcgtctctctatcttcaggcaatgttcgctcaggacacagcatggttcgatcagcaagccgtcggaaactctgtcacaagttatctga
ggacaccgacaacattcagtttaagtattgggctaaagttgagcgaatgttcagaatatacaagttgtttcggcctctcatcgtc
ctgtgtgtggctgaaactgactgctgtccctatccatgctccattcgttatcattggcttcggttcattcgggtgttgacagttac
ttaccagaaaagaatctctcgttacgctaaagctagtgctattgtcgaagaagttttcgtcgaatcgaacagtatatgcattcgc
cggagagcggaaagaggcgagacgttacggaagccattggaggatgcccgaaggtgggatcagacaagcaactgtttc
ggttgtcggcgggtttatggttcacgggtctatgcatcgtcactggtatgttgtaacggagtcctccgaactccgttattctcgcg
gatgccggtactgtcattctggtatcctaaatgttatcattggcagcatgttcctggcggagctctccgaactccgttattctcgcg
gcaaaatctcggcacatcatgttttgaaatcattgaacgtaaacctccaattgacaaggtcgagggtggctgaaaccagaatca
tctttcaacaattcgggttcaagatgtctcattgctatcccactcgaccagatactatggtcctaaacaactttctgtggtcgtgg
agcaaaatcaaacagttgcttcgtcggaccaagtggtgctggcaaaagcaccatcatgcaattattacaacgtctgtacgatcc
ggtagagggcaagatcacaattgatggtgctgatcgcactgagctggatctcagttggttcgagggtcaaacgggggctgtccaac
aagaaccagttctttaccggcactgttgagagaatattcgtttgggactggacgcccactgaatcagagggtgatcgaagca
gctaaacaagcgaatgctgcacgattcattgtcaagctacctgaggggtatcaaacccgaatcaacaaaaatgtaccggattat
cagttggtcaaaagcaacgtattgcaatcgcggcagccctggtacgcgaccacgcatcctatcctggacgaagccacatcgg
ctttggatagtcagtcagagacattggtcaagctgcatcaaccgagcctgtgttggtcgaactgtgatcatggtcgcgatcgtttg
tctacgggtgcgcaatgctgatcgcattgtggtttggatcgcggctcgttagtgagatgggacacatacggaaactggcacaagct
ggtggtatgtatgccactctgtgaaatgacagcaacatgccgtctcagatgatcagcagatcgaatgggagtaacgtgacga
gtgaaccaaataccgttctgccaactgaccgatccactgttaaccggaacggacaaagtcaacgatggtgatggtcaagcaa
caccacagctccacacgacttattcgggttagaaaaaccctcgttaccacgcaaccatcacgtacgctcggcaacaacgaa
aacctccgcttactctgtgtaatgcgactcagtcgcccgaatggtgtggtattgtctgggaagtctgtggtccatcgtgaccggg
gagattcaaccgattttgcatcctctattcggaaatgatgcatgttttaccatgaaaaccgatccagatcaaatgcaaacagaat
caattgaccgcggggattatgacattgtggtctcattcgcactagccagttccactttcaagcctacttttcggtgctcgtggacag
cggtaacaaaacgcttgcgactaacgctattgagtcattctcgcagggaattagctggttgacgaaccggacaatcaagttg
gaactttgaccgcccgtgtggccggggacgcaacaaagtgcattcaatctgtggttcgcaatgggtcagatagttgaatcggg
gatgtactgatcttctggtgctggcattgtctacaactggaaactcaccctgtcgtggctgtattctccgggtgatcgtatttcc
agtttatcaataaataaacagctcagattggcggagacagtgaggcgaaccgaggcagtgctgttgccacgaggcgttctc
cgctcatcgtaccgtggcgggttcgattggagcactatttcatcagcagttgcacatgcatcgggtcagcagagtaactggc
acttcgagcatcgttctcagcggtagtgacgcgctcgtcagctttaccaattgtcgtatgaggctgttctcatttgggtctca
cctgatgagtaaggtgaaatcaagctgatcgtatctccgagtggtcagcagatcagtttctcaggtctcggacgcact
tcgatttgggtcggctatgaaacaggcgggtgcagcagcatctcgcactttcgcactattgaacgttcacagcctatgcctgtga
gcaagggttacagcctaactggaattgaacaccgtccctattcattttcgccacgatcgttccggtaccctccagaccacgat
gcctgtgctcgggacttctcacacaatctgtcttgccgaaacagtcgatttgggtcattccggttggcgaagaccagcgtg
ctcaactgtccaacgattctatacaatcggcccgtgtgacttaaccggggcatctttgttggtgagacaccactggatcagctgg
ctcctgttggttaagaagtcagattggtatggtcagatcaggaaccgcatctgtttgatatacctctccagaagaatcgtctatggg
gataacgagcgggaggttctatggaagaggtatggaggcagcccgactggccgaaattcatgactcatagtcagttaccac
atggctatgaaaccctcggggtctcacgggttgtaactatctggcgggtgaaaacaacgcatagcaatcgcctcagctctgatt
cgacgtcccactctgttctgttgatgaggccacctcggcttggacacacaaactgagctccgaatacaatcaaaactgaatga
ggctctcagaggtcggactgctgtgatcagcgcacatcgtctgaccgagaccagtggtgcgaaactgtggtggttctggccgat
ggtcacaaatggaatcgggcaaacgggacgagcctaatacaactccacggagcctatcatgctttgaccacgctcaagcta
gagctgtag

Protein sequence

MRWKRPTEQQVNNVQSQKNATRDNTVRFTDLFRYATPSEKLMITSGILLSLLGAAFPFAIF
 VFRLIVNEFINGGSLDVSTAVYSTSLWFAVIALCAFIVAFQAQVALVEISSVRQAERIRLLYLQAI
 FRQDTAWFDQQAVGTLVTKLSEDTDNISLGLKSEFVQNISSFVGLFIALLCGWKLTAVA
 LSMLPFVIIGFGSFGGLTRYFTRKESLAYAKASAIIEEVFRSIRTVYAFAGERKEARRYGSHL
 EDAAKVGIRQATCFGFAGGFIGFTVYASAALVFWYGVQLLIINEYDAGTVILVFLNVIIGSMFL
 GGALPNFRYFFAAKISAHHVFEIERKPPIDKCRGGLKPESFFQQIRFQDVSFAYPTRPDTMV
 LNKLSVVVEQNQTVAFVGPSPGCGKSTIMQLLQRLYDPVEGKITIDGVDLTELDLSWFRGQTG
 AVQQEPVLFTGTVAENIRFGALDATESEVIEAAKQANAHDFIVKLPEGYQTRINQATGLSVG
 QKQRIAIARALVRDPRILILDEATSALDSQSETLVQAAINRACVGRVIMVAHRLSTVRNADRI
 VVLDGRVSEMGTHTELAQAGGLYATLLNAQQHAVSDVSAIANGSNVTSEPNTVSSNLTDP
 LLTRTDKVNDDGQATPQSPHDLFGLEKPSVTTQPSRTRRQQRKPSASLRVMRLSRPEWL
 WIVLGSLGAVTGAIQPIFAILYSEMYAIFTLKTDPDQMQRINLTAGIMALLGLIRLASSTFQAY
 FFGVAGQRLTKRLRLTLFESILRQELAWFDEPDNQVGTLTARVAGDANKVHPICGSAMGQIV
 ESVMILLIFSLVAVFYVNWKLTLVAVFFPVIAFSSFINIKQLRFGGDSAGETEAVRVAHEAFSA
 HRTVAGFALEHYFHQQFAHASGQQSQLALRASFRHAVVYALAQSLPICSYAAAFSFGAHLM
 SQGEIKLIAIFRVFAAISFAAALGRTSHLGPAMKQAGAAASRIFRIERSSAMPVVSQGVQPN
 WNLNTVPIHFRHVSFRYPSRPTMPVLRDFSHTICPGETVAFVGHSGCGKTSVLNLLQRFYTI
 GPCDSNRGIFVGETPLDRLAPCWLRISQIGMVDQEPHFDITLQKNIAYGDNEREVSMEEV
 EAARLAEIHDFIVSLPHGYETLAGPHGCELSGGEKQRIAIARALIRPHLFLLEATSALDTQT
 ELRIQSKLNEALRGRTALISAHRLTATSGAETVVVLADGHKLESKPDDELILHGAYHALYHA
 QANEL

FhepSLC6DNA sequence

atgcccaggaattcagttccaagtaaaagcagaaccgagctggcagcaactagttctattcatccagtggtcagagtgaaag
 atgaatgctctattattccggtttcatcatcctggcaaacacaaggaagtggaataacacctcgggaacaatggaagagacg
 tttgatttctgcttctctgtgtgctcgtgggattgggaaatatctggcgtttccgatatctgtgttacaagcacggtggaggtgcat
 ttctgataccttattcatcagatatttgcgctggactccagattctgtctgaagtactgtggccagataacagcacagggag
 gtattgctgctggaacattgtcctctcttccggggtatcggttttccagtttggtaccaactttgtctgattgtactacaactgatat
 tggcctgggactctactatttctctcgtctcactccactctccgtagactgtgtggacagtggtggaacacgccacaatgt
 gataacggatccgactgatcaacggaacagttgcaacagatccagcagcgaattctgggaaaatcgcgcttctggtttgcca
 aaggaatcgaacatctggggccagtgctgggatctggcattgtgttctattggcctggatcatagttccttctgattttcaaagg
 gatcaaaacgtccggaaggtatgtatgtgacagcaaccagtcctatatttcatgtttatcctattggttcgagcagcagcttgg
 aaggagcgtatggtatagcttattacatggtccccgactggagtaagcttgcggatgtacagatgtggcggacgccggtgc
 gcagatcttttcagttattctatcagtttgggaacgcttactgcacttgaagtataaattcgtttaccagaactctttcgagactgtttg
 gcttatgccacagtgatacgttacaagcttctggtgatttatcatttgcacaactcggccacatggcactgaaggctgactt
 gtccattgatcaggtggcgaatctggaccgggttggcgtctgctgatctatccgaaagcgattgggatgatgaaagccagtcatt
 ctggtctgtctgtttcttctgatgctcctctgctcggtatagacagtcagttgctggttgaaggattcatcacatcgattaccgacttt
 acccagactggtgctgcgccgaaacttcaataacttttggatcagctcgcctagctgttttctgtgtgcttaccatggtcaca
 gaggtggtatgtacctgtttcaactttcaaccattacgctggaagtcgaatcactgctgacggctttcttgaatgcattgctgctg
 gttacttctatggagcaaacgcatcgggtggtcacatgaaaaaatgcatggtcggggttaggtgttctgccgaggtatttggg
 cgtcattagctccggtttactctgggtttatttattgctcagtggttagtcacgaagaggtcagctatgagcgggcatcgaggacgg
 aagtttgcactttccgcaatggtccatcatatttgggttctgctgctgctgagttatcatgattccaataatcatggtattcgagtt
 attcgaaactccgggacttttgcagcggctcagaactctgagtcaccacaaactgactggtagtcagctgatgcgattgcagg
 gcagaaaaaccgaaaacgattcatctgttcaacagattcatccaacagtcgaagggtcaaaaaacgggttgacgaatgtagaa
 acgcaaacgaaagttggtgcaaacggttcttgaatgagaatcaacatcaataatttgaattag

Protein sequence

MRQEFSFPSKSRTELAATSSIHVFEVKDECSIIPVSSSLANTREVEKSPREQWKRRFDLL
SLVGLSVGLGNIWRFPYLCYKHGGGAFLIPYFISIFAAGLPVFLLEVTVGQITAQGGIAAWNIC
PLFRGIGFASLVTNFCLDCYYNVILAWALYYLFSSTSTLPWTLCGQWWNTPQCDNGSGLIN
GTVATDPAAEFWENRVLGLSKGIEHLGPVRWDLALCLLAWIIVFLCIFKGIKTSGKVMYVTA
TSPYIFMFILLVRAATLEGAIDGIRYYMVPDWSKLADVQMWADAGAQIFFSYSISLGTLTALG
SYNSFHQNSFRDCLAYATVNTLTSLLAGFIIFATLGHMALKADLSIDQVAESGPGLAFVIYPKA
IGMMKASPFWSVCFLLMLLLLGIDSQFAGVEGFITSITDFYPRLVLRPKLRILFVGSVCLACFL
VGLTMVTEGGMYLFQLFNHYAGSRIILLTAFFECIAAGYFYGAKRIGGHMCKMHGWGLGVLP
QVFWCVISPVFTLGLFIVSVVHVEVSYERASRTEVCHFPQWSIIFGWLLAACSVIMIPIIMVF
ELLRTPGTFSQRLRTLSHHKLTGSQLMRLQGRKTENDSSASTDSSNSRRSKNGLTNVETQT
KVVAKRFLNEESTSNLN

Zusammenfassung (Abstract german)

Fasciola hepatica, ein endoparasitärer Plattwurm der Klasse Trematoda, Stamm Platyhelminthes, auch bekannt als großer Leberegel, ist verantwortlich für die Krankheit Fasziole. Durch aktives Durchdringen der Darmwand und anschließender Migration in die Leber besiedelt der Leberegel schlussendlich die Gallengänge seines Endwirts.

Aufgrund dieser Erkrankung, welche eine große Bedeutung bei Weiderindern und Schafen spielt, entstehen finanzielle Verluste durch nicht verwertbare Fleischprodukte, oder schlecht genährter Tiere. Auch die Bedrohung für den Menschen nimmt einen immer größeren Stellenwert ein.

Aufgrund von fehlender präventiver medizinischer Vorsorge, wie zum Beispiel Impfungen gibt es momentan nur den Ansatzpunkt der Chemotherapie in Form des Anthelmintikums Triclabendazol, welches unter dem Markennamen Fasinex® verkauft wird. Dieses Medikament gehört der Gruppe der Benzimidazole an, welche dadurch charakterisiert sind, dass sie gegen β -Tubulin und daher am mitotischen Spindelapparat und dem Mikrotubulisystem wirken und diese Strukturen zerstören. Interessanterweise ist Triclabendazol das einzig bekannte Medikament, das gegen *Fasciola hepatica* Wirkung zeigt, zusätzlich mit dem großen Vorteil, dass es alle vorkommenden Entwicklungsstadien innerhalb des Endwirts bekämpft.

Allerdings wurde im Laufe der Zeit eine erhöhte Zahl an Resistenzen gegen dieses Medikament beobachtet.

Verschiedene Hypothesen versuchen diese aufkeimende Resistenz zu erklären. Eine vielversprechende Erklärung basiert auf einer publizierten Teilsequenz eines ABC Transporters (vom englischen ATP binding cassette) von Reed et al. aus dem Jahr 1998, die eine hohe Homologie zum humanen P-glycoprotein aufweist. Triclabendazol könnte als Substrat für einen oder sogar mehrere verschiedene ABC Transporter von *F.hepatica* dienen. Ungeachtet der Homologie zu P-gP handelte es sich bei dieser Teilsequenz um einen Halbtransporter. Daher war es von Interesse herauszufinden, ob diese Sequenz vollständig war, oder nicht.

Zusätzlich war es notwendig andere Transporter zu identifizieren.

Im Rahmen der vorliegenden Arbeit konnten zwei komplette cDNAs von *Fasciola hepatica* identifiziert, kloniert und exprimiert werden, welche für zwei verschiedene Transmembrantransporter kodieren – FhMDR und FhSLC6 (Taurin Transporter Homolog). FhMDR als repräsentatives Mitglied der ABC Transporter der Unterfamilie B, ist jener Transporter der eine Schlüsselrolle in den Mechanismen der Resistenzentwicklung einnehmen könnte.

Funktionellen Eigenschaften von FhMDR wurden mittels eines auf FACS basierendem Rhodamine123 Experiments getestet, welches für den humanen MDR Transporter schon gut etabliert ist.

Der zweite identifizierte Transporter erwies sich aufgrund seiner Sequenzhomologie als Taurintransporter (SLC6).

Obwohl es nicht zu erwarten war, dass Taurin eine Rolle in der Resistenzentwicklung gegen Triclabendazol spielt, war es trotzdem von großem Interesse zu erforschen wie dieser Transporter funktioniert, welche Substrate er transportieren kann und welche möglichen Antagonisten auf diesen Transporter einwirken können.

Curriculum Vitae

Sandra Pichler, BSc

Academic Career

- Since 2011 **[University of Vienna]** [Vienna] [Austria]
Master studies: *Molecular Biology (Molecular Medicine)*
Master thesis: "Transmembrane transporters of the liver fluke *Fasciola hepatica*"
- 2007 – 2010 **[Leopold-Franzens University]** [Innsbruck] [Austria]
Bachelor Studies: *Biology* (BSc)
Bachelor thesis: "High Resolution Melting Analysis"
- 2005 – 2007 **[Medical University]** [Vienna] [Austria]
Diploma Studies: Medicine
- 2002 - 2005 **[BG Nonntal]**, [Salzburg] [Austria]
Grammar school
- 1996 - 2002 **[BG/BRG Dr. Schauerstraße]**, [Wels] [Austria]
Grammar school
- 1992 – 1996 [Primary School 11 Lichtenegg], [Wels] [Upper Austria]

Work Experience (Laboratory)

- since 09/2012 **[Medical University of Vienna]**, [Vienna] [Austria]
Department: Center for Physiology and Pharmacology
Master thesis (PI: Univ. Prof. Dr. Harald Sitte) "Transmembrane transporters of the liver fluke *Fasciola hepatica*"
- Cell Culture techniques (Cultivation, Stable celllines)
 - Molecular Biology/Cell Biological/Biochemical Methods (PCR, Western Blot, Cloning, Gel electrophoresis, Tissue Preparation)
 - Pharmacological Assays (Uptake/Inhibition)
 - FACS (Fluorescence activated cell sorting)
 - Epifluorescence Microscopy
 - Tissue preparation from nude mice

- 01/20012 – 04/2012 **[Medical University of Vienna], [Vienna] ([Austria])**
 Department: Center for Physiology and Pharmacology
 Practical Course “Transmembrane Transporters of the liver fluke *Fasciola hepatica*”
- Cloning
 - Ligand Binding Assay / CalceinAM Assay
 - Expression systems (HEK293, Sf9 cells)
 - Generation of recombinant Baculoviruses
- 04/2011 – 06/2011 **[University of Vienna], [Vienna] ([Austria])**
 Department: Max F. Perutz Laboratories MFPL
 Practical Course “Plectin – A cytolinker protein and its function in focal adhesions”
- Cell Culture techniques (Crosslinking, Cultivation, Primary Fibroblasts)
 - Protein Purification (Ammonium Sulphate), Dialysis
 - FPLC (Fast Protein Liquid Chromatography)
 - Western Blot, SDS Page

Skills

EDP MS Office, GraphPadPrism5.0, BD Accuri™ C6 Analysis Software, Li-Cor Odyssey® CLx
 Image Studio

Languages *German (mother tongue)*
 English
 Spanish (school basics)

Posters

06/2014 “Identification and characterization of transmembrane transporters of the liver fluke *Fasciola hepatica*”
 Kudlacek O., **Pichler S.**
 10th Young Science Association (YSA) PhD Symposium 2014 (Vienna)

04/2013 “ABC transporters of the liver fluke *Fasciola hepatica*”
 Kudlacek O., **Pichler S.**
 Research Retreat of the Center for Physiology and Pharmacology (Haindorf/Lower Austria)